

**DESIGN AND DEVELOPMENT OF AN
ASSISTIVE HAND ORTHOSIS FOR HAND AND
FINGER MOTOR TRAINING**

WONG CHI HEIM

UNIVERSITI TUNKU ABDUL RAHMAN

**DESIGN AND DEVELOPMENT OF AN ASSISTIVE HAND
ORTHOSIS FOR HAND AND FINGER MOTOR TRAINING**

WONG CHI HEIM

**A project report submitted in partial fulfilment of the
requirements for the award of Bachelor of Biomedical
Engineering with Honours**

**Lee Kong Chian Faculty of Engineering and Science
Universiti Tunku Abdul Rahman**

October 2024

DECLARATION

I hereby declare that this project report is based on my original work except for citations and quotations which have been duly acknowledged. I also declare that it has not been previously and concurrently submitted for any other degree or award at UTAR or other institutions.

Signature :



Name : Wong Chi Heim

ID No. : 2006340

Date : 13/10/2024

APPROVAL FOR SUBMISSION

I certify that this project report entitled “**DESIGN AND DEVELOPMENT OF AN ASSISTIVE HAND ORTHOSIS FOR HAND AND FINGER MOTOR TRAINING**” was prepared by **WONG CHI HEIM** has met the required standard for submission in partial fulfilment of the requirements for the award of Bachelor of Biomedical Engineering with Honours at Universiti Tunku Abdul Rahman.

Approved by,

Signature

:



Supervisor

:

Ts. Dr. Loo Joo Ling

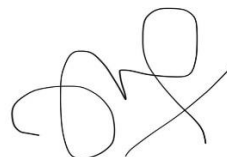
Date

:

13/10/2024

Signature

:



Co-Supervisor

:

Chong Yu Zheng

Date

:

13/10/2024

The copyright of this report belongs to the author under the terms of the copyright Act 1987 as qualified by Intellectual Property Policy of Universiti Tunku Abdul Rahman. Due acknowledgement shall always be made of the use of any material contained in, or derived from, this report.

© 2024, WONG CHI HEIM. All right reserved.

ACKNOWLEDGEMENTS

I would like to thank everyone who had contributed to the successful completion of this project. I would like to express my gratitude to my research supervisors, Ts. Dr. Loo Joo Ling and Mr. Chong Yu Zheng for their invaluable advice, guidance and their enormous patience throughout the development of the project.

In addition, I would also like to thank the Department of Mechatronics and Biomedical Engineering at Universiti Tunku Rahman for support and funding of this project.

ABSTRACT

There are currently lack of assistive devices connected to internet-of-things (IoT), which enables precise real-time, and remote control and monitoring of the patients during finger fine motor rehabilitation. This study aimed to enhance existing hand therapy tool by developing a portable, cost-effective (RM 383.29), lightweight (500 g) and remotely controllable active assistive hand orthosis (AHO) to enhance fine motor training of fingers. The AHO was designed to assist in actuating flexion-extension movements of all 4 fingers and thumb in the metacarpophalangeal (MCP) joint, and grasping movement. The mechanical frame was designed using computer-aided software (CAD) and additive manufactured with polylactic acid (PLA) filaments. The functional components include inertial measurement units (IMUs) that measure the range of motion of the index finger and thumb; servo motors that enable precise linear actuation in performing specific finger and thumb movements; a microcontroller as the control system; and a simple Internet of Things (IoT) user interface that aid the therapists in monitoring rehabilitation progress of individual patient during home-based rehabilitation, as well as controlling the exoskeleton remotely. This AHO can perform 4 fingers flexion/extension and thumb flexion/extension on subjects with various hand sizes (15.5 cm to 18 cm) consistently with a low standard deviation ($SD < 10$), and it can aid on users' grip strength with a percentage increase of 16.86% and 14.09% of index finger and thumb respectively. Experimental outcomes showed that the AHO was able to acquire, display and store relevant data accurately when assisting participants to perform repetitive flexion/extension movement and practice grasping on objects of various shapes and sizes. This proof of concept demonstrated the AHO can assist and has the potential to improve the effectiveness of fine motor trainings in hand and finger rehabilitation, besides providing more convenience to the users and therapists.

TABLE OF CONTENTS

DECLARATION		i
APPROVAL FOR SUBMISSION		ii
ACKNOWLEDGEMENTS		iv
ABSTRACT		v
TABLE OF CONTENTS		vi
LIST OF TABLES		x
LIST OF FIGURES		xi
LIST OF SYMBOLS / ABBREVIATIONS		xiv
LIST OF APPENDICES		xvi
 CHAPTER		
1	INTRODUCTION	1
	1.1 General Introduction	1
	1.2 Importance of the Study	3
	1.3 Problem Statement	4
	1.4 Aim and Objectives	4
	1.5 Scope and Limitation of the Study	5
	1.6 Contribution of the Study	5
	1.7 Outline of the Report	6
2	LITERATURE REVIEW	7
	2.1 Introduction	7
	2.2 Types of Actuators	7
	2.2.1 Electrical Motors	7
	2.2.2 Pneumactical Actuators	9
	2.2.3 Cable-Driven Systems	11
	2.2.4 Shape Memory Alloys	12
	2.2.5 Hydraulic Actuators	13
	2.3 Typical Sensors and Devices Used to Collect Biomechanical Parameters	13
	2.3.1 Sensors, Motion Capture Systems and Software used to Measure Joint ROM and Joint Kinematics	14

2.3.2	Sensors and Devices Used to Measure Forces Exerted by Fingers	16
2.3.3	Use of Electromyography (EMG) sensors with EMG Electrodes	17
2.4	Pros and Cons on Previously Developed Assistive Hand Orthoses	18
2.4.1	Electrically Actuated Assistive Hand Orthoses	18
2.4.2	Pneumatically Actuated Assistive Hand Orthoses	21
2.4.3	Cable-Actuated Assistive Hand Orthosis	22
2.4.4	Shape Memory Alloy-Actuated Assistive Hand Orthosis	23
2.5	Comparisons of Assistive Hand Orthoses	27
2.5.1	In Terms of Actuators Used	27
2.5.2	In Terms of Microcontroller Used and Types of Muscle Movements Involved	27
2.5.3	In Terms of Biomechanical Parameters Collected, and Sensors, Devices or Software Used to Collect Them	28
2.6	Summary	28
3	METHODOLOGY AND WORK PLAN	30
3.1	Introduction	30
3.2	Prototype Requirements	30
3.3	Prototype Development Process	31
3.4	Biomechanical Assessments	32
3.4.1	Finger Range of Motion (ROM)	32
3.4.2	Grip Strength	34
3.5	System Architecture of the Prototype	34
3.6	Mechanical Design Conceptualisation	35
3.7	Materials and Electrical Components Selection	37
3.7.1	3D Printing Material	37
3.7.2	Metal Gear Servo Motors	38
3.7.3	Portable Power Supply	39

3.7.4	ESP32 Microcontroller	39
3.7.5	Inertial Measurement Units	39
3.7.6	Multiplexer	40
3.7.7	Velcro Straps	41
3.7.8	Wrist Brace	41
3.7.9	Digital Force Gauge	41
3.7.10	Digital Goniometer	42
3.7.11	Stripboard (Printed Circuit Board)	42
3.8	Calibration of IMU Sensors	43
3.9	Circuit Design	43
3.9.1	Circuit Design with Breadboard	43
3.9.2	Circuit Design with Stripboard	45
3.10	Internet of Things (IoT) System	46
3.10.1	IoT Architecture	46
3.10.2	IoT System Program Flowchart	47
3.11	Libraries Used to Program the Components and IoT System	48
3.12	Experimental Protocols and Data Analysis Methods	49
3.12.1	Finger ROM Test	50
3.12.2	Grip Strength Test	51
3.12.3	Objects Grasping Test	53
3.13	Costs of Materials Used on the Prototype	53
3.14	Summary	54
4	RESULTS AND DISCUSSION	56
4.1	Introduction	56
4.2	Final Prototype Mechanical Design	56
4.2.1	Technical Drawings of Mechanical Design	56
4.2.2	Fabrication of Final Prototype	60
4.2.3	Circuit Design of Final Prototype	61
4.3	Types of Finger Movements Actuated	63
4.4	IoT User Interface Design	63
4.5	Prototype Mechanical Design Changes and Enhancements	64

4.5.1	4 Fingers Part Design Changes and Enhancements	65
4.5.2	Thumb Part Design Changes and Enhancements	68
4.5.3	Junction Box Design Changes and Enhancements	69
4.6	Code Used to Program the Components and IoT System	70
4.6.1	Servo Motor With IoT system Code	70
4.6.2	Inertial Measurement Units with Multiplexer Code	72
4.6.3	Blynk IoT System Code	75
4.7	Results of Performance Assessments of the Prototype	76
4.7.1	Inertial Measurement Unit Angle Accuracy Test	76
4.7.2	Finger Range of Motion Test	77
4.7.3	Grip Strength Test	79
4.7.4	Object Grasping Test	80
4.7.5	Finger Range of Motion and Grip Strength Tests Based on Gender	82
4.8	Summary	83
5	CONCLUSIONS AND RECOMMENDATIONS	84
5.1	Conclusions	84
5.2	Limitations	85
5.3	Recommendations for Future Work	85
	REFERENCES	87
	APPENDICES	94

LIST OF TABLES

Table 2.1:	Comparisons of Developed Assistive Hand Orthoses.	24
Table 3.1:	Costs of Materials Used on the Prototype.	54
Table 4.1:	Thumb IP Joint ROM Before and After Redesigning Thumb Part.	69
Table 4.2:	Percentage Difference Between Thumb IP Joint ROM Achieved and Its Typical Value.	69
Table 4.3:	Subjects of Various Right Hand Sizes Involved in the Testing on the Prototype.	76
Table 4.4:	Comparison of Angle Measurements on Prototype.	77
Table 4.5:	Percentage Differences in Angle Between Two Measurement Tools.	77
Table 4.6:	Finger Range of Motion for All Subjects.	78
Table 4.7:	Grip Strength With and Without the AHO.	79
Table 4.8:	Differences in Index Finger DIP joint ROM Between Male and Female Participants.	82
Table 4.9:	Differences in Grip Strength Without AHO and With AHO for Male and Female Participants.	82

LIST OF FIGURES

Figure 2.1:	A Linear Motor.	9
Figure 2.2:	A McKibben Air Muscle.	10
Figure 2.3:	EMG Board with Electrodes.	18
Figure 2.4:	An Assistive Robotic Hand Orthosis.	20
Figure 2.5:	The ExoGlove.	21
Figure 2.6:	A SMA Based Wrist Exoskeleton.	23
Figure 3.1:	Methodology Flowchart for the Prototype Development.	31
Figure 3.2:	Gantt Chart for Part 1 of the Project.	32
Figure 3.3:	Gantt Chart for Part 2 of the Project.	32
Figure 3.4:	Finger ROM Measurements Diagram.	33
Figure 3.5:	System Architecture of the Prototype	35
Figure 3.6:	Overall Prototype Mechanical Design Conceptualisation.	36
Figure 3.7:	Conceptualisation of 4 Fingers Part in Isometric View.	36
Figure 3.8:	Conceptualisation of Thumb Part in Isometric View.	37
Figure 3.9:	Conceptualisation of Junction Box in Isometric View.	37
Figure 3.10:	MG946R Metal Gear Servo Motor.	38
Figure 3.11:	Wemos D1 R32 Microcontroller.	39
Figure 3.12:	An Inertial Measurement Unit.	40
Figure 3.13:	A TCA9548A I2C multiplexer module.	40
Figure 3.14:	A Digital Force Gauge.	41
Figure 3.15:	A Digital Goniometer.	42
Figure 3.16:	A Stripboard.	42
Figure 3.17:	Method Used to Validate the IMU Angle Readings.	43
Figure 3.18:	Overall Circuit Design for the Prototype.	44

Figure 3.19:	Detailed Circuit Design involving IMUs and Multiplexer.	45
Figure 3.20:	Detailed Circuit Design with Stripboard.	46
Figure 3.21:	IoT Architecture of the Prototype.	47
Figure 3.22:	Program Flowchart for the Prototype IoT System.	47
Figure 3.23:	Finger ROM Test Performed When Wearing Prototype.	51
Figure 3.24:	Grip Strength Test on Index Finger When Wearing Prototype.	52
Figure 3.25:	Grip Strength Test on Thumb When Wearing Prototype.	53
Figure 4.1:	Drawing of Finalised 4 Fingers Part in Isometric View.	57
Figure 4.2:	Drawing of Final Prototype Servo Motor Holder for 4 Fingers Part in Isometric View.	58
Figure 4.3:	Drawing of Finalised Thumb Part in Isometric View.	59
Figure 4.4:	Drawing of Finalised Junction Box in Isometric View.	60
Figure 4.5:	Mechanical Design of the Final Prototype.	61
Figure 4.6:	Circuit Design of Final Prototype.	62
Figure 4.7:	Finger Movements Actuated by the Final Prototype a) 4 fingers flexion; b) 4 fingers extension; c) thumb flexion; d) thumb extension.	63
Figure 4.8:	IoT User Interface Design for Final Prototype.	64
Figure 4.9:	2nd Iterative 4 Fingers Part Drawing in Isometric View.	65
Figure 4.10:	Broken Frames of the Conceptualised 4 Fingers Part.	65
Figure 4.11:	3rd Iterative 4 Fingers Part Drawing in Isometric View.	66
Figure 4.12:	Misalignment of Rotational Axes for the Mechanical Joints of Each Finger for the Second Iterative 4 Fingers Part Frame	67
Figure 4.13:	Single Centre Point of Rotation and Rotational Axis at the Mechanical Joints in Between the Proximal and Distal Ends of the Final Prototype 4 Fingers Part.	67
Figure 4.14:	2nd Iterative Thumb Part Drawing in Isometric View.	68

Figure 4.15:	Variables For the Servo Motors Used on the Prototype.	70
Figure 4.16:	Code to Define the Pins on the Microcontroller to Be Connected With the Three Servo Motors' Signal Pins.	70
Figure 4.17:	Code to Set Rotational Angle of the Servo Motors When a 4 Fingers Flexion/Extension or Grasping Button Selected on the Blynk IoT Mobile App.	71
Figure 4.18:	Code to Set Rotational Angle of Servo Motors When a Thumb Flexion/Extension or Reset Button Selected on the Blynk IoT Mobile App.	72
Figure 4.19:	Code to Define the Variables Used for the Two IMUs and the I2C Channels to be Selected on the Multiplexer.	73
Figure 4.20:	Code to Initialise Both IMUs via the Multiplexer.	73
Figure 4.21:	Code to Program the IMUs to Collect its Accelerometer Readings.	74
Figure 4.22:	Code to Derive the IMU's Acceleration Data to Angular Data.	74
Figure 4.23:	Code Showing the Adjustments Made to IMUs' Angle Readings.	75
Figure 4.24:	Function Used to Connect Microcontroller to Blynk IoT.	75
Figure 4.25:	Function Used to Display Both IMUs Real-Time Angle Readings in Blynk IoT User Interface.	76
Figure 4.26:	Finger ROMs against Time During 5 Repeated Movements of a Participant in Flexion-Extension Directions.	79
Figure 4.27:	Average grip strength of the Index Finger for All Participants With and Without Wearing the AHO.	80
Figure 4.28:	Average grip strength of the Thumb for All Participants With and Without Wearing the AHO.	80
Figure 4.29:	The AHO Grasping Balls of Various Sizes, a) $D = 3$ cm ; b) $D = 6$ cm ; c) $D = 7$ cm ; d) $D = 8$ cm.	81
Figure 4.30:	The AHO Grasping Objects of Different Shapes, a) Cube ; b) Cylinder ; c) Sphere.	81

LIST OF SYMBOLS / ABBREVIATIONS

$\theta_{thumbIP,indexDIP}$	absolute angle of thumb IP and index finger DIP joint, °
a_x	acceleration in the x-axis, m/s ²
a_y	acceleration in the y-axis, m/s ²
a_z	acceleration in the z-axis, m/s ²
θ_z	angle along the z-axis, °
θ_D	DIP Joint's ROM, °
θ_M	MCP Joint's ROM, °
θ_P	PIP Joint's ROM, °
ADL	activities of daily living
AC	alternating current
AHO	assistive hand orthosis
ARHO	assistive robotic hand orthosis
CAD	computer-aided software
I/O	digital input/output
DC	direct current
DIP	distal interphalangeal
EMG	electromyography
FMG	force-myography
FSR	force sensitive resistors
GND	ground
IMU	inertial measurement units
V _{cc}	input voltage
IDE	integrated development environment
IoT	Internet of Things
IP	interphalangeal
MCP	metacarpophalangeal
NOHAS	Novel Orthotic Hand Actuated by Servo Motors
PAM	pneumatic artificial muscles
PLA	polylactic acid

PCB	printed circuit board
PIP	proximal interphalangeal
PWM	pulse width modulation
ROM	range of motion
SMA	shape memory alloy
sEMG	surface electromyography
3D	three dimensional

LIST OF APPENDICES

Appendix A: Technical Drawings of the Conceptualised 4 Fingers Part with Dimensions in Multiple Views.	94
Appendix B: Technical Drawings of the Conceptualised Thumb Part with Dimensions in Multiple Views.	94
Appendix C: Technical Drawings of the Conceptualised Junction Box with Dimensions in Multiple Views.	95
Appendix D: Technical Drawings of the Final Prototype 4 Fingers Part with Dimensions in Multiple Views.	95
Appendix E: Technical Drawings of the Final Prototype Servo Motor Holder for 4 Fingers Part with Dimensions in Multiple Views.	96
Appendix F: Technical Drawings of the Final Prototype Thumb Part with Dimensions in Multiple Views.	96
Appendix G: Technical Drawings of the Final Prototype Junction Box with Dimensions in Multiple Views.	97
Appendix H: Technical Drawings of the Second Iterative 4 Fingers Part with Dimensions in Multiple Views.	97
Appendix I: Technical Drawings of the Third Iterative 4 Fingers Part with Dimensions in Multiple Views.	98
Appendix J: Technical Drawings of the Second Iterative Thumb Part with Dimensions in Multiple Views.	98
Appendix K: Conference Manuscript Based on This Project Accepted to be Presented at the IECBES 2024 Conference.	99
Appendix L: An Assistive Robotic Hand Orthosis (Farinha, et al., 2019). Reprinted with permission from Copyright 2019 IEEE.	100
Appendix M: The ExoGlove (Yap, et al., 2015). Reprinted with permission from Copyright 2022 IEEE.	100
Appendix N: A SMA Based Wrist Exoskeleton (Serrano, et al., 2018). Reprinted with permission from Copyright 2018 IEEE.	100

CHAPTER 1

INTRODUCTION

1.1 General Introduction

People with fine motor disability on fingers face difficulties in performing precise and coordinated movements such as finger flexion/ extension, finger abduction/ adduction, and opposition/ reposition of thumb (Rad, 2023). This can impact their activities of daily living (ADL) like writing, drawing, buttoning clothes and more. Fine motor skills involve smaller and more precise movements using hands and wrists, whereas for gross motor skills, it involves coordinated movements of larger muscle groups and the whole body such as sitting, standing, walking, jumping, running and more, it involves leg muscles like quadriceps, hamstrings, calves and more (EJ Therapy, 2019). Besides that, people with fine motor disability hinders gripping, pinching and precision movements like flexion and extension of fingers (Enabnit and Warren, 2023).

Various conditions such as cerebral palsy, traumatic brain injury and more can lead to fine motor disability by damaging brain regions responsible in coordinating and control finger movements such as motor cortex, posterior parietal cortex and cerebellum. This disrupts brain signals which affects the brain's ability to communicate with the muscles involved in finger movement and these muscles are unable to contract and relax properly (Levin et al., 2009). Muscles involved in fine motor skills on fingers are mainly located on the upper limb like forearm extrinsic muscles like flexors, extensors, intrinsic muscles hand muscles like thenar and hypothenar muscles, and others like lumbrical muscles, palmaris longus and more (Physiopedia, n.d.). Therefore, these individuals would experience hand muscle weakness, spasticity, dystonia, loss of coordination, loss of dexterity, numbness on hand muscles and tremors as those seen in individuals having Parkinson's disease (Mayo Clinic, n.d.).

The motor cortex located on both sides of the brain, is responsible for planning and coordinating finger movements by sending signals to specific muscles to signify them to contract. The left motor cortex controls the right side of the body, and the vice versa (Cunnington, 2016). Moreover, people with stroke can have hemiparesis (Cleveland Clinic, 2023), that causes fine motor

skills disabilities only on one side of the body. This causes coordination problem between the movement of left-and right-hand fingers (Cunnington, 2016). This is due to stroke often damages the motor cortex on opposite side of the body's movement (Cleveland Clinic, 2023).

Moreover, people with bone fractures and dislocations have swelling on the affected areas and this causes the finger's bone alignment to be altered and joints to be unstable, which affects their finger movements. Furthermore, people with soft tissue injury burns and finger infections can cause tissue to be damaged, which disrupts finger structure and changes skin integrity that affects their finger movements (Tarr, 2022).

Therefore, individuals with fine motor disability in their fingers who are undergoing post-stroke and trauma injury recovery, having genetic disorders and others, require fine motor skills training to regain and improve their fine motor control, coordination, strength and dexterity of their fingers, to enable them to properly perform daily tasks with their fingers again. There are various ways of performing fine motor skills trainings. One way in performing fine motor skills rehabilitation is to attend occupational therapy sessions by performing hand and finger exercises like ball grip, pinching objects, gripping and grasping objects, opposition exercises and more to improve on pinch force and grip strength (Enabnit and Warren, 2023). During occupational therapy sessions, daily activities involving fine motor skills such as grooming, feeding and getting dressed are practiced. Furthermore, home exercise programs are developed by the occupational therapist using household items to allow participants to practice fine motor skills training independently at their homes. Occupational therapy differs from physiotherapy where occupational therapy focuses on fine motor skills enhancement and regaining them back, whereas physiotherapy focuses on gross motor skills to enhancement and regaining them back (Shea, 2021).

However, occupational therapy has some limitations such as high costs, time commitment and varying effectiveness for individuals (Painscale, n.d.). An alternative way is to use assistive devices designed to assist in fine motor training, which can be beneficial over occupational therapy as it offers precise support tailored to suit the user's individual fine motor skill training requirements unlike occupational therapy where it covers too wide range of fine

motor skills. Besides that, these assistive devices can provide instant assistance unlike occupational therapy which require gradual skill development to be carried out properly. Furthermore, using these assistive devices ensures consistent performance in practicing repetitive tasks unlike doing occupational therapy during fine motor skills training (Akyurek, et al., 2017). These assistive devices can help people with fine motor disabilities to improve and regain their dexterity, coordination and hand muscle strength, for activities requiring precise movements. Examples of assistive devices and aiding tools designed for fine motor skills training are adaptive utensils, pencil grips and writing aids, button hooks, and zipper pulls, adaptive scissors, video gaming tools, adaptive computer accessories, exoskeletons and more (Denslow, 2023). Advancements of technology can further enhance assistive devices to help individuals to perform fine motor trainings more effectively and easily. Examples of these technologies are specialised touchscreen apps, devices with brain-computer interfaces, virtual reality systems, speech-to-text software, gesture recognition technology, electrical simulation, robotics and more (Cowan, et al., 2012).

This study involves the design and development of an active assistive hand orthosis (AHO), actuated by servo motors, to actuate specific and precise finger movements such as flexion and extension for the 4 fingers (index, middle, ring and small fingers) and thumb, and grasping. It contains sensors such as inertial measurement units (IMUs) to provide accurate biomechanical data such as the finger range of motion (ROM) and grip strength, and to perform assessments on fine motor training progress and the performance of the device. This wearable active AHO also integrates with an Internet of Things (IoT) platform and facilitated with a simple and user-friendly interface that the enhances effectiveness of fine motor training by allowing therapists to monitor the patient's rehabilitation progress remotely and allowing therapist/patients to control it anywhere with ease. These two aspects are crucial for providing real-time feedback and data on the patient's progress, which helps in tailoring rehabilitation programs, in particular in a home-based setting.

1.2 Importance of the Study

The assistive hand orthosis can provide repeatable finger flexion and extension movements so that individuals with fine motor disabilities can use it to further

enhance their fine motor skills training. Besides that, assistive hand orthosis is equipped with sensors that can provide precise and accurate biomechanical data to assess on the fine motor training progress. Moreover, the assistive hand orthosis is integrated to a user-friendly IoT platform, allowing the patients and therapists to control the device with ease, and allowing the data from its sensors to be collected remotely, so that therapists can monitor patients' progression and provide targeted and customizable assistance to the patients based on the patients' rehabilitation needs.

1.3 Problem Statement

People who experienced stroke, hand or finger bone fracture, hand muscles damage, brain injury and more often experience fine motor impairments in their fingers, impacting activities of daily living and overall hand functionality. Current rehabilitation methods for finger motor training may lack the precision and adaptability needed for addressing unique needs, and qualitatively track and evaluate the performance of individual patient for fine motor skills training (Basteris et al., 2014). Therefore, there is a need of an active assistive orthosis, that can measure biomechanical assessments accurately and precisely, so that therapists can use these data to provide targeted and customizable assistance during their fine motor skills training. Moreover, there are a lack of assistive devices that has an IoT user interface that allows it to be controlled with ease and allow remote control and sensor data visualisation (Maciejasz et al., 2014).

1.4 Aim and Objectives

The aim of this study is to develop an assistive hand orthosis integrated with accurate sensors and have an IoT user interface that helps individuals with fine motor impairments to undergo more effective fine motor skills trainings and improve in fine motor skills' effectiveness, and to have remote control and sensor data visualisation.

Objectives of this study:

1. To analyse the current development in hand orthosis and commercial hand rehabilitation technology.

2. To develop a cost-effective, portable, lightweight and IoT-connected assistive hand orthosis with sensors that can measure biomechanical assessments accurately.
3. To conduct performance assessments on this assistive hand orthosis.

1.5 Scope and Limitation of the Study

The scope of this study is to develop an assistive hand orthosis for actuating finger flexion and extension, thumb flexion and extension, and finger grasping movements only. Besides that, the prototype developed in this study is only suitable for the right hand and not on the left hand. Moreover, the servo motors were used as actuator force to drive the prototype. In addition, biomechanical parameters of interest in this study are finger ROM and grip strength of right index finger and thumb. Furthermore, the sensors on this prototype were only placed at the index finger and thumb because the movement of the index, middle, ring and small finger are all moved together for the prototype so their ROMs are very similar.

One of the limitations of this study is that it is unable to assist in other fingers like finger opposition, adduction and abduction. Another limitation of this study is that individuals with extremely big or extremely small hands may not be able to wear and use this prototype effectively. The third limitation of this study is that this prototype must be connected to a Wi-Fi network in order to be able to control it remotely and visualise the data collected by the sensors via its IoT user interface.

1.6 Contribution of the Study

The assistive hand orthosis (AHO) designed and developed in this study aims to assist individuals with fine motor impairments in performing repeatable specific finger movements such as 4 fingers flexion/extension, thumb flexion/extension and grasping so that they could practice these movement and eventually regain their finger mobility to perform ADL again.

In addition, the AHO is designed to be lightweight so that it can be easily carried around and be used anywhere when needed. Besides that, this AHO is cost-effective so that it is affordable for patients or therapists. The AHO

is adjustable so that it allows users with various hand sizes, wrist sizes and finger diameters to wear this AHO.

Moreover, this AHO is also integrated with the Blynk IoT platform, which allows remote monitoring of sensor readings so that the physiotherapists can monitor the progression of the patient's fine motor trainings anytime and anywhere with ease. This allows the therapist to supervise the patients' rehabilitation progression more conveniently and flexibly. It has a user-friendly IoT interface on the Blynk IoT mobile app that allows patients to control this device easily without the therapists' assistance.

1.7 Outline of the Report

Chapter 1 of this report is about the background information on this study and stating the problems on current assistive hand orthoses developed as well as the aims, objectives, scope, limitations and the contributions of this study. Chapter 2 reviews on the types of actuators used in previously developed assistive hand orthoses, typical sensors, devices and sensors used to collect biomechanical parameters, the pros and cons on previously developed assistive hand orthoses, and the comparisons between previously developed assistive hand orthoses in several aspects. Chapter 3 illustrates on the prototype's requirements, development process, system architecture, mechanical design conceptualisation, materials and components selections, circuit designs, IoT system. Chapter 3 of this report also delves into the biomechanical parameters to be collected on the prototype, the IMU calibration method, libraries used to program the prototype's components and IoT system, and the experimental protocols on the performance assessments to be carried out on the prototype with the methods on the analysis of the data collected from these tests. Chapter 4 discusses on the final prototype mechanical design, types of finger movements that can be actuated by the prototype, the prototype's IoT user interface design, the prototype's mechanical design changes and enhancements, code used to program the components and IoT system, and the results of performance assessments done on the prototype. Chapter 5 of this report discusses on the conclusions, limitations and future works of this study.

CHAPTER 2

LITERATURE REVIEW

2.1 Introduction

This chapter delves into key information needed to know in order to design and develop an effective, safe and functional active assistive hand orthosis. Firstly, it covers on the various actuators that can be used to drive assistive hand orthoses, and the pros and cons of each of these types of actuators. Secondly, it discusses on the various sensors, devices or software that can be used to measure and collect biomechanical parameters to assess the performance of assistive hand orthoses. Thirdly, it explores on the pros and cons of the previously developed assistive hand orthoses to learn the positives and shortcomings of these assistive hand orthoses before designing and developing one. Lastly, it provides insights on the previously developed assistive hand orthoses and they were compared in terms of actuators and microcontroller used, the types of muscle movements they were involved in, the biomechanical parameters they had collected, and the sensors, devices or software used to collect these biomechanical parameters. Hence, these give us a better understanding on how to design and develop an active assistive hand orthosis.

2.2 Types of Actuators

In this section, the different types of actuators used to drive developed assistive hand orthoses such as electrical motors, pneumatic actuators, cable-driven systems, shape memory alloys and hydraulic actuators are discussed and compared.

2.2.1 Electrical Motors

Servo motors are a type of electrical motor that can be used to drive an assistive hand orthosis. An assistive hand orthosis called NOHAS developed by Mercyshalinie and co-workers (Mercyshalinie, et al., 2023), and a 3D-Printed Hand Exoskeleton Based on Force-Myography Control developed by Esposito and co-workers (Esposito, et al., 2022), are examples of assistive hand orthoses being actuated by servo motors.

Servo motors are a type of electrical motor that converts electrical energy to mechanical energy to produce rotational torque and velocity based on the current or voltage supplied to them. They consist of a DC or AC motor to rotate the output shaft, a sensor (such as potentiometers and encoder) to measure the position, speed or torque of the output shaft, a gear assembly to adjust the revolution per minute and increase the motor's torque, and a controller that provides feedback on the motor shaft's position. A servo motor has 3 pins, one is the Vcc pin (the red wire) for current and voltage supply, ground pin (the brown wire) to ground for connection grounding and control pin (the orange wire) for motor control. The servo motor is controlled using Pulse with Modulation (PWM) signals, where input electrical pulses from the microcontroller are sent to the control wire. These pulses should occur every 20 ms, with the electrical pulse width determining the degree of rotation of the shaft. For example, when the width of the pulse increases by 0.5 ms, the servo motor's shaft rotates clockwise by 90 degrees. Servo motors can usually rotate between 0 to 180 degrees. This is how servo motors are controlled (Apoorve, 2015).

Based on research, servo motors are highly used as actuators for developed assistive hand orthosis. There are several reasons for this. Firstly, due to servo motors employ PWM control, this allows them to be controlled precisely which is ideal for actuating assistive hand orthoses that assist in fine motor skills that requires highly precise movements. Another reason is because they are small and lightweight, with a weight of 55 grams only (Cytron Technologies, n.d.b), so it minimizes the added weight to the assistive hand orthoses and this which easier actuation compared to other heavier electrical motors as lesser force is required for actuation. Its small size also makes them easy to attach to assistive hand orthoses, enhancing their suitability for actuating assistive hand orthosis (Heason, 2020).

Linear motors, as shown in Figure 2.1, are also a type of electrical motor that can be used to actuate assistive hand orthoses. Examples of developed assistive hand orthoses that uses linear motors to drive them are an underactuated finger exoskeleton (Li et al., 2021), and Assistive Robotic Hand Orthosis (ARHO) (Farinha, et al., 2019).

Linear motors are a type of electrical motor that produces linear motion by generating linear force along their length. They consist of a stator that

generates a magnetic field, and a slider with a coil that moves along its field, so when there are alternating current directions flowing through the coil, this allows the slider to move back and forth along the stator. The speed of linear motors' movement can be controlled by the magnitude of the current flow through the coils (Electricity-Magnetism, n.d.b). Based on research, linear motors are also commonly used as an actuator for developed assistive hand orthoses. This is due to their ability to provide precise motion control, making them suitable in actuating assistive hand orthoses that assists in fine motor skills requiring highly precise movements (Electricity-Magnetism, n.d.b).



Figure 2.1: A Linear Motor.

In another report, an extra robotic thumb and exoskeleton robotic fingers (Ismail, et al., 2017), uses both linear motors and servo motors to actuate it. The linear motors on this device, actuates the linear motion of the four fingers of the exoskeleton and the servo motors on it actuates the rotative motion of its extra robotic thumb (Ismail, et al., 2017).

2.2.2 Pneumactical Actuators

A soft exoskeletal glove utilised pneumatic artificial muscles (PAMs), which is a type of pneumatic actuator, to drive their assistive hand orthosis (Skaramagkas, Andrikopoulos and Manesis, 2020).

Pneumatic artificial muscles, also known as McKibben air muscles, as shown in Figure 2.2, consist of an inflatable inner bladder made with materials such as latex rubber, silicone rubber and more, enclosed in a braided mesh with clamps at each end. The inflatable inner bladder has to be thin for it to be more efficient as it requires less energy to stretch it, but excessive thinness of it can

cause it to be easily damaged during PAM contraction. The PAM's braided mesh helps to convert radial expansion into linear contraction, while the end clamps hold the whole PAM together so that the mesh and the inner bladder would not slip during PAM contraction and relaxation and provides attachment points to attach the PAMs. A standard McKibben air muscle can contract linearly to approximately 25 percent, which is around 75 percent of its relaxed length (Soft Robotics Toolkit, n.d.).

The change in the PAMs' size, bladder stiffness and more can affect the performance of the PAM in its force exertion. Larger PAMs with greater diameters generate larger forces but requires more air, while increasing its original length can raise the contraction limit. Based on isometric testing of the PAMs, the force-pressure relationship of the PAMs is unaffected by its stiffness, with stiffer PAMs taking a longer time to reach a certain force. Plus, at the same air pressure, the less stiff PAMs can achieve higher contraction amounts and exert greater contraction force (Soft Robotics ToolKit, n.d.).



Figure 2.2: A McKibben Air Muscle.

PneuNets Bending Actuators are also a type of pneumatic actuator that can be used to drive assistive hand orthosis. A wrist rehabilitation exoskeleton (Fahaam, Davis and Meziani, 2016), and the ExoGlove (Yap, et al., 2015), are examples of developed assistive hand orthoses that are actuated by PneuNets bending actuators.

PneuNets bending actuators are soft actuators developed by a research group at Harvard University. It consists of a series of channels and chambers

inside a single and homogenous elastomer, typically made with materials such as latex rubber, silicone rubber and more, similar to those used in McKibben air muscles. When PneuNets bending actuators are pressurised, they inflate, which generates motion, with expansion happens in the least stiff areas of it and mainly on its thinnest structures. Designers can control their behaviour by adjusting the geometry of the embedded chambers, material properties of chamber walls and wall thicknesses to achieve the desired motion types (Soft Robotics Kit, n.d.).

Based on research, pneumatic artificial muscles and PneuNets bending actuator are more commonly used to actuate assistive hand orthoses compared to pneumatic cylinders. This is due to PAMs and PneuNets actuator having much lighter weight and smaller size than pneumatic cylinder, with the PAM having a weight of 27 g per meter (Baiju, 2022), compared to a pneumatic cylinder which has a weight of 647 g per meter (RS Malaysia, n.d.), and this makes them easier to incorporate into devices without adding extra weight or requiring excessive contraction force. Moreover, PAMs and PneuNets actuators provide smoother operation compared to pneumatic cylinders because they lack sliding parts such as pistons (Baiju, 2022). However, PAMs and PneuNets bending actuators are more susceptible to being damaged especially when PAMs' inner bladder and PneuNets' elastomer material are too thin, unlike pneumatic cylinders, which are more robust (Soft Robotics ToolKit, n.d.).

2.2.3 Cable-Driven Systems

Cable-Driven systems use cables to transmit forces from other types of actuators such as linear motors, servo motors and more. Examples of developed assistive hand orthosis that were driven by cable-driven systems are a hand exoskeleton (Nycz, et al., 2016), and an electrooculogram-activated Wearable Soft Hand Exoskeleton (Shahid, et al., 2021).

For the hand exoskeleton developed by Nycz and co-workers, they used Bowden cables driven by the linear motors to actuate it. They chose to use Bowden cables for its actuation because of its cheap components, ease of construction and ease of compatibility with the linear motors. The push-pull Bowden cable transmission with linear motors as the actuator for the hand exoskeleton allows it to exert both tensile and compressive forces that allow finger flexion and extension.

For the electrooculogram-activated Wearable Soft Hand Exoskeleton developed by Shahid and co-workers, they utilise a cable-pulley mechanism actuated by 2 servo motors. The cables are used to transmit the power of the servo motors to the fingers to drive finger flexion and extension. One servo motor is used to drive the pulley for finger flexion, while other one is used to drive the pulley for finger extension. In the soft hand exoskeleton developed by Shahid, et al., 2021, the cables are routed around the glove, and the pulley was 3D printed with polylactic (PLA) material which is fixed at the end of the motor shaft.

2.2.4 Shape Memory Alloys

Shape memory alloys (SMA) are a type of actuator that can be used to actuate assistive hand orthoses. An example of assistive hand orthosis that uses SMA to actuate it is a SMA based wrist exoskeleton developed by Serrano, et al., 2018. The SMAs in the SMA based wrist exoskeleton developed by Serrano, et al., 2018 are used to actuate it to perform wrist extension, wrist radial deviation and wrist ulnar deviation movements.

SMA is a metallic alloy known for its shape memory effect it can recover to its original shape after it has been deformed when heated beyond the transformation temperature, which is between a low and high temperature phase, this transformation is known as the reversible phase transformation. The geometrical change during this transformation allows the SMA to perform mechanical work, causing it to exert force. During heating, it causes the SMA to return to its original shape, while cooling induces deformation which transitions the SMA to a low-temperature phase. This allows force, motion and displacement of the SMA, to be precisely controlled by controlling the temperature applied to it. The SMA has several advantages such as having high force to weight ratios and low energy consumption during phase transitions, and having precise force control, which makes it suitable to be used as an actuator for assistive hand orthoses. The SMA alloy used in the SMA based wrist exoskeleton developed by Serrano, et al., 2018, is Nitinol (Motzki and Rizzello, 2023).

2.2.5 Hydraulic Actuators

Hydraulic cylinder is a type of hydraulic actuator that converts hydraulic energy into mechanical energy to provide linear motion. Its key components include a piston dividing the cylinder into two chambers, a rod transmitting force to the external load, seals to prevent fluid leakage and maintain pressure in the cylinder, ports connected to hydraulic valves controlling fluid flow, and a hydraulic pump. For the hydraulic cylinder to work, the hydraulic fluid pressurised from the pump enters the cylinder, pushing the piston to generate linear force, which is then transmitted to the external load by the piston rod (IQS Directory, n.d.).

Based on research, recent developments of assistive hand orthoses do not use hydraulic actuation for several reasons. Firstly, hydraulic actuators have limited motion control capabilities, particularly for assistive hand orthoses, as they require many stops and changes in velocity. Another reason is because basic hydraulic actuators lack programmability, leading to imprecision in manual adjustments of force and velocity, while servo-hydraulic actuation systems can be programmed but they require a lot of components that add complexity, space requirements and costs. In addition, hydraulic actuators are less energy efficient compared to electrical actuation as they require continuous energy input to operate the hydraulic pump and the pressure in the system has to be maintained. Moreover, hydraulic actuators include hydraulic pumps, hydraulic fluids and more, that adds significant weight to devices, and this restricts its mobility (Tolomatic, 2016). These factors contribute to why recent developments of assistive hand orthoses do not use hydraulic actuation.

2.3 Typical Sensors and Devices Used to Collect Biomechanical Parameters

This section discusses the typical sensors and devices used to measure and collect the data of various biomechanical parameters to assess the performance of assistive hand orthoses.

2.3.1 Sensors, Motion Capture Systems and Software used to Measure Joint ROM and Joint Kinematics

Inertial measurement units (IMUs), potentiometers, flex sensor, Hall-effect sensors and more are the sensors that can be used to measure joint range of motion (ROM). Motion capture systems can also be used to measure joint ROM. IMUs and motion capture systems can be used to measure joint kinematics like joint angular velocity and acceleration.

An IMU is a sensor that can be used to obtain a joint ROM and joint kinematics. It is made up of 3 components, gyroscope, accelerometer and magnetometer. Gyroscope measures the angular velocity or rotational rate along one or more axes. Accelerometer detects linear acceleration along one or more axes by detecting changes in velocity, and magnetometer measures the strength and direction of the Earth's magnetic field which can be used to determine the IMU's orientation relative to the Earth's magnetic field, this provides a reference for orientation (Vectornav Technologies, n.d.). The Exofinger, a finger exoskeleton developed by Ceccarelli and Cruz, 2021, uses IMU to measure the angle displacements, angular velocities, and linear acceleration at the metacarpophalangeal (MCP) and DIP (distal interphalangeal) joints on the fingers.

Potentiometers are a device that can be used to obtain a joint ROM. Potentiometers consists of a circular track with a wiper attached to a central shaft. When the shaft rotates, the resistance between its fixed terminal and wiper changes. As a result, the output voltage across the potentiometer changes. This voltage change is proportional to the shaft rotational angle (Positek, n.d.). By performing calibration of the potentiometer, it involves correlating various output voltages with the corresponding shaft rotational angles. This calibration process allows the joint ROM to be determined (Othman, et al., 2017). Examples of assistive hand orthoses that uses potentiometers to obtain joint angle/ROM and position of the thumb is an extra robotic thumb and exoskeleton robotic fingers developed by Ismail, et al., 2017 and an SMA based wrist exoskeleton developed by Serrano, et al., 2018.

Flex sensors can also be used to obtain a joint ROM. Flex sensors function as variable resistors with its resistance altering when flexed. The degree of bending of flex sensors directly correlates with the change in resistance across

the flex sensor. By measuring the change in resistance across the flex sensor using an ohmmeter, the bending degree can be determined, and this makes it useful for angle measurement and movement detection (Butt, n.d.). An electrooculogram-activated wearable soft hand exoskeleton developed by Shahid, et al., 2021 uses flex sensor to obtain the MCP joint angle. Hall-effect sensors are also another type of sensor that can be used to obtain a joint ROM. The Hall-effect sensors rely on the change in voltage induced by change in magnetic field to determine angular position. Hall-effect sensors consist of a magnet, Hall element and rotating axis. Hall-effect sensors detect shift in angular position by monitoring the changes in the magnetic field and the output voltage changes accordingly. Through calibration on the Hall-effect sensors, it establishes the correlation between the angle changes and voltage shifts, this allows joint ROM to be obtained (Positek, n.d.). An underactuated finger exoskeleton developed by Li et al., 2021 uses Hall-effect sensors to obtain the joint ROM on it.

Motion capture systems can be also used to obtain the joint ROM and joint kinematics. In these motion capture systems, it typically uses reflective markers being placed at the joints, and there are multiple cameras capturing the markers' movement in 3-dimensional space so the motion capture system can track the movement and orientation of the body segments relative to each other. The motion capture system will then analyse the markers' position data and calculate the angles between the segments and joint kinematics using techniques such as inverse kinematics or rigid body transformation (Motion Analysis, 2023). Examples of assistive hand orthoses that uses motion capture systems to obtain joint ROM and joint kinematics are the ExoGlove developed by Yap, et al., 2015, and hand exoskeleton developed by Nycz, et al., 2016. Based on research, motion capture systems are not frequently used to obtain joint ROM and joint kinematics on assistive hand orthoses. This is because it is very costly to set up as it requires a combination of software and equipment like high-resolution cameras and there are way cheaper alternatives to obtain joint ROM and joint kinematics, although it can provide high precision and accuracy of joint ROM and joint kinematics (Meta Motion, n.d.).

There is also software such as Matlab and Kinovea that can be used to obtain joint ROM and joint kinematics. Matlab is a simulation software that can be used to obtain joint ROM and joint kinematics by using a combination of mathematical equations (Yuan, et al., 2023). An exoskeleton finger rehabilitation training robot developed by Yuan, et al., 2023 uses the Matlab simulation software to obtain the change in angle, angular displacement, angular velocity and angular acceleration of the finger joints. The Kinovea software has tools that can measure the joint ROM and joint kinematics. The 3D-Printed Hand Exoskeleton Based on Force-Myography Control developed by Esposito, et al., 2022 uses Kinovea software to compute the trajectories of each phalanx of index finger and time required by the exoskeleton for closing and opening of the hand.

2.3.2 Sensors and Devices Used to Measure Forces Exerted by Fingers

Force sensitive resistors, dynamometer, load cells and more are sensors and devices that can be used to measure the forces exerted by the fingers and the arm while using assistive hand orthoses. Dynamometer is a device that can be used to measure forces exerted by the fingers. It works by squeezing it and the force on the finger tips is applied on it, and its digital screen shows the value of the force exerted by the fingers on the dynamometer (Basaraba, 2024). An underactuated finger exoskeleton developed by uses a dynamometer developed by Li et al., 2021 uses a dynamometer to measure the maximum finger-tip force.

Force sensitive resistors (FSRs) can be used to measure the force exerted by the finger when using assistive hand orthoses. Force sensitive resistors work by changing its resistance when a force or pressure is applied on them (Electricity-Magnetism, n.d.a). Examples of assistive hand orthoses that uses FSRs to measure force exerted on the fingers are the ExoGlove developed by Yap, et al., 2015, the Novel Orthotic Hand Actuated by Servo Motors (NOHAS) exoskeleton developed by Mercyshalinie, et al., 2023 and a soft exoskeleton glove developed by Skaramagkas, Andrikopoulos and Manesis., 2020. Based on research, FSRs are commonly used in measuring the force exerted by the fingers. The reasons are because FSRs are much cheaper than dynamometers, FSRs are simpler to use compared to load cells, and they are thin and flexible which makes them easy to be integrated into assistive hand

orthoses, even though it has lower precision, limited force detection range, prone to damage and can exhibit drift over time (Electricity-Magnetism, n.d.a).

Load cells can also be used to measure force exerted by fingers. Load cells are force transducers that convert applied force into electrical signals. Load cells work based on the piezo-resistivity principle, the resistance changes with the applied force and this changes the output voltage. By calibrating the load cell, it establishes the relationship between electrical output signal from the load cell and the force exerted on it, which can accurately obtain the force exerted by the fingers (Park, et al., 2020). A 3D-printed hand exoskeleton based on force-myography control developed by Esposito, et al., 2022, uses a load cell attached to a rigid cylindrical handlebar to measure the grip strength while using this device.

2.3.3 Use of Electromyography (EMG) sensors with EMG Electrodes

Electromyography (EMG) sensors with EMG electrodes can be used to capture muscle activities during finger or arm movements facilitated by the assistive hand. EMG sensors with EMG electrodes consists of surface electrodes placed on skin over targeted muscle areas and these electrodes can detect the electrical signals generated by muscle fibres during the contraction and relaxation of these muscles. The EMG signals are then amplified, processed and filtered, and can be visualised on a software for analysis of muscle activity (Harrison, 2023). Examples of assistive hand orthoses that uses EMG sensors with EMG electrodes to measure the arm or finger muscle activities while using these devices are assistive robotic hand orthosis developed by Farinha, et al., 2019, extra robotic thumb and exoskeleton robotic fingers developed by Ismail, et al., 2017 and the ExoFinger developed by Ceccarelli and Cruz, 2021



Figure 2.3: EMG Board with Electrodes.

2.4 Pros and Cons on Previously Developed Assistive Hand Orthoses

There were various different kinds of previously developed assistive hand orthoses which were actuated by different types of actuators for different objectives, and they all focus on assisting the user in specific movements on the wrist or fingers. They all also used different types of microcontrollers and control systems for controlling the actuators and processing data from the sensors. Each of them carried out different biomechanical assessments on the users. In this section, the pros and cons on the previously developed assistive hand orthoses will be analysed and discussed on.

2.4.1 Electrically Actuated Assistive Hand Orthoses

An underactuated finger exoskeleton developed by Li et al. (2021), is an electrically actuated assistive hand orthosis aimed to assist elderly with weak muscle strength on grasping tasks. An advantage of this device is that it is lightweight and portable as it has an overall weight of only 476 g, so this allows the user to use this exoskeleton to assist in ADL. Another advantage of this device is that it can carry out many biomechanical assessments such as man-robot interaction forces, finger joint angles, without the need of an external device to assess the performance of this device as it has force sensor, dc motor encoder and Hall-effect sensor with magnets embedded to it. Another advantage of this device is that it can achieve finger reshaping and can adapt to the object's shape and size while grasping using this device, according to this study, it mentioned that it is the first exoskeleton developed to achieve it. A disadvantage

of this device is that it requires an external device such as the dynamometer to measure the maximum fingertip force (Li et al., 2021).

A Novel Orthotic Hand Actuated by Servo Motors (NOHAS) developed by Mercyshalinie et al. (2023), is an electrically actuated assistive hand orthosis aimed to assist in stroke rehabilitation. An advantage of this device is that it is portable and lightweight, as it weighs less than 500 g, so it can be carried around and used anytime and anywhere. Another advantage of this device is that its glove has Velcro straps which allows the glove of this device to be adjusted according to the user's hand and finger size, so this makes it comfortable for the user to wear it. Moreover, another advantage of this device is that it can connect to an Internet of Things (IoT) app called Blynk, that allows the user to control the device remotely, not a lot of assistive hand orthoses can do so. A disadvantage of this device is that the servo motors on this device produces sharp noises by its gear vibrations that has a noise level of approximately 40 dB, and this can cause discomfort to the user (Mercyshalinie, et al., 2023). Another disadvantage of this device is that it relies on video tracking software, external to this device, to obtain the bending angles of each finger joint, which can be inaccurate and imprecise as the angle of the camera, and the lack of quality and clarity of the footage can also affect the data accuracy obtained from this software (Gutierrez and Biswas, 2023).

A 3D-printed hand exoskeleton based on force-myography (FMG) control developed by Esposito et al. (2022), is an electrically actuated assistive hand orthosis that use an FMG to control it and its aim is to provide assistance and motor rehabilitation for stroke survivors who have impaired voluntary hand movements. An advantage of this device is that it has Velcro straps that allows this device to be adjustable according to the user's finger shape so the user will feel comfortable when wearing it. Another advantage of this device is that its frame on its fingers, wrist and arm are 3D printed with polylactic acid (PLA), so this makes it lightweight and portable, which makes it easy for the user to carry it around. A disadvantage of this device is that it relies on a video tracking software, external to this device, to compute the trajectories each phalanx of index finger and time required by the exoskeleton for closing and opening of the hand. This can lead to data inaccuracy and imprecision due to camera angle, and footage quality and clarity concerns (Gutierrez and Biswas, 2023). Another

disadvantage of this device is that the forearm and finger muscles electrical activity, and the finger joints ROM cannot be measured without the use of external devices, software or motion capture system. The third disadvantage of this device is that the thumb support of this device can only be fixed in adduction or abduction position, and the four fingers and thumb of this device cannot be moved together, so more actuators are needed which increases the complexity of the mechanics and controller of this device (Esposito, et al., 2022).

An Assistive Robotic Hand Orthosis (ARHO) developed by Farinha et al. (2019), is an electrically actuated assistive hand orthosis controlled with muscle electrical activity in the forearm for object grasping. An advantage of this device is that it has Velcro straps which makes it adjustable according to the user's finger shape, so this makes it comfortable for users while wearing it. Another advantage of this device is that its frame on its fingers, wrist and arm is 3D printed with PLA, so this makes it lightweight and easy to carry around. A disadvantage of this device is that it can only measure one biomechanical assessment, which is the muscular activity in the forearm, to assess the performance of this device as it only has sEMG sensors as the only type of sensor embedded to this device (Farinha, et al., 2019).

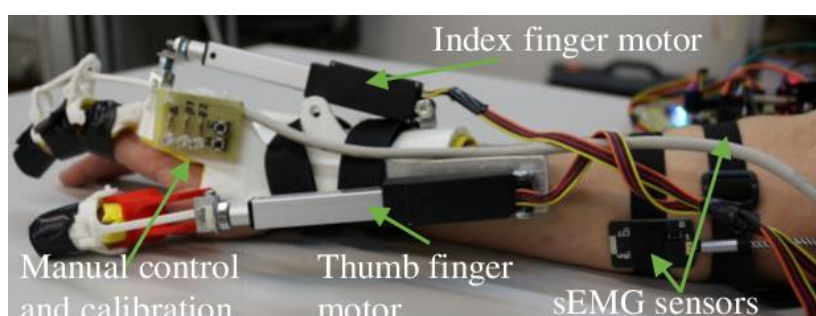


Figure 2.4: An Assistive Robotic Hand Orthosis (Farinha, et al., 2019).

Reprinted with permission from Copyright 2019 IEEE.

A disadvantage of electrically actuated assistive hand orthoses is that they pose a risk of electric shocks as they are powered by electrical power sources, so they require safety features such as emergency stop buttons to stop the operation of the device in case of emergencies.

2.4.2 Pneumatically Actuated Assistive Hand Orthoses

The ExoGlove developed by Yap et al. (2015), is a pneumatically actuated assistive hand orthosis for assistance in hand motions and hand rehabilitation. An advantage of this device is that it is lightweight and easy to wear because it is actuated by soft pneumatic actuators, which are much lighter compared to hydraulic cylinders and electrical motors, and it consists of a glove that can be worn easily and it has very few components, which makes it light. Another advantage of this device is that at different localities of this device, the stiffness of the soft pneumatic actuators can be changed, which allows it to be customised for different hand sizes and this allows different hand therapy exercise to be conducted while using this device. A disadvantage of this device is that it uses gloves which could be difficult for people with deformed fingers due to the post-effects of stroke and more, to wear it comfortably and fit it properly. Another disadvantage of this device is that there is no emergency stop button which makes it dangerous to use if the pressure regulator connected to pneumatic air source fails. This is because it could cause explosion and failure of the soft actuators of this device (Yap, et al., 2015).

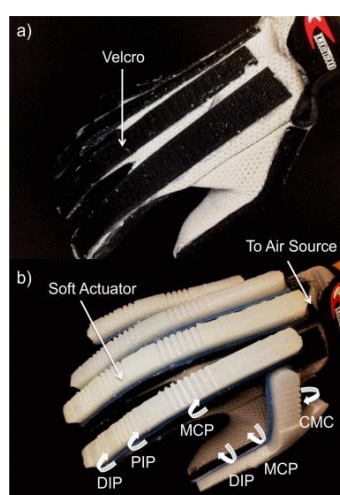


Figure 2.5: The ExoGlove (Yap, et al., 2015). Reprinted with permission from Copyright 2015 IEEE.

A wrist rehabilitation exoskeleton developed by Fahaam, Davis and Meziani (2016), is a pneumatically actuated assistive hand orthosis for wrist joint rehabilitation. An advantage of this device is that it has a lightweight design with a weight of only 150 g, due to it having very few components. Plus,

it uses soft pneumatic soft actuators, which are lightweight compared to electrical motors and hydraulic cylinders. Besides that, it involves the use of a glove that makes it easy to wear. Moreover, this device is made up low-cost materials, which makes it affordable. Another advantage of this device is that it can provide universal fit because it is made up of stretchy materials. A disadvantage of this device is that there are no sensors embedded to it to carry out biomechanical assessments to assess the performance of the device. (Fahaam, Davis and Meziani, 2016).

A soft exoskeletal glove developed by Skaramagkas, Andrikopoulos and Manesis (2020), is a pneumatically actuated assistive hand orthosis with the purpose of Reducing hand tremors in patients with essential tremor condition. An advantage of this device is that it is lightweight as it consists of lightweight components such as McKibben air muscles and a soft glove. Another advantage of this device is that it can conduct many biomechanical assessments such as exerted resistive force on index finger and metacarpal, and the acceleration of the distal phalanges of the index and thumb, along with the metacarpal and forearm regions, to assess the performance of this device without the need of an external device. A disadvantage of this device is that there is no emergency stop button if the pressure regulator connected to the pneumatic air source fails, which can cause danger to the user as the McKibben air muscles will fail and may explode.

A disadvantage of these two developed pneumatically actuated assistive hand orthoses is that they require a tube connection to a pneumatic air compressor to supply air to the PAMs and PneuNets bending actuators, so this makes them not portable.

2.4.3 Cable-Actuated Assistive Hand Orthosis

An electrooculogram-activated wearable soft hand exoskeleton developed by Shahid et al. (2021), is a cable-actuated assistive hand orthosis that can be controlled by eye electrical signals to assist patients with hand paralysis to improve their quality of life. An advantage of this device is that it is lightweight weighing only 110g as it consists of a lightweight PLA 3D printed pulley, fabric glove, lightweight cables and lightweight servo motors. A disadvantage of this device is that this device cannot assist in abduction and adduction movements.

Another disadvantage of this device is that it can only conduct one biomechanical assessment, which is the MCP joint angle due to the fact that it is only embedded with a flex sensor at the MCP joint.

2.4.4 Shape Memory Alloy-Actuated Assistive Hand Orthosis

A SMA based wrist exoskeleton developed by Serrano et al. (2018), is a shape memory alloy actuated assistive hand orthosis for rehabilitation therapy. An advantage of this device is that it is very lightweight, and it is noiseless while it is used. This is because the shape memory alloys used to drive this device are small sized, lightweight and do not generate noise. Another advantage of this device is that it is symmetrical which means it can be used for both left and right wrist by changing the glove to the hand. A disadvantage of this device is that it can only conduct one biomechanical assessment which is the position of wrist exoskeleton during flexion-extension and radial-ulnar deviation as it only has potentiometers embedded to it (Serrano, et al., 2018).

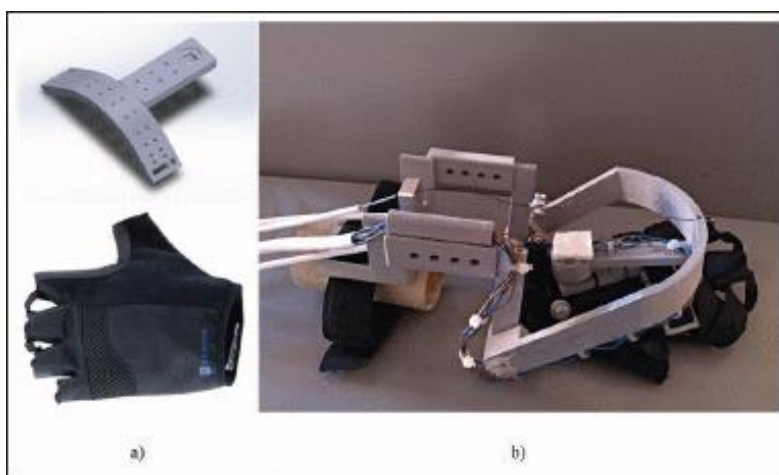


Figure 2.6: A SMA Based Wrist Exoskeleton (Serrano, et al., 2018). Reprinted with permission from Copyright 2018 IEEE.

Table 2.1: Comparison of Developed Assistive Hand Orthoses.

Assistive Hand Orthosis Name	Actuator	Microcontroller	Sensors/Software/Devices	Movements Involved	Biomechanical Parameters	Reference
<i>ExoGlove</i>	PneuNets bending actuators	Arduino Mega microcontroller	Motion Capture System, Flexible force sensitive resistors	Finger extension and flexion	Range of Motion and maximum force output for hand grasping and pinching	Yap et al. (2015)
<i>Underactuated Finger Exoskeleton</i>	Linear motor	Microcontroller, model not specified	Force sensor, Dynamometer Hall-effect sensor with, magnets , Dc motor encoder	Finger extension and flexion	Man-robot interaction forces, maximum finger-tip force, passive back driveability force, finger joints angle	Li et al. (2021)
<i>Wrist Rehabilitation Exoskeleton</i>	PneuNets bending actuators	Arduino Mega microcontroller	Pressure sensor	Wrist extension/flexion, wrist radial /ulnar deviation	None	Fahaam, Davis and Meziani (2016)
<i>NOHAS</i>	Servo motor	ESP8266 microcontroller	Video tracker software, force-sensing resistors	Finger extension and flexion	Bending angles of each finger joint, force output	Mercyshalinie et al. (2023)
<i>Exoskeleton Finger Rehabilitation Training Robot</i>	Pneumatic tendon actuator	Mitsubishi PLA control system	Matlab Simulation Software	Finger extension and flexion	Change in angle, angular displacement, angular velocity and angular acceleration of the connecting rods	Yuan et al. (2023)

<i>3D-Printed Hand Exoskeleton Based on Force-Myography Control</i>	Servo motor	Arduino Uno R3 microcontroller	FSR on FMG armband, Kinovea software, Rigid cylindrical handlebar containing a single axis load cell	Finger extension and flexion	Force output on flexor carpi ulnaris and the extensor digitorum muscles, trajectories of each phalanges of index finger and time required by the exoskeleton for closing and opening of the hand, grasping force output	Esposito et al. (2022)
<i>SMA Based Wrist Exoskeleton</i>	Shape Memory Alloy	STM32F407VG microcontroller	Potentiometer	Wrist extension/flexion and wrist radial/ulnar deviation	Position of wrist exoskeleton during flexion-extension and radial-ulnar deviation	Serrano et al. (2018)
<i>Soft Exoskeletal Glove</i>	McKibben Pneumatic Artificial Muscle	National Instruments USB-6215 and Arduino Mega microcontrollers	Accelerometer, Force sensitive resistor	Finger extension and flexion	Exerted Resistive force on index finger and metacarpal, Acceleration of the distal phalanges of the index and thumb, along with metacarpal and forearm regions	Skaramagkas, Andrikopoulos and Manesis (2020)
<i>Assistive Robotic Hand Orthosis (ARHO)</i>	Linear motor	Arduino Mega 2560 microcontroller	Surface Electromyography sensor	Finger extension and flexion	Muscular activity in the forearm	Farinha et al. (2019)

<i>Hand Exoskeleton</i>	Bowden Cable driven by linear motors	Arduino Mega 2560 microcontroller	Motion capture system, Force sensor	Finger extension and flexion	Angular change in finger flexion, corresponding positional change of the exoskeleton fingertip caused by bending the Bowden cable	Nycz et al. (2016)
<i>Extra Robotic Thumb and Exoskeleton Robotic Fingers</i>	Linear motor and servo motor	Arduino Nano microcontroller	Potentiometer, Myo Armband electromyography	Finger extension/flexion, and thumb circumduction and flexion/extension	Position of stroke, muscle activity	Ismail et al. (2017)
<i>Electrooculogram-Activated Wearable Soft Hand Exoskeleton</i>	Cables driven by servo motor	Arduino Mega microcontroller	Flex sensor	Finger extension and flexion	MCP Joint angle	Shahid et al. (2021)
<i>Exofinger</i>	Servo motor	Arduino Nano and Arduino Mega microcontrollers	IMU, EMG sensors	Finger extension and flexion	Angle displacements, angular velocities, and linear acceleration on the MCP and DIP joints, Finger electrical activity	Ceccarelli and Cruz (2021)

2.5 Comparisons of Assistive Hand Orthoses

In this section, different developed assistive hand orthoses developed are compared in terms of their actuators, microcontroller/control system, types of muscle involved when using them and the biomechanical assessments done, and the sensors, software or Systems used to assess the performance of them.

2.5.1 In Terms of Actuators Used

For the developed assistive hand orthoses, different types of actuators are used to actuate them such as electrical motors, pneumatic actuators, cable-driven systems and shape memory alloys.

The underactuated finger exoskeleton developed by Li et al. (2021), the NOHAS developed by Mercyshalinie et al. (2023), the 3D-printed hand exoskeleton based on force-myography control developed by Esposito et al. (2022), and the ARHO developed by Farinha et al. (2019), are all driven by electrical motors. However, not all of them are driven by the same type of electrical motors. The underactuated finger exoskeleton and the ARHO are driven by linear motors, whereas the NOHAS and 3D-printed hand exoskeleton based on force-myography control are driven by servo motors. Besides that, the ExoGlove developed by Yap et al. (2015), the wrist rehabilitation exoskeleton developed by Fahaam, Davis and Meziani (2016), and the soft exoskeletal glove developed by Skaramagkas, Andrikopoulos and Manesis (2020), are driven by pneumatic actuators. The ExoGlove and the wrist rehabilitation exoskeleton are driven by PneuNets bending actuators, whereas the soft exoskeletal glove is driven by McKibben PAMs. Moreover, the SMA based wrist exoskeleton developed by Serrano et al. (2018), and electrooculogram-activated wearable soft hand exoskeleton developed by Shahid et al. (2021), are driven by SMA and a cable-driven system respectively, which are different types of actuators compared to the other actuators discussed here.

2.5.2 In Terms of Microcontroller Used and Types of Muscle Movements Involved

Different assistive hand orthoses use different microcontrollers. Most of the assistive hand orthoses discussed here used the Arduino Mega microcontroller to control them. This is mainly because Arduino Mega microcontroller has 54

digital input/output (I/O) pins and 16 analogue input pins (Arduino, n.d.), so this allow a lot of devices and sensors that output analogue signals can be connected to this microcontroller. Besides that, it has a larger memory and processing power compared to other microcontroller models. allowing these exoskeletons to work effectively (Arduino, n.d.). Only the NOHAS, the 3D-printed hand exoskeleton based on force-myography control, the SMA based wrist exoskeleton, and the soft exoskeletal glove use the ESP8266, Arduino Uno R3, STM32F407VG and National Instruments USB-6215 microcontroller respectively.

For the types of muscle movements involved, most of the assistive hand orthoses discussed here are involved in finger extension and flexion. Only the wrist rehabilitation exoskeleton, and the SMA based wrist exoskeleton are involved in muscle movements at the wrist joint such as wrist extension/flexion and wrist radial /ulnar deviation.

2.5.3 In Terms of Biomechanical Parameters Collected, and Sensors, Devices or Software Used to Collect Them

Different assistive hand orthoses collected different biomechanical parameters to assess the performance of them, and they used different sensors, devices or software to collect these biomechanical parameters.

Most of the assistive hand orthoses mentioned here have measured the finger ROMs/finger joint angles, and finger joint kinematics, but with different sensors, devices and software such as the motion capture system, Hall-effect sensors, video tracker software, Kinovea software, potentiometer, accelerometer, IMUs, flex sensors and more. For the forces exerted by the fingers, a few assistive hand orthoses such as the ExoGlove, the underactuated finger exoskeleton, the NOHAS, the 3D-printed hand exoskeleton based on force-myography control and the soft exoskeletal glove measured them, with the use of mainly FSRs, load cell and dynamometer. For the muscle electrical activity, only the ARHO measured it using sEMG sensors.

2.6 Summary

In the literature review on previously developed assistive hand orthoses, it was found that the recent developments of these devices were mostly actuated by

electric motors such as servo motors and linear motors. For assistive hand orthoses developed a while back, they are usually actuated by hydraulic cylinders, pneumatic actuators and cable-driven systems. Besides that, it was found that most previously developed assistive hand orthoses used the Arduino Mega microcontroller, although some of them used other microcontroller models and control systems. Moreover, it was discovered that most of the previously developed assistive hand orthoses were involved in actuating finger flexion and extension movements, and some of them were also involved in actuating movements at the wrist joint. Furthermore, it was found that most of the previously developed assistive hand orthoses collected angles at the fingers' joints, fingers' joints kinematics using sensors, systems and software such as IMUs, motion capture systems, Kinovea software, Hall-effect sensors, potentiometers, flex sensors and more to assess their performance. Lastly, it was also found that some of previously developed assistive hand orthoses have measured forces exerted on foot using sensors such as FSRs, load cell and dynamometer, and some of them collected muscles activity using EMG sensors with electrodes, to assess their performance.

CHAPTER 3

METHODOLOGY AND WORK PLAN

3.1 Introduction

This chapter outlines the technical processes and procedures employed in the design and development of an assistive hand orthosis, which includes the requirements of the prototype, the prototype development process, the prototype mechanical design conceptualisation, the prototype system architecture and the biomechanical assessments to be conducted to assess the performance of the prototype. It also discusses on the choice of materials and electrical components to be used on developing the prototype, the IMUs calibration and validation methods and the circuit design of the prototype with breadboard and stripboard. Additionally, it delves into the prototype IoT system's platform choice, architecture and program flowchart. Moreover, the libraries used to program the prototype components and IoT system, and the experimental protocols for the three tests (finger ROM test, grip strength test and objects grasping tests) to evaluate the functionality and effectiveness of the prototype in improving fine motor training outcomes are also discussed here. The methodology section provides insights into the project's technical framework and the rationale behind key decisions made throughout its execution.

3.2 Prototype Requirements

The requirements of the prototype are that it has to be lightweight, fully portable, durable, cost-effective, adjustable according to the user's finger diameter and shape to enhance comfortability to the user, able to obtain highly accurate data from the sensors and devices used and have IoT connectivity.

It is focused on being lightweight and fully portable so that it can be carried around easily and it can be used anywhere. Besides that, it has to be durable, so that it can be used for a long period of time as fine motor skills training typically takes long duration to complete (Lelong, et al., 2021), and it should be able to last until the fine motor skills training ends, which is when the patient can perform ADL again without any assistance. Moreover, it is also focused on being cost-effective as assistive hand orthoses on the market are

generally quite expensive to develop (Ison and Artemiadis, 2014). Lastly, this prototype needs to be able to connect to an IoT platform, so that it can be controlled remotely, and enabling sensor data visualisation for data analysis of sensor data, so that the therapists can monitor patients' progressions during fine motor trainings more conveniently and control the device with ease.

3.3 Prototype Development Process

Figure 3.1 shows the methodology flowchart for the development of the prototype. It started with a literature review and mechanical design conceptualization, where research and initial design ideas were formed. After this, SOLIDWORKS drawings of the first prototype were created. The first prototype was then 3D-printed and assembled and went through functionality testing to identify the shortcomings and limitations of the mechanical design. After that, necessary modifications on mechanical design were made to improve the movement of the joints on the mechanical frame. At the same time, software development for the prototype such as the program to control the rotational angle of the servo motor, enabling the two IMUs to output their angle readings and to integrate them together into a single program. Then, the Blynk IoT user interface design and its program were developed. Once the changes to its mechanical design were implemented, the final prototype was 3D-printed and assembled. Finally, the final prototype was tested to gather data and analyze its performance, ensuring that it meets the desired requirements and objectives. This iterative process ensures continuous refinement and improvement of both the mechanical design and software. The Gantt charts for part 1 and 2 of this project are shown in Figure 3.2 and 3.3.

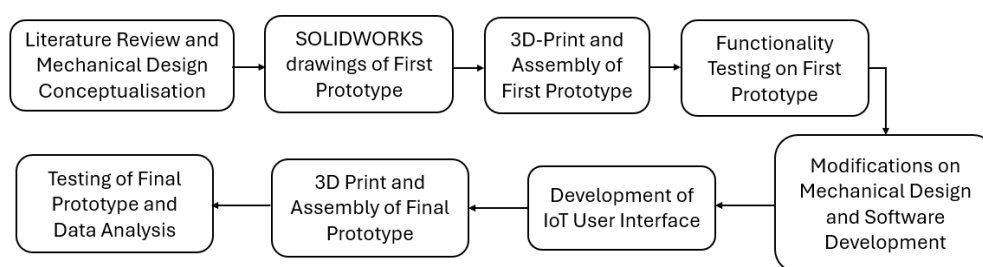


Figure 3.1: Methodology Flowchart for the Prototype Development.

Gantt Chart Part-1															
No.	Project Activities	W1	W2	W3	W4	W5	W6	W7	W8	W9	W10	W11	W12	W13	W14
M1	Background research, Problem formulation, Aim and Objectives, Scope and Limitation.	█	█	█	█										
M2	Literature review -Determine scope and relevant content		█	█	█	█	█	█	█	█					
M3	Methodology part 1 - Identify hardware, software, integration system - Design conceptualisation - Sourcing for hardware, software and integration system, and finalising them					█	█	█	█	█					
M4	Methodology part 2 - Completing mechanical design on CAD software - Assembling mechanical design on CAD software - Finalising circuit design										█	█	█	█	
M5	Report writing & Presentation									█	█	█	█	█	█

Figure 3.2: Gantt Chart for Part 1 of the Project.

Gantt Chart Part-2															
No.	Project Activities	W1	W2	W3	W4	W5	W6	W7	W8	W9	W10	W11	W12	W13	W14
M1	Prototype Fabrication and Software Development	█	█	█	█	█									
M2	Integration of Hardware and Software			█	█	█	█								
M3	Data Callibration, Collection and Validation						█	█	█						
M4	Improvement and Testing						█	█	█	█	█	█			
M5	FYP Poster											█			
M6	FYP2 Report Writing and Oral Presentation								█	█	█	█	█	█	█

Figure 3.3: Gantt Chart for Part 2 of the Project.

3.4 Biomechanical Assessments

Finger range of motion (ROM), and grip strength are the biomechanical assessments to be conducted on this prototype to evaluate the performance of it and to show that the prototype can provide repeatable finger flexion/extension movements and assist in the user fingers' grip strength.

3.4.1 Finger Range of Motion (ROM)

The finger range of motion (ROM) on the distal interphalangeal (DIP) joint of the index finger and the interphalangeal (IP) joint of the thumb on the right hand were measured by two inertial measurement units (IMUs) attached at the side of the distal phalanx of the index finger of the 4 fingers part and the thumb part of this prototype.

In Figure 3.4, it shows the MCP, DIP and PIP joints' angle/ROM for the index finger labelled as θ_M , θ_P and θ_D respectively. The same method is used to measure the MCP and IP joint angle/ROM of the thumb.

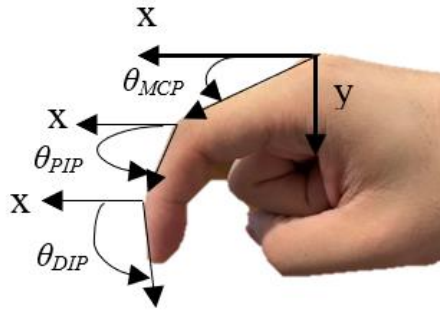


Figure 3.4: Finger ROM Measurements Diagram.

The MPU6050 accelerometer was utilised to measure the finger ROM. It first measures the gravitational acceleration along the 3 axes. The angular data was then derived using trigonometry. The index finger DIP and thumb IP joint angles changes along the Z-axis due to the orientation attachment of the IMUs on the exoskeleton, and the angle along the Z-axis were determined using Equation 3.1:

$$\theta_z = \tan^{-1} \left(\frac{\sqrt{a_y^2 + a_x^2}}{a_z} \right) \times \pi \quad (3.1)$$

where

θ_z = angle along the z-axis, °

a_x = acceleration in the x-axis, m/s²

a_y = acceleration in the y-axis, m/s²

a_z = acceleration in the z-axis, m/s²

The absolute angle of the thumb IP and index finger DIP joints along the Z-axis, were then calculated using Equation 3.2:

$$\theta_{thumbIP, indexDIP} = \theta_z - 90^\circ \quad (3.2)$$

where

$\theta_{thumbIP,indexDIP}$ = Absolute angle of thumb IP and index finger DIP joint, °

θ_z = angle along the z-axis, °

3.4.2 Grip Strength

Grip strength refers to the maximum force exerted by the fingertip with contraction of the person's forearm muscles. Grip strength is used in ADL such as opening jars, carrying objects, turning door knobs and more (Physiopedia, n.d.). Thus, it will be useful for users with fine motor disability to use this assistive device to regain grip strength. The grip strength exerted on the index finger and thumb on the right hand by the prototype were measured with the use of a digital force gauge.

3.5 System Architecture of the Prototype

The system architecture depicted in this Figure 3.5 revolves around a control unit (microcontroller) that manages the inputs and outputs of the system. The IMU sensors provide real-time data regarding the finger ROMs, which is sent to the microcontroller for processing. The microcontroller is powered by a portable power supply, ensuring that the system can operate independently without a constant external power source. Based on the sensor data, the microcontroller controls the actuation system, which consists of servo motors. These motors drive the mechanical frame responsible for finger flexion, extension, and grasping movements, enabling precise mechanical control of finger motions. The system includes a user interface developed using Blynk IoT, allowing the user to interact with the system remotely. Through this interface, the user can monitor the system's status, control the actuators, and observe the movements of the mechanical structure. The integration of IMU sensors, servo motors, and an IoT interface ensures that the system can operate efficiently and be controlled and monitored by the user in real-time.

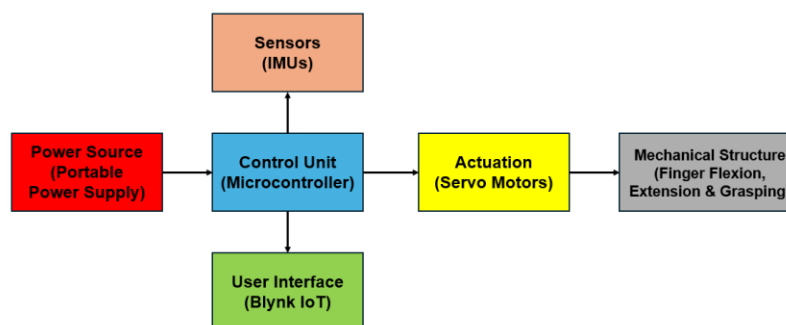


Figure 3.5: System Architecture of the Prototype

3.6 Mechanical Design Conceptualisation

Figure 3.6 shows the overall mechanical design conceptualisation of various parts of the prototype drawn using the SOLIDWORKS software. It consists of a wrist brace, two lithium-ion rechargeable batteries with a 2-slot battery holder, a 3D-printed 4 fingers part for the 4 fingers (index finger, middle finger, ring finger and small finger), 3D-printed thumb part for the thumb. The prototype's mechanical design planned to have 3 servo motors on it with 2 connected to the 4 fingers part to actuate the 4 fingers' MCP and DIP joints, and 1 connected to the thumb part to actuate the thumb IP joint. It was also planned to have a 3D-printed junction box that houses an ESP32 microcontroller and a multiplexer. It was planned to have Velcro straps placed in between the rigid supports on each phalanx of the thumb and the index finger, and two IMUs attached at the side of the index finger's the proximal and distal phalanges of the 4 fingers part to measure the index finger MCP and DIP joint ROM, and two IMUs attached at the side of the thumb's proximal and distal phalanges of the thumb part to measure the thumb MCP and IP joint ROM.

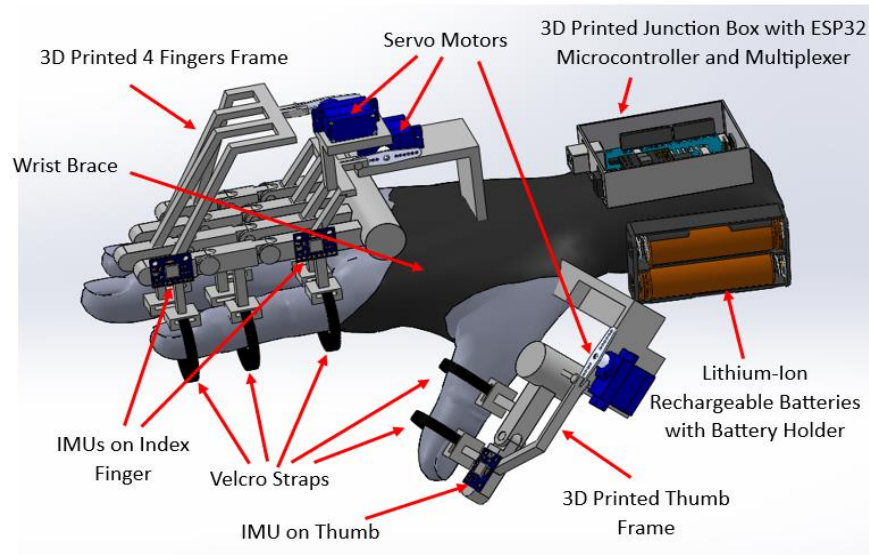


Figure 3.6: Overall Prototype Mechanical Design Conceptualisation.

Figures 3.7, 3.8 and 3.9 shows the conceptualisation of the 3D-printed 4 fingers part, thumb part and junction box in isometric view respectively created using SOLIDWORKS. Additionally, the technical drawings of the conceptualised 4 fingers part, thumb part and junction box with their dimensions in multiple views drawn in the SOLIDWORKS software are shown in Appendices A, B and C respectively.

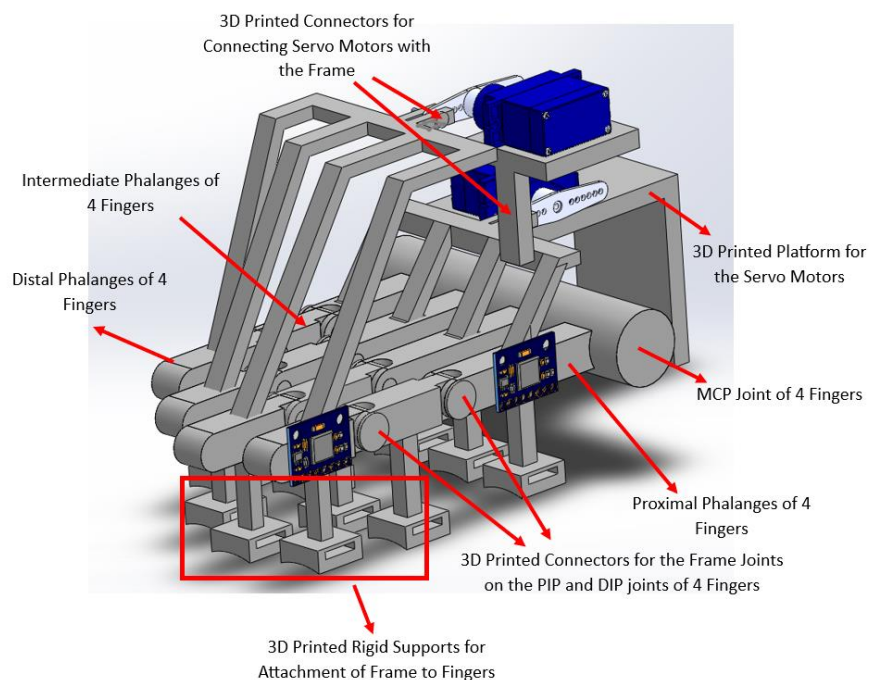


Figure 3.7: Conceptualisation of 4 Fingers Part in Isometric View.

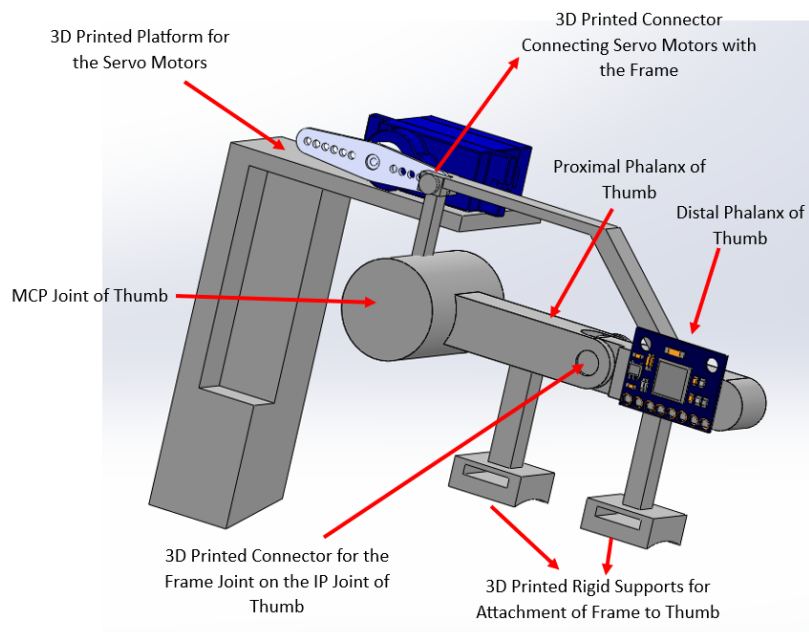


Figure 3.8: Conceptualisation of Thumb Part in Isometric View.

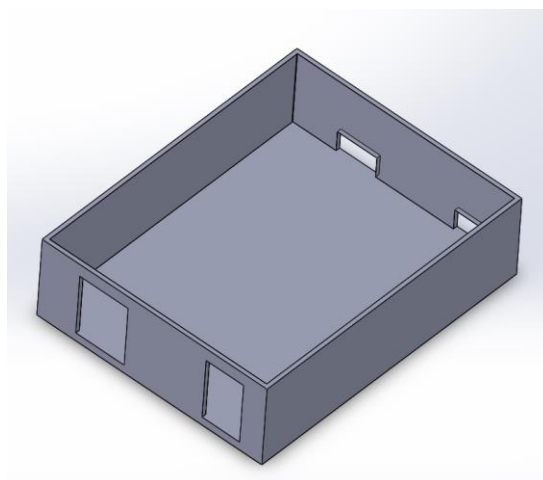


Figure 3.9: Conceptualisation of Junction Box in Isometric View.

3.7 Materials and Electrical Components Selection

3.7.1 3D Printing Material

The mechanical frame of the 4 fingers and thumb parts, and the junction box of this prototype were 3D printed with polylactic acid (PLA) filaments. This is because PLA filament was easy to print, did not produce fumes and not expensive, even though it has a low melting point at high temperatures, they can get soft or deform at high temperatures and it is quite brittle as it can break quite easily (Barrett, 2020) This prototype is mainly used in indoor areas, so these limitations of PLA do not affect the functionality of this device.

3.7.2 Metal Gear Servo Motors

Three MG946R micro servo motors (Cytron Technologies, n.d.b) shown in Figure 3.10, was used to actuate this prototype. This servo motor operates at 4.8 to 6 VDC and can provide a torque of 13 kg.cm or 1.274 N.m (Cytron Technologies, n.d.b), which is sufficient to actuate finger movements as the hands are very light, with an average weight of 0.46 kg (What Things Weigh, n.d.). It is also able to provide a 180 degree rotation angle, which is sufficient for the operation of this assistive device.

There are several reasons why this metal gear servo motors were chosen to drive this prototype instead of other electrical motors and other types of actuators. Firstly, this is because metal gear servo motors are relatively lightweight, with a weight of only 55 g (Cytron Technologies, n.d.b). Besides that, the torque of the micro servo motors can be precisely controlled through PWM principles which aligns well with the need for precise movement in assisting fine motor skills, which are highly precise movements. Moreover, metal gear servo motors are small which enables them to be easily attached to this prototype (Heason, 2020).

Other actuators like hydraulic cylinders are so heavy as it requires fluid and other metallic components (Tolomatic, 2016), and pneumatic actuators are noisy, require a pneumatic air compressor to work, which makes them not portable, and they are difficult to be controlled precisely due to the difficulty of keeping the compressed air under constant pressure and flow rate (Hankun, 2023), which makes them not suitable to be used to actuate this prototype.



Figure 3.10: MG946R Metal Gear Servo Motor (Cytron Technologies, n.d.b).

3.7.3 Portable Power Supply

A power supply was used to power the servo motors, microcontroller and the IMUs of the prototype. It is also portable which allows the prototype to be carried around easily and to be used anywhere. It has a regulated 5V output which prevents excessive voltage or current being supplied to the electrical components, this ensures that this assistive device is safe for users to use it and the electrical components on the prototype will be protected at all times.

3.7.4 ESP32 Microcontroller

A microcontroller was used to control the torque generated by the servo motors, and process the data received from the IMUs to obtain the finger ROMs. The Wemos D1 R32 microcontroller (Cytron Technologies, n.d.c) shown in Figure 3.11, is the ESP32 microcontroller model chosen to be used in this prototype due to its ability to connect to the Wi-Fi and internet wirelessly without requiring the use of a Wi-Fi Module, unlike some Arduino Uno R3 and Arduino Nano microcontrollers. This enables the prototype to connect to an IoT platform. Besides that, it also contains sufficient analogue and digital input/output pins (Last Minute Engineers, n.d.) to connect all the electrical components used on this prototype.



Figure 3.11: Wemos D1 R32 Microcontroller (Cytron Technologies, n.d.c).

3.7.5 Inertial Measurement Units

Two Inertial measurement units (IMU) were used to obtain the finger ROM on the DIP joint of the right index finger and the IP joint of the right thumb. The MPU-6050 (Cytron Technologies, n.d.a) shown in Figure 3.12, is the IMU model chosen to be used on this assistive device. The MPU-6050 IMU has 6 degrees of freedom, and it is a combination of 3-axis gyroscope and

accelerometer with a digital motion processor (Electronic Wings, n.d.), which allows it to be able to measure angular velocity through the gyroscope and acceleration through the accelerometer (Vectornav Technologies, n.d.). The main reason why IMUs are chosen to obtain the finger ROMs, is because IMU can provide continuous and real-time data, facilitating dynamic joint angle tracking during movement (Inertial Labs, 2023). Furthermore, IMUs are small and lightweight, which makes it easy to be attached on this assistive device. An IMU will be placed at the side of the distal phalanx of the index finger of the 4 fingers part and the thumb part of the prototype.



Figure 3.12: An Inertial Measurement Unit.

3.7.6 Multiplexer

A Multiplexer is a device which allows devices with the same I2C addresses to be connected to one microcontroller (Mybotic, n.d.). TCA9548A 12C Multiplexer Module (Mybotic, n.d.) shown in Figure 3.13 was the multiplexer model used in this prototype. A multiplexer was used in this prototype due to the limitation of the microcontroller, which cannot handle simultaneous reading and writing of multiple devices with identical I2C addresses. Therefore, with two IMUs needed to be used on this prototype, the TCA9548A I2C multiplexer I2C module solves this issue by facilitating individual control of the IMUs via the microcontroller, which allows effective communication between them on the same bus (Mybotic, n.d.).

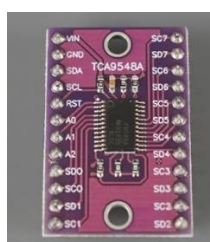


Figure 3.13: A TCA9548A I2C multiplexer module.

3.7.7 Velcro Straps

Velcro straps were used to enable the attachment of the 3D-printed 4 fingers and thumb parts of the prototype to the fingers of the user to be adjustable according to user's finger diameter and shape to enhance its comfortability to the use while wearing it. This also allows patients with deformed finger shape after suffering from stroke, neurological damage, finger bone fractures and more, to wear it comfortably.

3.7.8 Wrist Brace

A wrist brace was used to house the prototype's 4 fingers part, thumb part junction box and servo motors, so that it is easy for this prototype to be worn by the user, making it user-friendly. Besides that, the wrist brace can fix the position of the wrist while wearing this assistive device, so that the wrist can be stabilized and stay in position to prevent the results of the finger ROMs to be affected. It has straps to enable adjustments according to the size of the user's wrist size, which enhances the comfortability of the user while wearing it.

3.7.9 Digital Force Gauge

A digital force gauge shown in Figure 3.14 was used to measure the grip strength on the index finger and thumb exerted by the prototype. This is due to its ability to provide accurate and precise grip strength readings (Tkachuk and Horn, 2020). It has a zero button to prevent zero error during the grasping force measurements.



Figure 3.14: A Digital Force Gauge.

3.7.10 Digital Goniometer

A digital goniometer shown in Figure 3.15 was used to validate the IMU's angle readings. This is to ensure that the IMU's angle readings are correct and accurate. It also has a zero button to prevent zero error during the angle measurements,



Figure 3.15: A Digital Goniometer.

3.7.11 Stripboard (Printed Circuit Board)

A stripboard which is a type of printed circuit board (PCB) shown in Figure 3.16, was used to connect the circuit for the final developed prototype so that the connections of the components' pins are secured and not loose when the prototype is running. stripboard was chosen instead of donut board (perfboard) to connect the circuit for the final developed prototype is because it's easier to construct complex circuits due to it having pre-connected strips, this reduces the need for using excessive jumper wires to manually connect each point which is needed for a donut board. Besides that, a stripboard allows more compact circuit design compared to a donut board due to its ability to make multiple connections of the same pin on the same strip, which is suitable for my prototype as the 3D-printed junction box can be designed with a smaller size. (RAYPCB, n.d.).

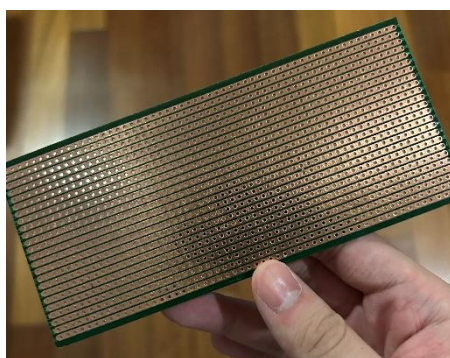


Figure 3.16: A Stripboard.

3.8 Calibration of IMU Sensors

The methods to perform calibration on the IMUs to ensure accurate and reliable data output from these sensors are discussed here.

The IMUs need to be calibrated to ensure their angle readings are accurate so that the finger ROMs collected will be accurate and reliable. The calibration of the IMUs were done by applying Equation 3.3 (Chillibasket, 2015):

$$\text{True Angle Reading} = \text{IMU Measured Angle Reading} - \text{Offset} \quad (3.3)$$

to remove the offsets on the IMU angle readings. The IMU angle readings are only considered accurate when the IMU angle readings in 30 degree intervals between 0 and 90 degrees are close to the actual angle measured using a digital goniometer. (with their percentage differences lesser than 10%). The method used to validate the IMU angle readings with the actual angle measured using a digital goniometer is shown in Figure 3.17.

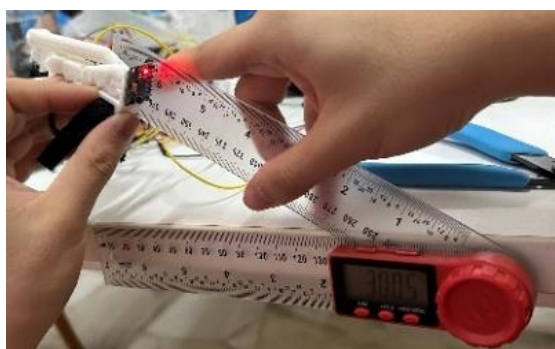


Figure 3.17: Method Used to Validate the IMU Angle Readings.

3.9 Circuit Design

The pins connected to the components in the circuit design with the breadboard and stripboard will be discussed in detail here.

3.9.1 Circuit Design with Breadboard

Figure 3.18 shows the overall circuit design for the prototype with a breadboard, it consists of an ESP32 microcontroller, three servo motors, two IMUs, a 5V power supply and a multiplexer. Figure 3.18 shows an Arduino Uno

microcontroller which has similar design with ESP32 microcontroller used in this prototype, to visualise roughly where the pin connections would be placed.

The three servo motors' signal pins were connected to the IO27 (actuates the 4 fingers' proximal phalanges), IO25 (actuates the 4 fingers' distal phalanges) AND IO26 (actuates the thumb's distal phalanx) digital input/output pins of the ESP32 microcontroller. The input voltage (Vcc) pins of the servo motors were connected in series with the Vcc wire of the power supply via the breadboard for it to supply electricity for the servo motors to work. The ground (GND) pins of the servo motors were connected in series with the GND wire of the power supply via the breadboard to create a complete circuit between the servo motors, microcontroller and power supply.

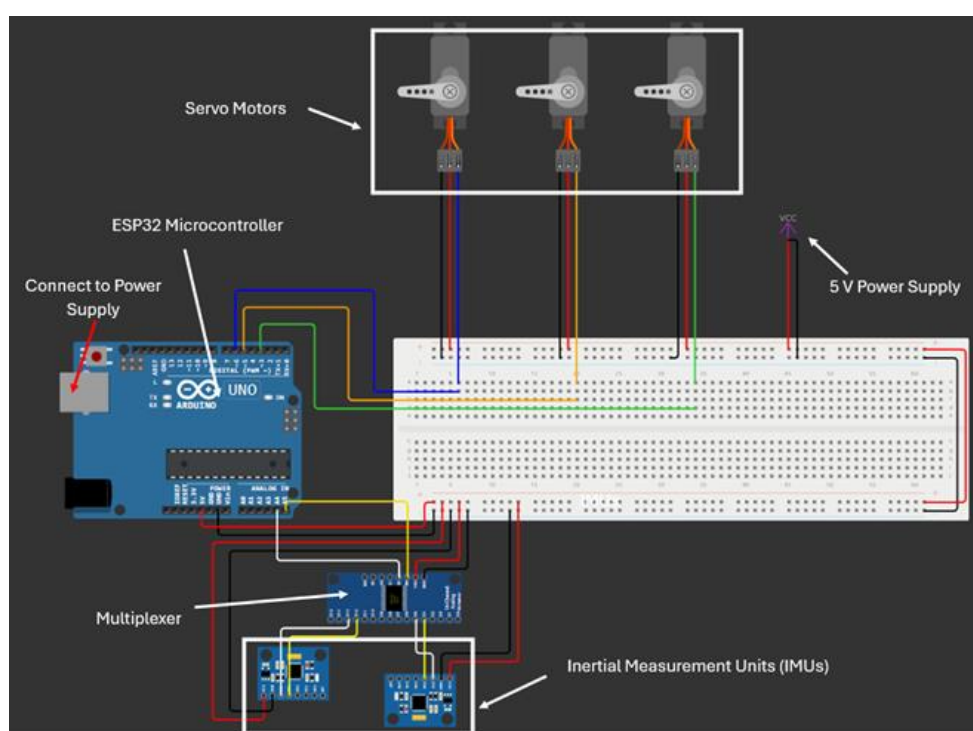


Figure 3.18: Overall Circuit Design for the Prototype.

Figure 3.19 shows the detailed circuit design involving the IMUs and multiplexer. The multiplexer and IMUs' Vcc pins are connected in series with the Vcc wire of the power supply via the breadboard, The multiplexer and IMUs' GND pins are also connected in series with the GND wire of the power supply via the breadboard to complete the circuit. The SCL and SDA pins of the

multiplexer is connected to the SCL and SDA pins of the ESP32 microcontroller. The SCL and SDA pins of the first IMU (measures the thumb IP joint ROM) are connected to the SC2 and SD2 pins of the multiplexer respectively, and the SCL and SDA pins of the second IMU (measures the index finger DIP joint ROM) is connected to the SC6 and SD6 pins of the multiplexer respectively.

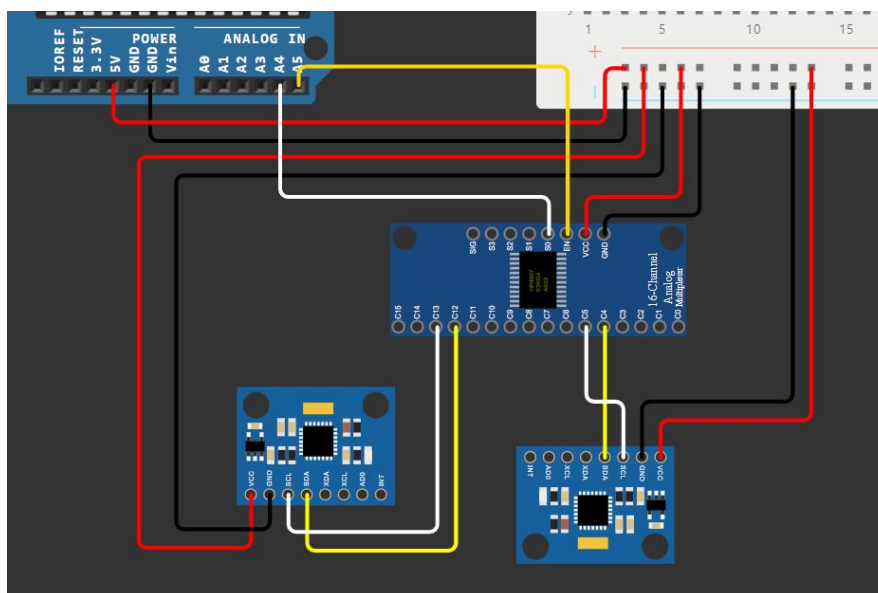


Figure 3.19: Detailed Circuit Design involving IMUs and Multiplexer.

3.9.2 Circuit Design with Stripboard

Figure 3.20 shows the detailed circuit design with stripboard for all the prototype's components. The stripboard of the prototype has many female head pin connectors soldered on the board that allows the wires to be connected onto the stripboard. Grey coloured boxes signify ground (GND) pins, peach coloured boxes mean input voltage (Vcc) pins, yellow coloured boxes are SDA pins and white coloured boxes are SCL pins to be connected onto the stripboard. Blue, orange and green coloured boxes are each of the three servo motors' signal (Sig) pins to be connected onto the stripboard. The two black lines signifies that the parts of the stripboard where the copper on the stripboard will be scratched off to prevent the pins of the same row to be connected to each other as they are different types of pins, which may cause short circuits that can potentially damage the components if the copper on the board are not scratched off properly.

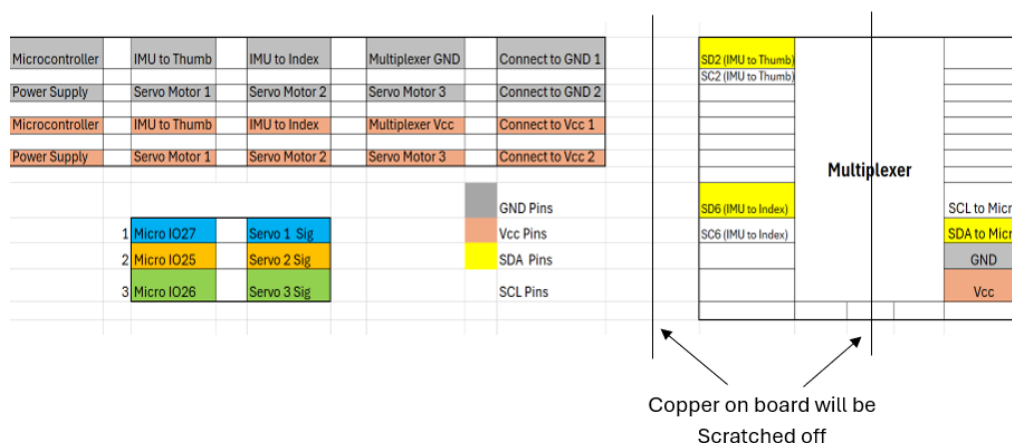


Figure 3.20: Detailed Circuit Design with Stripboard.

3.10 Internet of Things (IoT) System

Blynk was the IoT platform chosen to be connected to this prototype for several reasons. Firstly, it is because it is designed for IoT projects to be created easily due to its user-friendly interface. Besides that, it has custom dashboards that can be built to display the data collected by the sensors connected to this prototype in the form of graphs and charts. Moreover, it supports a wide range of devices such as ESP32, Arduino Uno, ESP8266 and other popular microcontrollers (Indian Institute of Embedded Systems, n.d.).

3.10.1 IoT Architecture

The Prototype's IoT architecture shown in Figure 3.21 consists of 4 main layers, which are the physical layer, network layer, middleware layer and application layer. The first layer, the sensing layer, involves sensors and devices like the IMUs for collecting data, servo motors used to drive this prototype, and the ESP32 microcontroller to process and send input control signals to input devices connected to it, and sending information to the cloud server. The next layer, the network layer, involves the integrated Wi-Fi component on the ESP32 microcontroller which establishes communication and Wi-Fi network connections between the microcontroller and the cloud server. The third layer, middleware layer, involves the Blynk Cloud which is responsible for managing and storing data (Dychen, 2023), in its cloud server so that it can be connected to the application layer. The last layer, the application layer, involves the Blynk

IoT mobile app which allows this prototype to be controlled remotely and real-time data to be visualised on its user interface.



Figure 3.21: IoT Architecture of the Prototype.

3.10.2 IoT System Program Flowchart

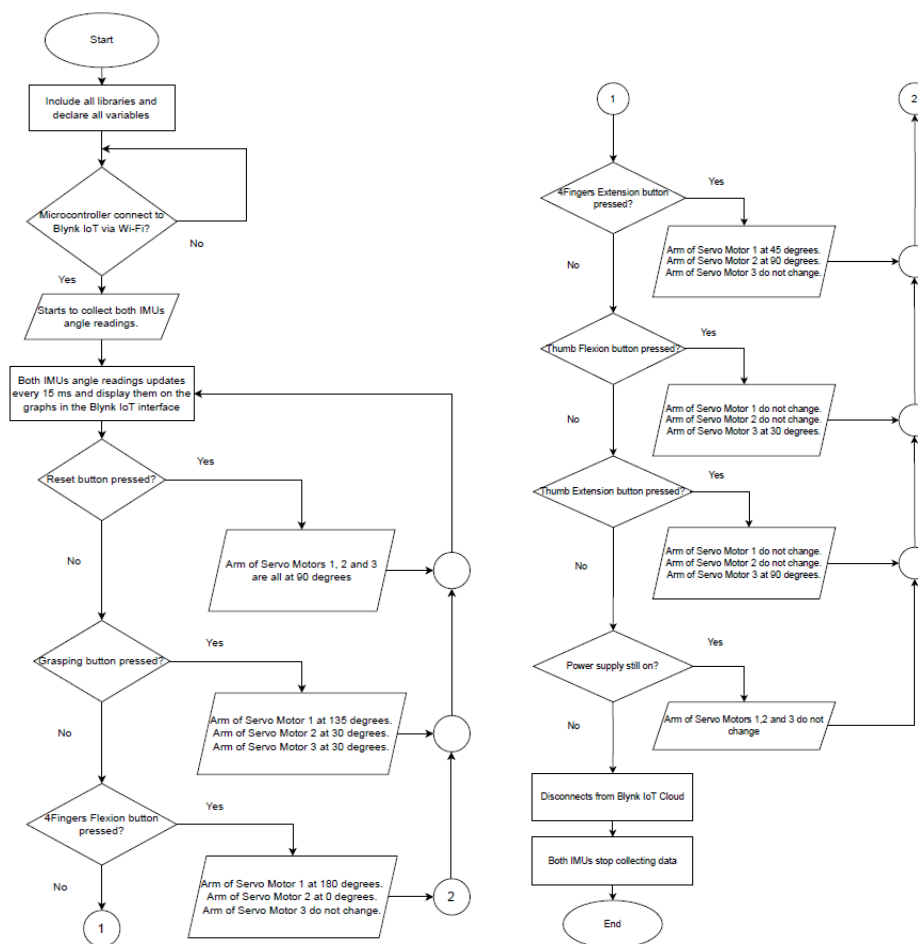


Figure 3.22: Program Flowchart for the Prototype IoT System.

Figure 3.22 shows the program flowchart for the prototype IoT system. It starts when the power supply is turned on. After that, the system would include all the libraries and declare all the variables in its program. Then, the prototype's microcontroller would try to connect to the Blynk IoT Cloud via Wi-Fi, if cannot

then it would try to reconnect to the Blynk IoT Cloud, usually this happens when there is no connection established with the Wi-Fi network. If the microcontroller could connect to the Blynk IoT Cloud, the system would start to collect both IMUs angle readings and updates their angle readings every 15 ms which would be displayed on the graphs in the Blynk IoT user interface. Then, the system checks whether the reset button is pressed, if it's pressed, the arm of Servo Motors 1, 2 and 3 would be all at 90 degrees or else the system checks whether the grasping button is pressed. If the grasping button is clicked, the arm at Servo Motor 1 would be at 135 degrees, and the arm of Servo Motors 2 and 3 would be at 30 degrees. The system then checks whether the 4Fingers flexion button is pressed, if its pressed, the arm of Servo Motor 1 would be at 180 degrees, the arm of Servo Motor 2 would be at 0 degrees and arm of Servo Motor 3 would not change from its current position, or else the system checks whether the 4 fingers extension button is pressed. If its pressed, the arm of Servo Motor 1 would be at 45 degrees, the arm of Servo Motor 2 would be at 90 degrees, and the arm of Servo Motor 3 do not change.

Followed by this, the system checks whether the thumb flexion button is pressed, if its pressed, the arm of Servo Motor 1 and 2 do not change, whereas the arm of Servo Motor 3 would be at 30 degrees, or else the system checks whether the thumb extension button is pressed. If its pressed, the arm of Servo Motors 1 and 2 do not change and the arm of Servo Motor 3 would be at 90 degrees. Then, the system checks whether the power supply is still on, if it's still on, the system loops back to updating both IMUs angle readings and display them on the graphs in the Blynk IoT interface, and it rechecks whether all the buttons on the Blynk IoT user interface have been pressed or not. If the power supply is turned off, the system disconnects from the Blynk IoT cloud, and both IMUs would stop collecting data. This signals the end of the program for the system.

3.11 Libraries Used to Program the Components and IoT System

There were 10 types of libraries used to program and components and IoT system for them to work. The WiFi.h library was used to provide the functionality for the ESP32 microcontroller to connect to a Wi-Fi network, so that the microcontroller can connect to the Blynk IoT Cloud for the Blynk IoT

user interface to work. The BlynkSimpleESP32.h library was used to enable the integration and interaction of the ESP32 microcontroller with the Blynk IoT platform that enable remote control of the prototype and data visualisation of the IMU angle readings on the Blynk IoT mobile app. The ESP32Servo.h library was used to control the servo motors with the ESP32 microcontroller to perform the specific finger movements. It helps in the generation of pulse width modulation (PWM) signals that are necessary to control the servo motors' positions.

The Adafruit_Sensor.h library was used to provide the standardisation of the sensor data format when reading from IMUs, it helps to handle the IMUs data in a consistent and reliable manner. The Adafruit_BusIO_Register.h library was used to aid in low-level communication with the IMUs, allowing the ESP32 microcontroller to interact with the IMUs' registers to read or configure their settings. The Adafruit_I2CDevice.h enables the communication between the ESP32 and the IMUs via the I2C interface, which is used to gather acceleration data that will be converted to angular data. The Adafruit_I2CRegister.h library was used to interact with specific register on the IMUs, allowing the ESP32 to configure and extract their data. The Adafruit_MPU6050.h was used to provide easy access to the IMUs' acceleration data. Lastly, the Wire.h library was used for the ESP32 to communicate with the IMUs via the I2C protocol.

3.12 Experimental Protocols and Data Analysis Methods

The objectives, procedures and method of data collection and data analysis, potential risks for the three tests on the assistive hand orthosis namely the finger ROM test, grip strength test and objects grasping test are described here. Six healthy individuals (3 male and 3 female) with a mean age of 24 were recruited for this study. Inclusion criteria required participants to be between the ages of 20 to 29 years old. Individuals who were suffering from neurological disorders and injuries on finger joint or the upper extremities were excluded from the study. Ethical approval was obtained from UTAR Scientific and Ethical Review Committee (U/SERC/28/2023), and written informed consent was obtained from all participants prior to enrolment in the study. During all these tests, subjects were closely monitored during the experiment to ensure their safety. The device would be stopped immediately if there is any discomfort or adverse

reactions. All subjects' data were protected through private storage and restricted access.

3.12.1 Finger ROM Test

The objectives of this test were to assess whether this assistive hand orthosis was able to perform flexion, extension and grasping movements on the thumb and the other four fingers close to the typical Finger ROMs and compare the finger ROMs during 4 fingers flexion and 4 finger extension movements between male and female subjects. The equipment and software used in this test are the assistive hand orthosis, inertial measurement units, Blynk IoT and Microsoft Excel. Each movement was repeated 5 times for each subject.

The procedure for the finger ROM test began with the subject wearing the assistive hand orthosis. The subject was then instructed to align their fingers horizontally and place their wrist on an object shown in Figure 3.23. The experimenter used the Blynk IoT app, first clicking the 'Reset' button, followed by the '4 Fingers Flexion' button, and data for the range of motion (ROM) at the index finger's DIP joint was recorded for 15 seconds. The experimenter then clicked the '4 Fingers Extension' button, recording the ROM data for another 15 seconds. This process was repeated four more times. Next, the subject aligned their thumb horizontally and placed the side of their wrist on an object. The experimenter once again clicked the 'Reset' button on the app, followed by the 'Thumb Flexion' and 'Thumb Extension' buttons, recording the ROM data at the thumb's IP joint for 15 seconds each. This process was repeated four more times for the thumb. Finally, after the test is done, the subject was instructed to remove the assistive hand orthosis.

The data to be collected in this test were the index finger DIP joint and thumb IP joint ROMs with the assistive hand orthosis for finger flexion/extension and thumb flexion/extension movements. These data could be obtained from the data streamed in Microsoft Excel and analysed by calculating the mean and standard deviation. Besides that, the percentage error was calculated between the index DIP joint ROM of this assistive hand orthosis and another developed hand orthosis during finger flexion and extension. Additionally, the percentage error for the thumb IP joint ROM was compared with typical ROMs during finger flexion and extension. The standard error and

mean squared error for the index DIP joint ROM were also analysed during four fingers' flexion and extension between male and female subjects.

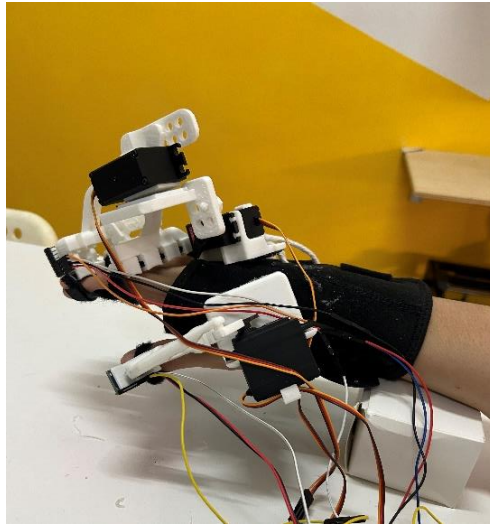


Figure 3.23: Finger ROM Test Performed When Wearing Prototype.

3.12.2 Grip Strength Test

The objectives of this test are to assess the amount grip strength that can be produced on the index finger and thumb by the actuation of the assistive hand orthosis during grasping movements and compared the value of grip strength that could be produced on the index finger and thumb with and without the assistive hand orthosis for all subjects and in terms of gender. The equipment and software used in this test are the assistive hand orthosis, digital hand gauge, Blynk IoT and Microsoft Excel. Index finger and thumb grip strengths with and without the assistive hand orthosis were performed 3 times for each subject.

The procedure for the grip strength test began by turning on the digital force gauge and setting it to zero. The subject was instructed to place their palm above an object and align their index finger on the digital force gauge's measuring head. They were then instructed to perform a grasping movement, pressing their index finger on the measuring head with maximum force for 5 seconds. The reading of the index finger's grip strength was recorded, and the process was repeated two more times for each subject. After setting the gauge to zero and peak, the subject placed the side of their palm above the object and aligned their thumb on the measuring head. They performed the same grasping

movement for the thumb, and the grip strength was recorded, repeating the process two more times.

Next, the subject was instructed to wear the assistive hand orthosis, and the experimenter clicked the 'Reset' button on the Blynk IoT app. After setting the gauge to zero and peak, the subject aligned their index finger on the gauge as shown in Figure 3.24, and the experimenter clicked the 'grasping' button on the app. After 5 seconds, the grip strength was recorded. This process was repeated two more times. The gauge was again set to zero and peak, and the subject aligned their thumb on the measuring head as shown in Figure 3.25. The experimenter clicked the 'grasping' button, and after 5 seconds, the thumb grip strength was recorded. The process was repeated two more times for each subject, with the experimenter resetting the device back to default (fingers kept straight) after each trial. Finally, after the test is done, subject was instructed to remove the assistive hand orthosis.

The data to be collected with and without the assistive hand orthosis are the index finger and thumb grip strength with the assistive hand orthosis for grasping movements, using a digital force gauge, and they were recorded in Microsoft Excel. These data collected were analysed by calculating the mean and standard deviation of the index finger and thumb grip strength with and without assistive hand orthosis and the percentage differences between the index finger and thumb grip strengths with and without the assistive hand orthosis for all subject and on each gender separately.

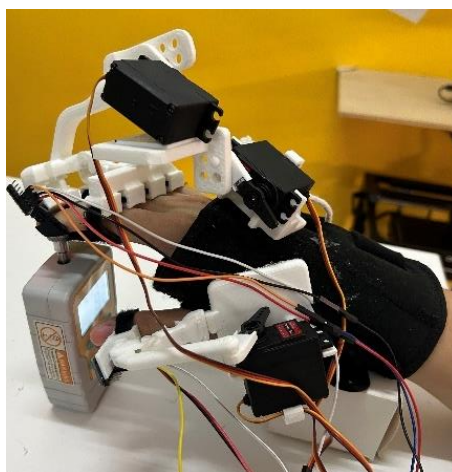


Figure 3.24: Grip Strength Test on Index Finger When Wearing Prototype.

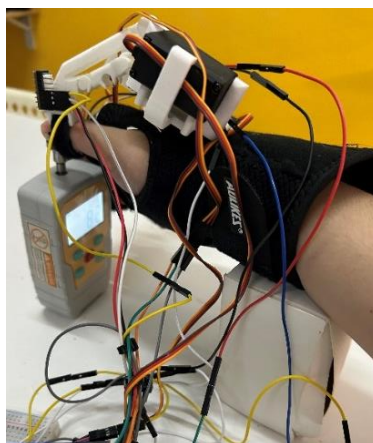


Figure 3.25: Grip Strength Test on Thumb When Wearing Prototype.

3.12.3 Objects Grasping Test

The objective of this test is to assess the the ability of the assistive hand orthosis to grasp on and pick up objects of different shapes and sizes. The equipment and software used in this test are the assistive hand orthosis, objects with different shapes (sphere, cube and cylinder), spherical objects with sizes between 3 to 8 cm, Blynk IoT and Microsoft Excel. This experiment would determine the range of object sizes that could be grasped by the subject when wearing the prototype.

The procedure for the objects grasping test began with the subject wearing the assistive hand orthosis and keeping their fingers horizontally. The experimenter then clicked the ‘Reset’ button on the Blynk IoT app. The subject was instructed to move their fingers above the object that needed to be picked up. The experimenter clicked the ‘grasping’ button on the app, and whether or not the object could be grasped and picked up with the assistive hand orthosis was recorded. If the object was successfully picked up, the subject placed the device near the table, and the experimenter clicked the ‘Reset’ button to release the object. This process was repeated for objects of different shapes and sizes. Lastly, after this test is done, the subject was instructed to remove the assistive hand orthosis.

3.13 Costs of Materials Used on the Prototype

Table 3.1 shows the costs of all the materials used on the prototype, which has a total of RM 383.29, indicating its cost-effectiveness.

Table 3.1: Costs of Materials Used on the Prototype.

No.	Item Name	Quantity	Total Cost (RM)
1	Adjustable Wrist Guard	1	17.08
2	Stripboard	1	2.25
3	Velcro Tapes	1	5.90
4	PLA Filament, 1 kg	1	50.00
5	Breadboard	2	5.40
6	MPU6050 Inertial Measurement Unit	2	21.00
7	Portable Power Supply	1	77.93
8	Cable Ties, 100 pcs	1	0.74
9	40 Ways Male to Male Jumper Wire	1	2.50
10	40 Ways Male to Female Jumper Wire	1	2.50
11	40 Ways Female to Female Jumper Wire	1	2.50
12	Wemos D1 R32 ESP32 Microcontroller	1	29.00
13	USB Micro B Cable	1	4.00
14	MG946R Metal Gear Servo	3	87.00
15	Digital Goniometer	1	27.49
16	Extra 3D Printing Costs	1	48.00
Grand Total Cost (RM)			383.29

3.14 Summary

The prototype requirements include lightweight, portable, comfortable, cost-effective, able to collect accurate biomechanical assessments, IoT connected and adjustable making it suitable to be used on users with different finger shape and diameter, and wrist sizes. The mechanical design conceptualisation of the prototype involves the 3D-printed 4 fingers part, thumb part and junction box, and the IMUs and servo motors placement locations on the prototype. The development process of the prototype starts from research and the mechanical conceptualisation of the prototype, then proceeds to SOLIDWORKS drawings, 3D printing and assembly of the first prototype design, followed by modifications on the mechanical design, software development, development of IoT user interface, and ends with 3D printing, assembly, and testing of final prototype with data analysis of the testings' results. The system architecture of the prototype involves a power supply, a microcontroller for control, Blynk IoT user interface for interaction with prototype, servo motors for actuation, IMUs to collect finger ROMs and specific finger movements by servo motors actuation.

The materials and electrical components will be used on this prototype are PLA, micro servo motors, ESP32 microcontroller, IMUs, digital force gauge and more. The IMUs were calibrated to ensure the data collection by them are accurate and reliable and their angle readings are validated by a digital goniometer. The prototype will be connected to the Blynk Cloud for storing and managing its data, remote controlled, and visualisation of real-time data on its IoT user interface in the Blynk IoT mobile app. Various libraries were used to program the components, and the IoT system followed a structured flowchart for data collection, control, and monitoring. Experimental protocols involving tests to assess finger ROM, grip strength, and object grasping capability, and these tests' data analysis methods were discussed. These three tests provided the data to analyse the prototype's performance. The total costs of all the materials used on the prototype is RM 383.29, which indicates its cost-effectiveness.

CHAPTER 4

RESULTS AND DISCUSSION

4.1 Introduction

The current chapter discusses on the final prototype developed such as its mechanical design on SOLIDWORKS, actual mechanical design, the actual circuit built for the final prototype and its IoT user interface design. The mechanical design changes and enhancement done from the first to the final prototype; the code used to program and integrate the components and IoT system. Furthermore, it discusses on the results of the four tests (inertial measurement unit angle accuracy test, finger ROM test, grip strength test and objects grasping test) carried out on the prototype to evaluate the final prototype's performance on all subjects and also on each gender.

4.2 Final Prototype Mechanical Design

The final prototype comprised of 3D-printed parts such as the final iterative of the 4 fingers part, thumb part, servo holder for 4 fingers part and junction box were designed and drawn separately using the SOLDIWORKS software. They were then 3D-printed and assembled along with three servo motors, two IMUs, a microcontroller, a PCB, a wrist guard, cable ties, cables, a portable power supply and Velcro straps to develop the final prototype.

4.2.1 Technical Drawings of Mechanical Design

Figure 4.1 shows the drawing of the finalised 4 fingers part which consists of rigid attachments to attach the frame to the 4 fingers proximal and distal phalanges, and there are holes at them to allow Velcro straps to be placed through them. Besides that, there are mechanical joints at the attachments to the 4 fingers distal phalanges to increase the flexibility at the distal end of the frame. Moreover, there is a platform at the attachment to the distal phalanx of the index finger to attach an IMU on it. Furthermore, there are mechanical joints at the middle of the frame that mimics the MCP, PIP and DIP joints for the index, middle, ring and small fingers. Additionally, there are holes at the proximal ends

of the frame to fit the slots which are used to attach the ends of the servo motors to the frame allowing the servo motors to move the proximal and distal ends of the 4 fingers part frame. Lastly, there is a platform at the left proximal end of the frame to place the servo motor which actuates the distal parts of the 4 fingers part frame. The technical drawing of the final prototype 4 fingers part with its dimensions in multiple views is shown in Appendix D.

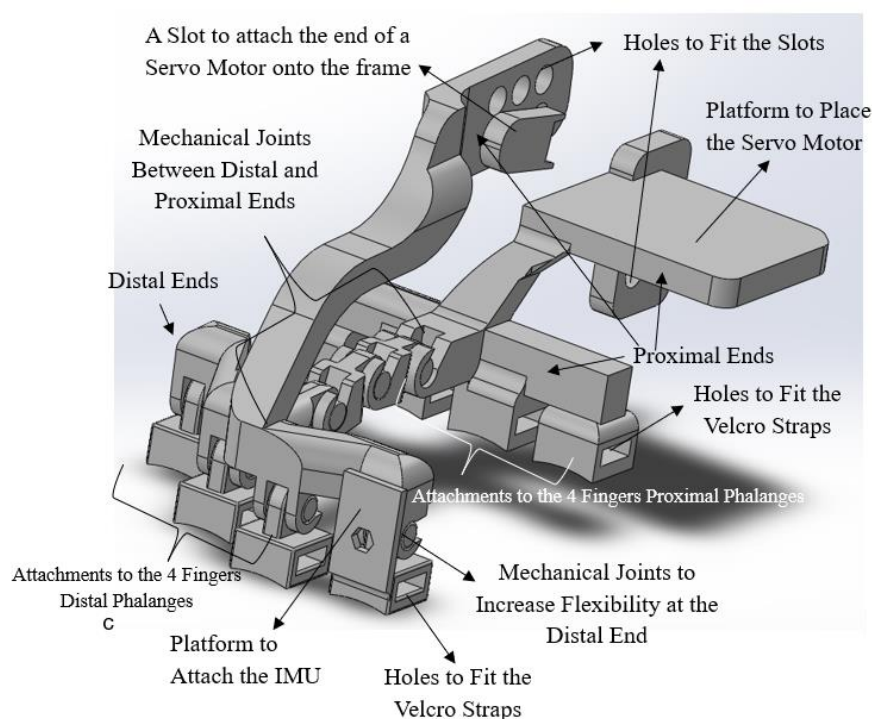


Figure 4.1: Drawing of Finalised 4 Fingers Part in Isometric View.

Figure 4.2 shows the drawing of the servo motor holder for the 4 fingers part on the final prototype. This servo motor holder holds the servo motor that is responsible for actuating the proximal ends of the 4 fingers part frame. The servo motor holder is designed to hold the servo motor in place according to its shape and size, and to attach the servo motor onto the wrist guard. The technical drawing of the final prototype servo motor holder for 4 fingers part with its dimensions in multiple views is shown in Appendix E.

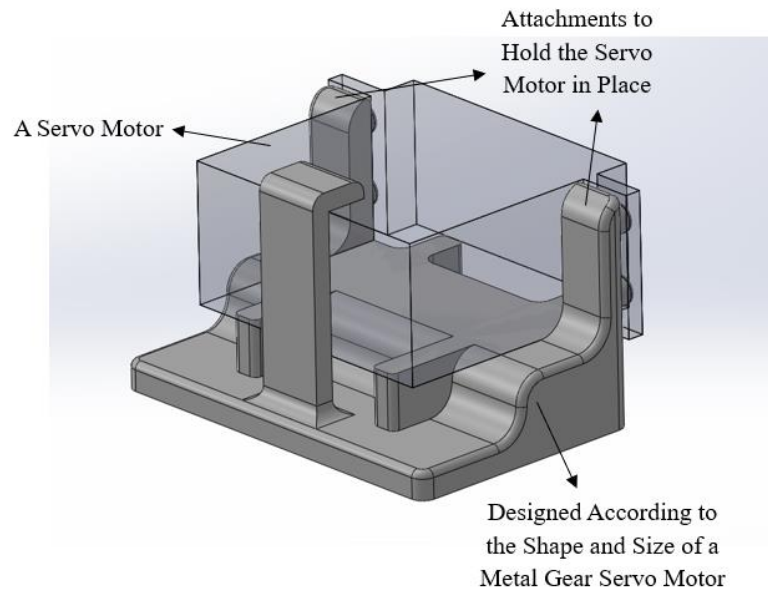


Figure 4.2: Drawing of Final Prototype Servo Motor Holder for 4 Fingers Part in Isometric View.

Figure 4.3 shows the drawing of finalised thumb part. It consists of rigid attachments to attach the frame to the thumb proximal and distal phalanx, and there are holes at them to allow the Velcro straps to pass through it. In addition, there is a platform at the attachment to the thumb distal phalanx to attach an IMU on it. Besides that, there are mechanical joints at the middle of the frame that mimic the thumb joints. At the proximal end of the frame, there is a platform to place the servo motor onto the wrist guard and there are attachments designed to hold the servo motor according to its shape and size. There is a hole at the proximal end of the frame to fit the slot which attaches the end of the servo motor allowing the servo motor to move the thumb part frame. The technical drawing of the final prototype thumb part with its dimensions in multiple views is shown in Appendix F.

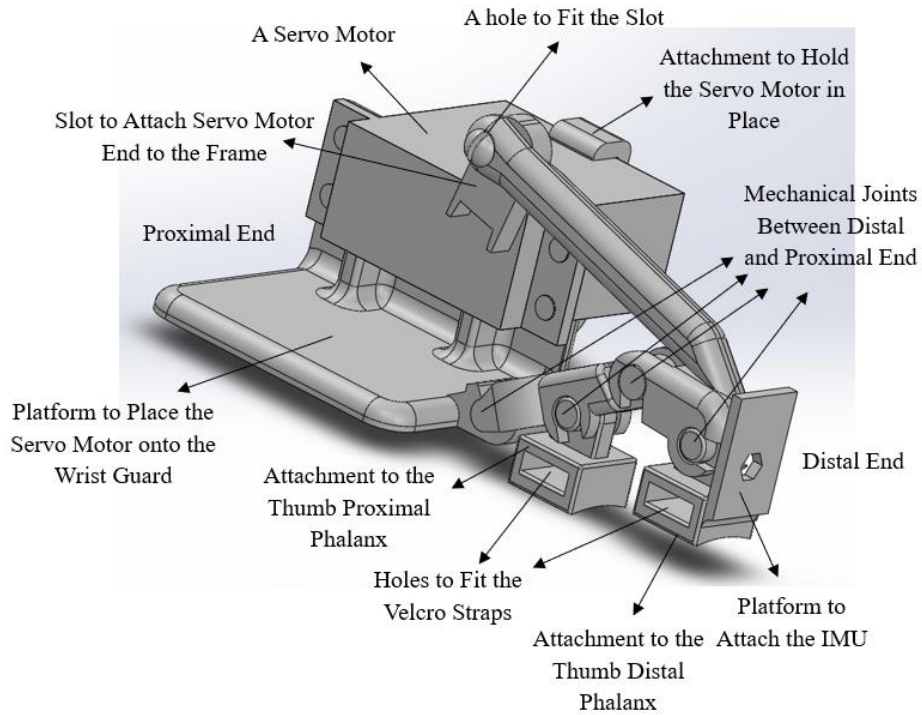


Figure 4.3: Drawing of Finalised Thumb Part in Isometric View.

The junction box for the final prototype is designed with a lid to allow the microcontroller and PCB to be covered up. It has a hinge designed to move the lid up and down, and there are ends designed to hold the lid when it's closed. Moreover, it is designed to have the PCB attached underneath the lid, and there are small gaps shown in Figure 4.4 to fit the microcontroller in place inside the junction box. The technical drawing of the final prototype junction box with its dimensions in multiple views is shown in Appendix G.

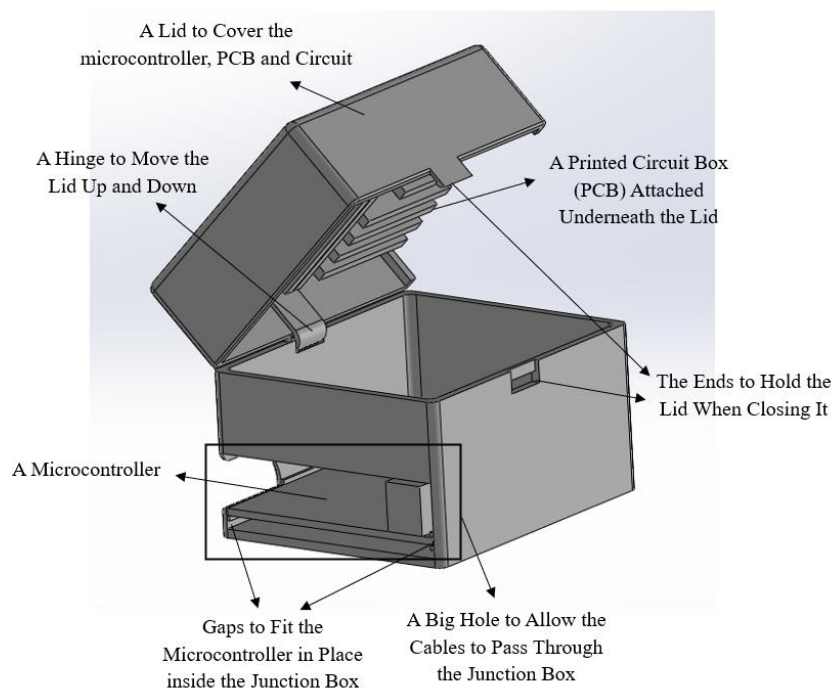


Figure 4.4: Drawing of Finalised Junction Box in Isometric View.

4.2.2 Fabrication of Final Prototype

Figure 4.5 shows the final prototype developed based on the final drawings. It consists of a portable power supply used to power up the microcontroller, IMUs and servo motors. For the 3D-printed mechanical frame of the prototype, it consists of two main parts: the 4 fingers part and thumb part. The 4 fingers part was designed to be attached to the 4 fingers (index finger, middle finger, ring finger and small finger) and able to move the 4 fingers simultaneously when actuated by the servo motors. The 4 fingers part have two servo motors attached to the left and right proximal ends of the frame with one actuating the proximal end of the 4 fingers part, and another one actuating the distal end of the 4 fingers part. The thumb part is designed to be attached to the thumb only and there is a servo motor attached to it to actuate the distal end of the thumb part.

Besides that, it consists of a microcontroller that act as the communication, processing and control unit for the prototype to control which servo motor will move and the degree of their rotation to actuate a specific finger movement, to process the data collected by the IMUs and to connect the prototype to the Blynk IoT platform via Wi-Fi. Moreover, there are two IMUs with one attached at the rigid attachment to the index finger to measure the index

finger DIP joint ROM and another one attached at the rigid attachment to the thumb to measure the thumb IP joint ROM. Additionally, there are Velcro straps at all the rigid attachments of the 4 fingers and thumb part to attach the mechanical frames to the fingers of the user, and Velcro Straps provides adjustability that allows users with various finger diameters and users with deformed fingers to wear it. Furthermore, it has a wrist guard which houses all of the prototype's electrical components, the junction box and the 3D-printed mechanical frames, so that the user can easily wear it. The wrist guard also contains straps that allows users with various wrist sizes to wear it. Lastly, it consists of a 3D-printed junction box that houses the microcontroller, PCB and circuit of the prototype. The total weight of the final prototype is 500 g, which proves that it is lightweight. The total cost of the materials of the final prototype is RM 383.29, which indicates its cost-effectiveness.

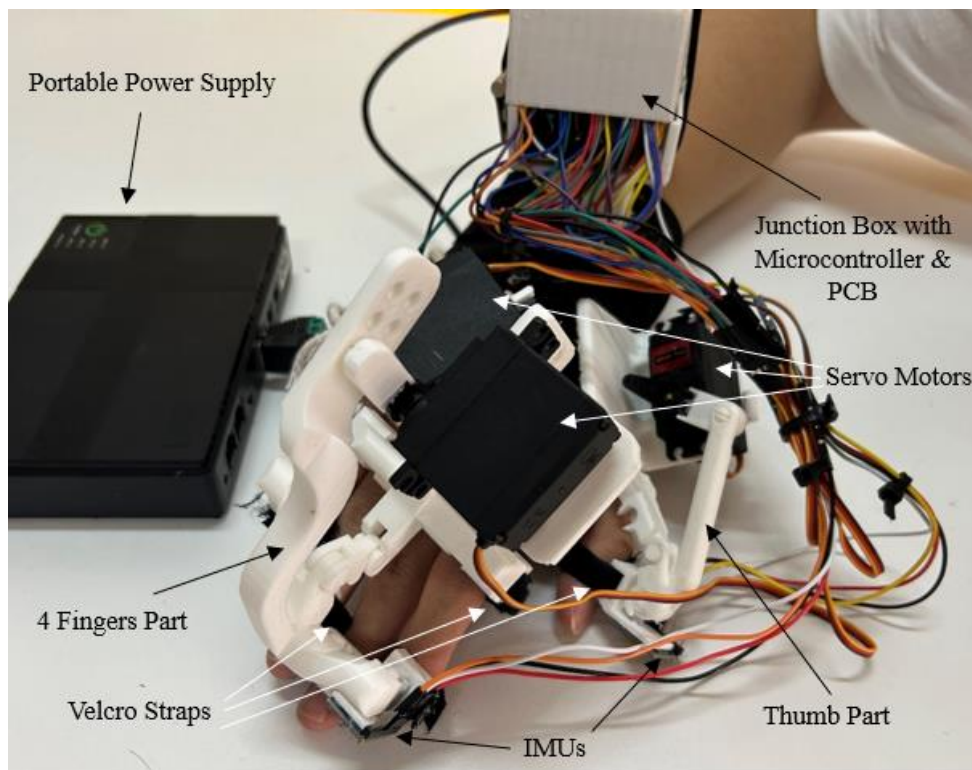


Figure 4.5: Mechanical Design of the Final Prototype.

4.2.3 Circuit Design of Final Prototype

Figure 4.6 shows the circuit design of the final prototype. It consists of a printed-circuit board (stripboard) which was soldered with female pin header connectors

to allow cables to connect to it. It was used instead of a breadboard to ensure that the circuit connections are secured and more compact for it to be able to fit inside the junction box. Additionally, the PCB houses the circuit of the prototype with cables connected to it that were also connected to the pins of the microcontroller, servo motors, IMU and multiplexer. The multiplexer was soldered to the PCB to ensure more organised circuit connections and to ensure the circuit connections relating to the multiplexer were more secured. It also consists of a power jack which is connected the Vcc and ground pins on the printed circuit board which connects to the power supply so that the power supply can power the all the prototype's components. Cables ties were used to tie the cables together especially for those connecting to the two IMUs and the three servo motors to ensure that the cables are well managed, not messy and would not hinder the movement of the frames during the servo motors' actuation.

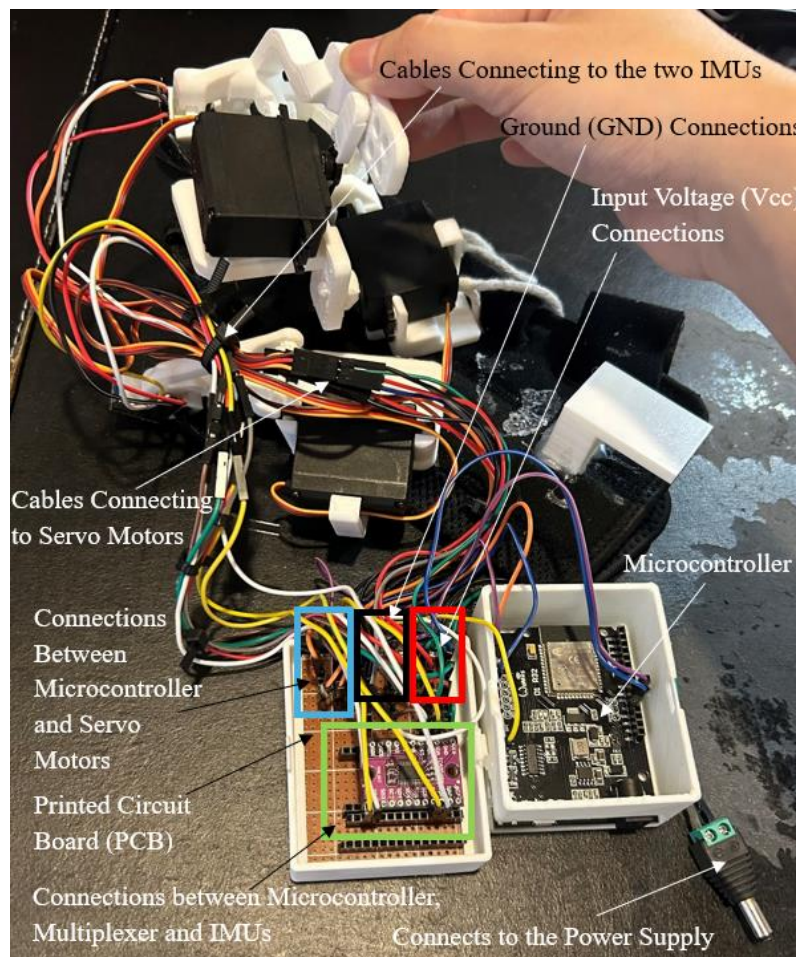


Figure 4.6: Circuit Design of Final Prototype.

4.3 Types of Finger Movements Actuated

Figure 4.7 shows the various finger movements that could be actuated by the final prototype such as 4 fingers flexion (a), 4 fingers extension (b), thumb flexion (c), and thumb extension (d). Grasping movement can also be actuated by the final prototype and the results of the objects able to be grasped when using it will be discussed later on in this chapter.

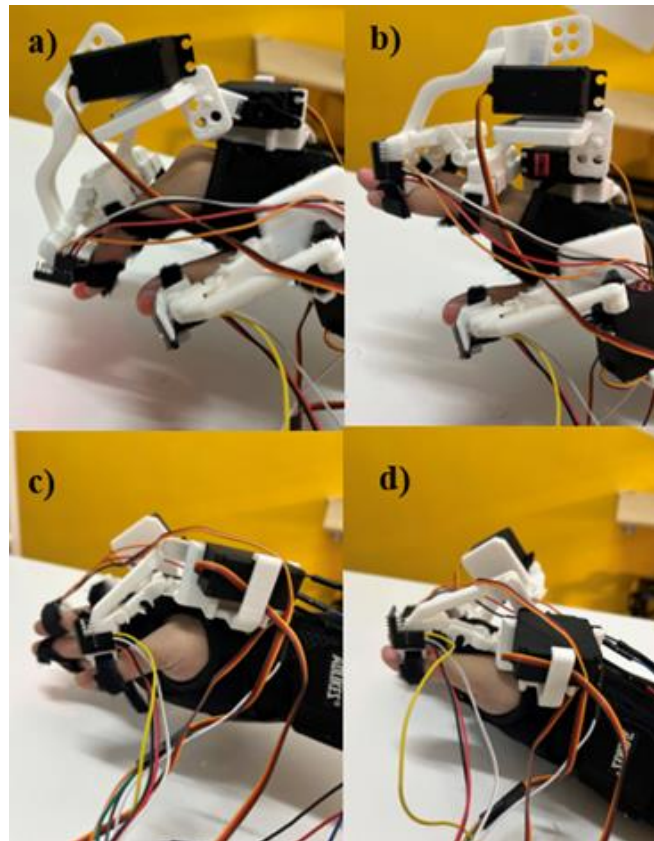


Figure 4.7: Finger Movements Actuated by the Final Prototype a) 4 fingers Flexion; b) 4 fingers Extension; c) Thumb Flexion; d) Thumb Extension.

4.4 IoT User Interface Design

The IoT user interface for the final prototype shown in Figure 4.8 featured Blynk IoT Cloud as the backend platform. Enables compatibility to the user interface on the Blynk IoT mobile app. The IoT user interface have push buttons to signal the prototype to perform the actuation of specific fingers and thumb movements such as finger flexion/extension, thumb flexion/extension and grasping, in a remote manner through Blynk IoT mobile app. It also consists of graphs displaying the real-time index finger DIP joint and thumb IP joint ROMs

measured by the two IMUs. The Blynk IoT cloud platform enables real-time acquisition of joint ROM by the IMUs, visualisation of biomechanical data, cloud data storage and retrieval. Lastly, it also has a reset push button to reset the prototype to its default state for the safety of the user in the event if there is discomfort felt by the user or uncommon bugs in the servo motor control during its actuation.

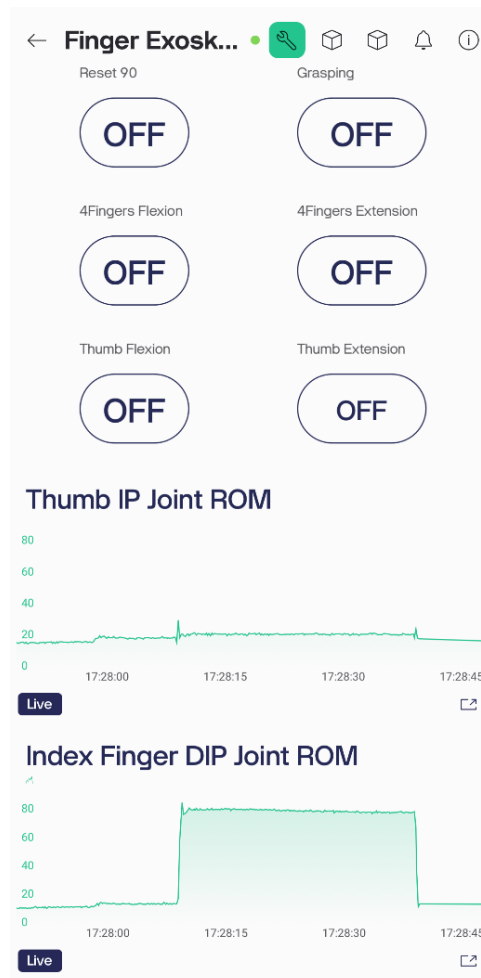


Figure 4.8: IoT User Interface Design for Final Prototype.

4.5 Prototype Mechanical Design Changes and Enhancements

The changes and enhancements in the mechanical design for the 3D-printed parts, which are the 4 fingers part, thumb part and junction box, after carrying out functional tests on them are discussed here. The technical drawings of the 4 fingers part, thumb part and junction box iterative designs with its dimensions in multiple views are shown in Appendix H to J.

4.5.1 4 Fingers Part Design Changes and Enhancements

After performing performance testing of the conceptualised 4 fingers part, all of its frames' height were shortened by half as shown in Figure 4.9, to reduce its bulkiness. Besides that, the thinner frame parts of the 3D-printed conceptualised 4 fingers part frame were broken as shown in Figure 4.10, during the removal of the 3D-printing supports and functionality testing on it. It was identified that this was caused by some of its frames being too thin. Hence, most of the thinner frames on the conceptualised 4 fingers part were modified to be twice thicker as shown in Figure 4.9. This ensures that the frames would not break when the servo motors actuate the frames.

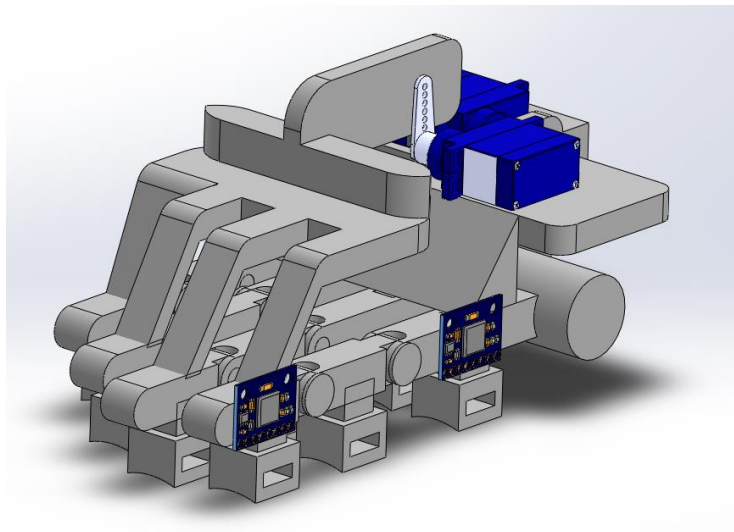


Figure 4.9: 2nd Iterative 4 Fingers Part Drawing in Isometric View.



Figure 4.10: Broken Frames of the Conceptualised 4 Fingers Part.

After performing functionality testing on the second iterative 4 fingers part, it was found that the rigid attachments that attaches the frame to the 4 fingers' distal phalanges were too rigid. Hence, the mechanical joints were added at them as shown in Figure 4.11 to increase flexibility at the distal end of the frame so that a higher finger ROM can be achieved when the device performs 4 finger flexion movements. Besides that, the proximal ends to the frame were modified to be thicker and bigger in size, and the mechanical joints between the proximal and distal ends of the frame were redesigned so that they would not break when the servo motors actuate the frame.

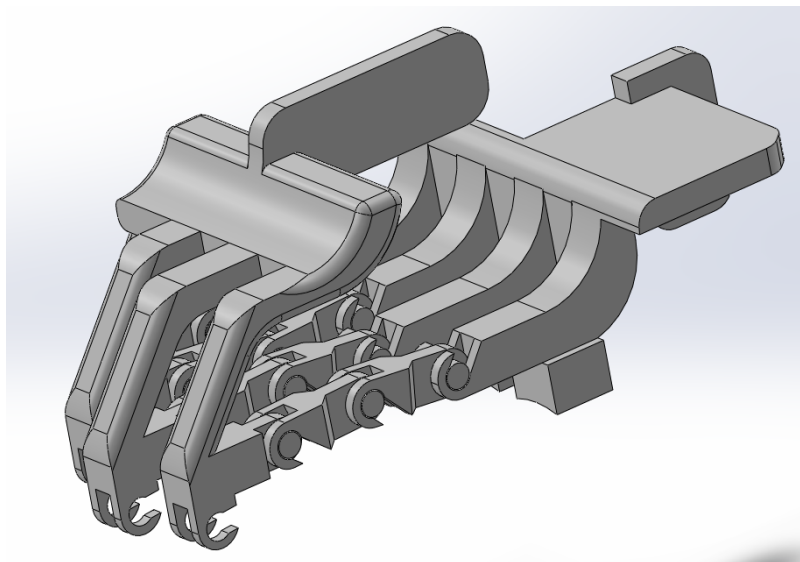


Figure 4.11: 3rd Iterative 4 Fingers Part Drawing in Isometric View.

After performing functionality testing on the third iterative 4 fingers part, it was found that the mechanical joints in between the proximal and distal ends of the second iterative 4 fingers part were not smooth enough. It was discovered that it is mainly due to the rotational axes for all the 4 fingers weren't aligned with each other as shown in Figure 4.12. The coloured dots refer to the estimated centre points of rotation for the mechanical joints on each of the 4 fingers and the coloured dotted lines corresponds to the rotational axis for each of the 4 fingers, which are the same colour as the dots. Misaligned rotation axes can cause inconsistent force transmission on the mechanical joints for each of the 4 fingers by the servo motors' actuation (Rincon et al., 2013), making the mechanical joint movements to be rough.

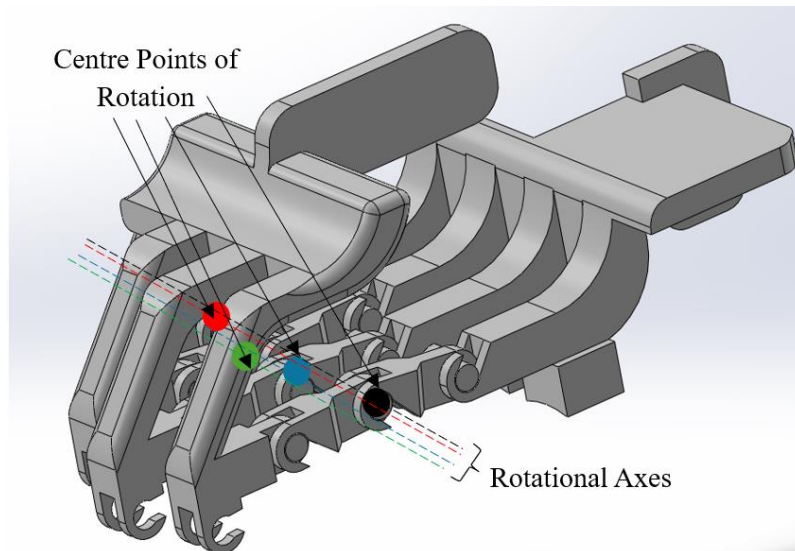


Figure 4.12: Misalignment of Rotational Axes for the Mechanical Joints of Each Finger for the Second Iterative 4 Fingers Part Frame

Hence, the mechanical joints in between the proximal and distal end of the 4 fingers part were modified to only have a single centre point of rotation and rotational axis shown in Figure 4.13. Besides that, holes were added at the proximal end of the third iterative 4 fingers frame to allow the slots to be fitted on it so that the servo motors ' end can attach to the frame of the 4 fingers part more securely, without it falling off while providing actuation to the frame.

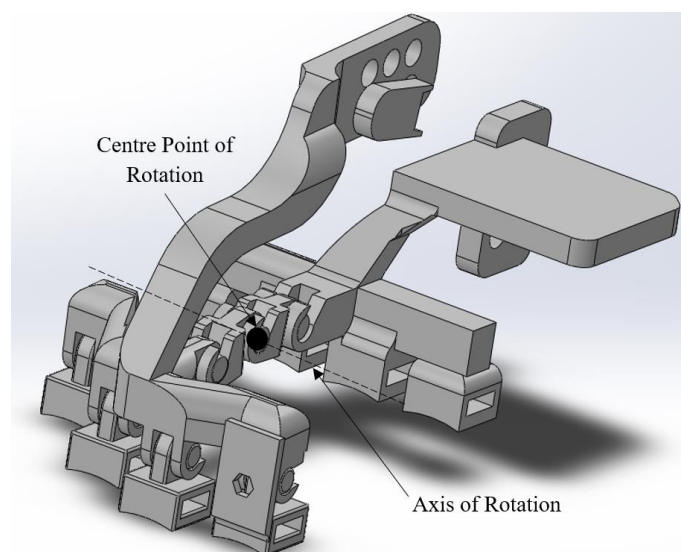


Figure 4.13: Single Centre Point of Rotation and Rotational Axis at the Mechanical Joints in Between the Proximal and Distal Ends of the Final Prototype 4 Fingers Part.

4.5.2 Thumb Part Design Changes and Enhancements

After performing functionality testing on the conceptualised thumb part, it was found that the proximal end of it is too thin, which may break when the servo motor actuates the thumb part. Therefore, the proximal end of the thumb part was redesigned to be larger and thicker as shown in Figure 4.14, to prevent it from breaking during servo motor actuation.

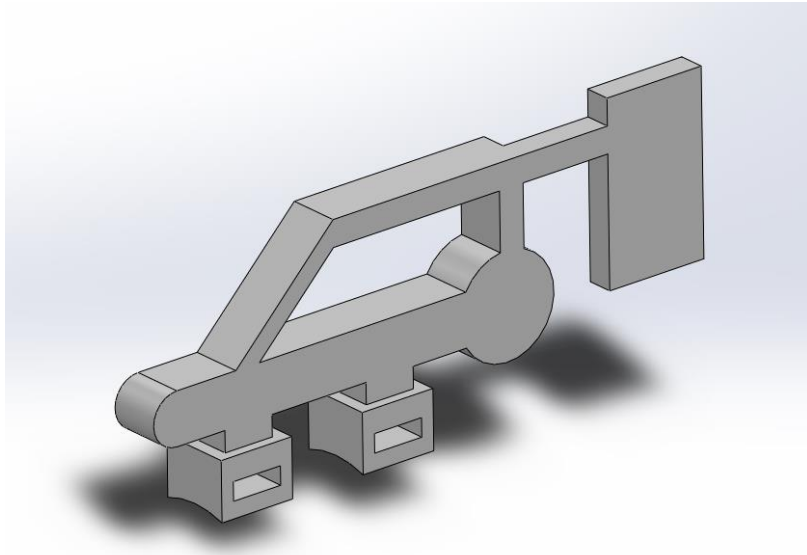


Figure 4.14: 2nd Iterative Thumb Part Drawing in Isometric View.

After performing functionality testing on the second iterative thumb part, it was discovered that the thumb flexion is insufficient. The results shown in Table 4.1 shows the mean thumb IP joint ROM achieved after redesigning the thumb part is greater for thumb flexion and lower for thumb extension. This signifies improvement in the thumb IP joint ROM for both thumb flexion and extension because the thumb IP joint ROM after redesigning the thumb part for both thumb flexion and thumb extension have a much lower percentage difference of 41.04% and 17.8% respectively shown in Table 4.2, when comparing them to their typical thumb IP joint ROM values. The typical thumb IP joint ROM for thumb flexion is 85° and for thumb extension is 5° (Physiotutors, n.d.).

Table 4.1: Thumb IP Joint ROM Before and After Redesigning Thumb Part.

Type of Movement	Thumb IP Joint ROM (°)	
	<i>Before</i>	<i>After</i>
<i>Thumb Flexion</i>	20.45 ± 0.88	50.11 ± 1.42
<i>Thumb Extension</i>	10.69 ± 0.57	4.11 ± 0.47

Table 4.2: Percentage Difference Between Thumb IP Joint ROM Achieved and Its Typical Value.

Type of Movement	Percentage Difference (%)	
	<i>Before</i>	<i>After</i>
<i>Thumb Flexion</i>	75.94	41.04
<i>Thumb Extension</i>	113.80	17.80

4.5.3 Junction Box Design Changes and Enhancements

Several changes were made on the junction box between the conceptualised junction box and the final prototype's one. Firstly, it was found that the PCB and microcontroller in the conceptualised junction box will move around inside it when the prototype was moving, which could result in loose circuit connections that can affect the circuit of the prototype. Therefore, there are small gaps added to the final prototype junction box to enable the microcontroller and PCB to fit into the junction box nicely so that both of them will stay in position while the prototype is moving. Besides that, the conceptualised prototype junction box was found to not have a lid which means the PCB and microcontroller may fall off if drastic movements were made by the user, which can result in loose circuit connections. Hence, the final prototype junction box was designed to have a hinge to enable the opening and closing of the junction box, and ends to hold the lid while its closed, so that the PCB and microcontroller would not fall off easily. Moreover, it was found that there are not enough room for the wires exit the junction box to connect to the IMUs and servo motors, so the final prototype junction box was designed to have a big gap at the side of it to allow space for the wires to exit the junction box.

4.6 Code Used to Program the Components and IoT System

Code used to program the components such as the servo motors, multiplexer and IMUs, with the Blynk IoT system used for this prototype are discussed here.

4.6.1 Servo Motor With IoT system Code

Figure 4.15 shows the code used to define the three servo motors that was used to actuate the prototype to perform specific finger movements as a variable for each. Servo1 (first servo motor) is the servo motor attached to the right proximal end of the 4 fingers part, servo2 (second servo motor) is the servo motor attached to the left proximal end of the 4 fingers part and servo3 (third servo motor) is the servo motor attached to the proximal end of the thumb part.

```
Servo servo1;  
Servo servo2;  
Servo servo3;
```

Figure 4.15: Variables For the Servo Motors Used on the Prototype.

Figure 4.16 illustrates the pins that the three servo motors signal pins would be connected to the microcontroller in order for them to receive the signals from the microcontroller to control them. According to Figure 4.16, the first, second and third servo motor signal pin would attach to the GPIO27, GPIO17 and GPIO26 pins on the microcontroller respectively.

```
servo1.attach(27);  
servo2.attach(17);  
servo3.attach(26);
```

Figure 4.16: Code to Define the Pins on the Microcontroller to Be Connected With the Three Servo Motors' Signal Pins.

Figure 4.17 shows the code used to set and control the rotational angle of the three servo motors for 4 fingers flexion, 4 finger extension and grasping movements depending on the button being pressed on the prototype IoT user interface via the Blynk IoT mobile app. When the 4 fingers flexion button was pressed on the Blynk IoT mobile app, the first and second servo motor would

be at 180 degrees and 0 degrees respectively, and the third servo motor would not change its position. When the 4 fingers extension button was pressed on the Blynk IoT mobile app, the first and second servo motor would be at 45 degrees and 90 degrees respectively, and the third servo motor would not change its position. Whereas, when the grasping button is pressed on the Blynk IoT mobile app, the first servo motor would be at 135 degrees, and the second and third servo motor would be at 30 degrees.

```
//4Fingers Flexion Button
BLYNK_WRITE(V0)
{
  servo1.write(180);
  servo2.write(0);
}

//4Fingers Extension Button
BLYNK_WRITE(V2)
{
  servo1.write(45);
  servo2.write(90);
}

//Grasping Button
BLYNK_WRITE(V5)
{
  servo1.write(135);
  servo2.write(30);
  servo3.write(30);
}
```

Figure 4.17: Code to Set Rotational Angle of the Servo Motors When a 4 Fingers Flexion/Extension or Grasping Button Selected on the Blynk IoT Mobile App.

Figure 4.18 shows the code used to control the rotational angle of the three servo motors when thumb flexion, thumb extension or reset button was being pressed on the prototype IoT user interface via the Blynk IoT mobile app. When the reset flexion button was pressed on the Blynk IoT mobile app, all three servo motors would be at 90 degrees to return it to its default state, which was presumed to be keeping the fingers straight. When the thumb flexion button is pressed on the Blynk IoT mobile app, only the third servo motor would be at 30 degrees, the first and second servo motor would not change their positions.

Furthermore, when the thumb extension button is pressed on the Blynk IoT mobile app, only the third servo motor would be at 90 degrees, the first and second servo motor would not change their positions.

```
//Reset Button (All Fingers Straight)
BLYNK_WRITE(V8)
{
  servo1.write(90);
  servo2.write(90);
  servo3.write(90);
}

//Thumb Flexion Button
BLYNK_WRITE(V9)
{
  servo3.write(30);
}

//Thumb Extension Button
BLYNK_WRITE(V10)
{
  servo3.write(90);
}
```

Figure 4.18: Code to Set Rotational Angle of Servo Motors When a Thumb Flexion/Extension or Reset Button Selected on the Blynk IoT Mobile App.

4.6.2 Inertial Measurement Units with Multiplexer Code

The first two lines in the code shown in Figure 4.19 are the variables that defined the first IMU (mpu1) which measured the thumb IP joint ROM and the second IMU (mpu3) which measured the index finger DIP joint ROM. The float variables in the code are the variables that were used for the derivation of the finger ROMs from the data collected by the IMUs' accelerometers with the use of trigonometry. TCAADDR 0x70 sets the default I2C address of the multiplexer. MOX1 was defined as 2, which indicated that first IMU was connected to multiplexer's third I2C channel (slot 2). MOX2 was defined as 6, which indicated the second IMU was connected to the multiplexer's seventh I2C channel (slot 6). The tcselect(uint8_t i) function was responsible to check which of the multiplexer's I2C channel (slot 0 to 7) was selected in this program.

```

//MPU6050
Adafruit_MPU6050 mpu1 = Adafruit_MPU6050(); // 1st imu
Adafruit_MPU6050 mpu3 = Adafruit_MPU6050(); //2nd imu

float mpu1_anglex; float mpu1_angley; float mpu1_anglez;
float mpu3_anglex; float mpu3_angley; float mpu3_anglez;
float mpu1_anglezz; float mpu3_anglezz;
float Ax, Ay, Az;
float Gx, Gy, Gz;
float pi=1.0/(3.142/180.0); //value of pi for radian to angle

//Multiplexer
#define TCAADDR 0x70
#define MOX1 2 // scl sda at slot 2
#define MOX3 6 // scl sda at slot 6

void tcselect(uint8_t i)
{
  if (i > 7) return;
  Wire.beginTransmission(TCAADDR);
  Wire.write(1 << i);
  Wire.endTransmission();
}

```

Figure 4.19: Code to Define the Variables Used for the Two IMUs and the I2C Channels to be Selected on the Multiplexer.

Before the IMUs could run with the program, they needed to be initialised first. The `tcselect(MOX1)` and `tcselect(MOX3)` functions shown in Figure 4.20 were responsible for initialising the first and second IMUs via the multiplexer. If any of the IMUs couldn't be initialised by the microcontroller, it would print out a message on the serial monitor in the Arduino integrated development environment (IDE) software showing that the IMU couldn't be found.

```

//First, to initiate 1st imu
tcselect(MOX1);
if (!mpu1.begin()) {
  Serial.println(F("Failed to find MPU6050 chip 1"));
  delay(5000);
}

//Second, to initiate 2nd imu
tcselect(MOX3);
if (!mpu3.begin()) {
  Serial.println(F("Failed to find MPU6050 chip 3"));
  delay(5000);
}

```

Figure 4.20: Code to Initialise Both IMUs via the Multiplexer.

Figure 4.21 shows the code used to program the IMUs to collect its accelerometer readings for every 100 milliseconds. The Blynk.run() function instructs the Blynk IoT to start collecting the IMUs accelerometer readings. In Figure 4.21, tcasselect(MOX1) function and tcasselect(MOX3) function select the first and third IMU respectively to collect its accelerometer data in the x, y and z axis.

```
void loop(){
//Run the Blynk
Blynk.run();

//MPU6050
/* Get new sensor events with the readings */
sensors_event_t a, g, temp;

//1st IMU
tcasselect(MOX1);
mpu1.getEvent(&a, &g, &temp);

float mpu1_ay = a.acceleration.y / 10;
float mpu1_ax = a.acceleration.x / 10;
float mpu1_az = a.acceleration.z / 10;

//2nd IMU
tcasselect(MOX3);
mpu3.getEvent(&a, &g, &temp);

float mpu3_ay = a.acceleration.y / 10;
float mpu3_ax = a.acceleration.x / 10;
float mpu3_az = a.acceleration.z / 10;
```

Figure 4.21: Code to Program the IMUs to Collect its Accelerometer Readings.

The code shown in Figure 4.22, contain the variables that represents the angular data in x, y and z axis derived from both IMU's accelerometer's readings with the use of trigonometry for every 100 milliseconds.

```
//Formulas to Convert Acceleration Data to Angular Data
mpu1_angley = atan(mpu1_ay/sqrt(mpu1_ax*mpu1_ax+mpu1_az*mpu1_az))*pi;
mpu1_anglex = atan(mpu1_ax/sqrt(mpu1_ay*mpu1_ay+mpu1_az*mpu1_az))*pi;
mpu1_anglez = (atan(sqrt(mpu1_ay*mpu1_ay+mpu1_ax*mpu1_ax)/mpu1_az)*pi);

mpu3_angley = atan(mpu3_ay/sqrt(mpu3_ax*mpu3_ax+mpu3_az*mpu3_az))*pi;
mpu3_anglex = atan(mpu3_ax/sqrt(mpu3_ay*mpu3_ay+mpu3_az*mpu3_az))*pi;
mpu3_anglez = (atan(sqrt(mpu3_ay*mpu3_ay+mpu3_ax*mpu3_ax)/mpu3_az)*pi);
```

Figure 4.22: Code to Derive the IMU's Acceleration Data to Angular Data.

The code shown in Figure 4.23 shows the adjustments made due to the orientation placement of the IMUs being attached on the prototype and to remove the offsets of both IMUs angle readings, in order to make their angle readings more accurate.

```

if (mpu1_anglez>0)
{
  mpu1_anglezz = mpu1_anglez - 90 + 5;
}

else if (mpu1_anglez<0)
{
  mpu1_anglez += 90;
  mpu1_anglezz = mpu1_anglez + 8;
}

if (mpu3_anglez>0)
{
  mpu3_anglez -= 90;
}

else if (mpu3_anglez<0)
{
  mpu3_anglez += 90;
}

```

Figure 4.23: Code Showing the Adjustments Made to IMUs' Angle Readings.

4.6.3 Blynk IoT System Code

Function 4.24 shows the function used to connect the microcontroller to the Blynk IoT via Wi-Fi connection. The code used to display the real-time index finger DIP joint and thumb IP joint ROM readings by both IMUs on the graphs in the prototype IoT user interface via the Blynk IoT mobile app every 100 milliseconds is shown in Figure 4.25.

```

//Connect to Blynk IoT
Blynk.begin(auth, ssid, pass);

```

Figure 4.24: Function Used to Connect Microcontroller to Blynk IoT.

```
Blynk.virtualWrite(V1, mpu1_anglezz);
Blynk.virtualWrite(V4, mpu3_anglez);
```

Figure 4.25: Function Used to Display Both IMUs Real-Time Angle Readings in Blynk IoT User Interface.

4.7 Results of Performance Assessments of the Prototype

This section displays the results of the various assessments done on the prototype to evaluate the performance of it in carrying out various finger movements and to test the accuracy of the IMUs finger ROM readings.

Subjects of various right hand sizes shown in Table 4.3, were involved in the performance assessments being carried out on the prototype. The data in Table 4.3 indicates that the prototype was able to be worn and used on subjects with various right hand sizes, hence this proven its adjustability to various right hand sizes.

Table 4.3: Subjects of Various Right Hand Sizes Involved in the Testing on the Prototype.

Right Hand Sizes	Range Length (cm)
<i>Middle Finger to Wrist</i>	15.5 - 18.0
<i>Across the Palm</i>	7.0 - 8.5
<i>Thumb to Wrist</i>	10.0 - 12.0

4.7.1 Inertial Measurement Unit Angle Accuracy Test

Table 4.4 illustrates the index finger DIP and thumb IP joint ROM measured by each of the two IMUs being attached on the final prototype and their corresponding actual angles measured by a digital goniometer in 30 degree intervals. The results indicated that after the calibration of both IMUs, they have quite consistent finger ROM readings with low variability as their finger ROM readings have low standard deviations of less than 2.

Table 4.4: Comparison of Angle Measurements on Prototype.

Actual Angle (Degree)	Mean \pm SD (Degree)	
	Index DIP	Thumb IP
0	0.59 \pm 0.23	0.43 \pm 0.42
30	30.53 \pm 0.43	29.34 \pm 0.70
60	60.08 \pm 0.75	61.11 \pm 0.67
90	85.99 \pm 1.35	88.86 \pm 0.51

The results in Table 4.5 proved the finger ROM readings of both IMUs being attached on the final prototype are quite accurate after calibrating them as they have very low percentage differences of less than 5% when comparing their finger ROM readings with their corresponding actual angles measured by a digital goniometer in 30-degree intervals.

Table 4.5: Percentage Differences in Angle Between Two Measurement Tools.

Actual Angle (Degree)	Percentage Difference in Angle (%)	
	Index DIP	Thumb IP
30	1.77	2.20
60	0.13	1.85
90	4.46	1.27

4.7.2 Finger Range of Motion Test

The results in Table 4.6 shows that the Finger ROM readings for both index finger DIP joint and thumb IP joint are quite consistent during 4 fingers flexion/extension and thumb flexion/extension movements, with them having low standard deviations of less than 8 between all participants.

The results also indicates that the mean index finger DIP joint ROM achieved by the final prototype for finger flexion is close to the typical ROM at the DIP joint for finger flexion with a low percentage difference of 10.1% when comparing it to its typical DIP joint ROM. Furthermore, the mean index DIP joint ROM for finger extension achieved by the final prototype is 23.78°, which is lower than that measured by the finger exoskeleton developed by Ceccarelli and Cruz, 2021 (36.81°). This indicates that this prototype can perform finger

extension better than the finger exoskeleton developed by Ceccarelli and Cruz, 2021, as it can produce a mean index finger DIP joint ROM with a lower percentage difference of 18.9% when comparing it to its typical DIP joint ROM. This means the prototype can perform finger extension closer to its typical DIP joint ROM than the finger exoskeleton developed by Ceccarelli and Cruz, 2021. The typical finger DIP joint ROM for finger flexion is 85° and for finger extension is 20° (Physiotutors, n.d.).

Based on the results shown in Table 4.6, the mean IP joint ROM for thumb flexion achieved by the final prototype was also close to its typical IP joint ROM for thumb flexion with a small percentage difference of around 20%. However, the mean IP joint ROM for thumb extension achieved by the final prototype was far below its typical ROM of 85 degrees (Physiotutors, n.d.), with a percentage error of 41.18%. The reason for the disparity is most likely due to the design limitation of the servo motor's arm, therefore it is recommended to use a linear actuator instead for future work.

Table 4.6: Finger Range of Motion for All Subjects.

Movement	Range of Motion	Mean \pm SD (Degree)
<i>4 Fingers Flexion</i>	<i>Index DIP</i>	80.29 \pm 3.91
<i>4 Fingers Extension</i>	<i>Index DIP</i>	23.78 \pm 7.70
<i>Thumb Flexion</i>	<i>Thumb IP</i>	50.11 \pm 1.42
<i>Thumb Extension</i>	<i>Thumb IP</i>	4.11 \pm 0.47

Figure 4.26 shows the finger ROMs response of a participant in flexion-extension directions during 5 repeated movements, with green line indicating the index finger DIP joint ROM and red line indicating the thumb IP joint ROM. This graph shows that the prototype can actuate repeatable 4 fingers flexion/extension and thumb flexion/extension, which is beneficial for people with fine motor trainings as repeatable finger movements can help improve finger muscle strengths, finger flexibility (Husam and Husi, 2021), and help stimulate neuroplasticity (Singh et al., 2021). This means it can help improve

fine motor trainings' effectiveness when this prototype is used to practice on these finger movements during these sessions.

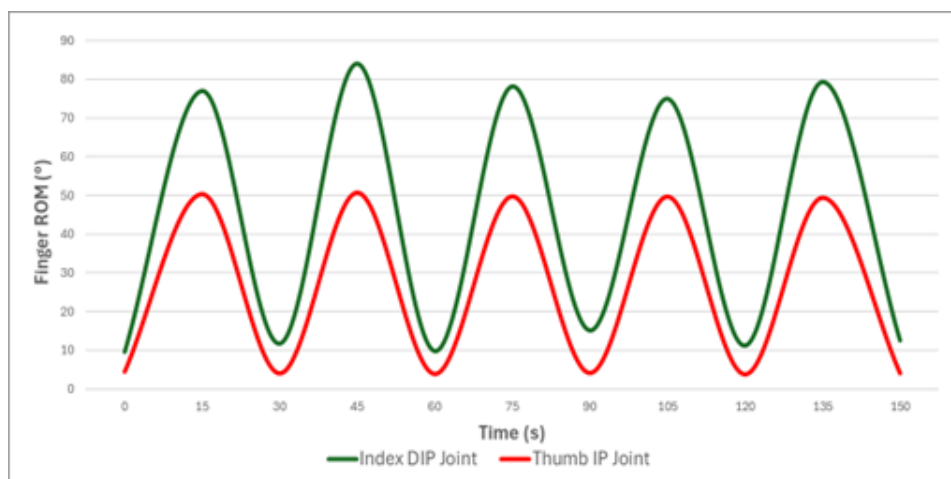


Figure 4.26: Finger ROMs against Time During 5 Repeated Movements of a Participant in Flexion-Extension Directions.

4.7.3 Grip Strength Test

The results of the grip strength test carried out with and without the final prototype (assistive hand orthosis, AHO) on all the participants' index finger and thumb after the grasping movement being actuated by the AHO are shown in Table 4.7. The results in Table 4.7, Figures 4.27 and 4.28 shows that the average grip strength for both index finger and thumb were found to be higher when wearing the AHO when compared to without wearing it, with a 14% and 16% increase, for the index finger and thumb respectively. This indicates that the AHO is able to improve on grip strength for both the index finger and thumb when grasping movement is being actuated by the AHO.

Table 4.7: Grip Strength With and Without the AHO.

Finger	Mean \pm SD (°)		% Increase
	Without AHO	With AHO	
<i>Index</i>	28.76 \pm 9.15	33.61 \pm 12.37	16.86
<i>Thumb</i>	33.93 \pm 9.67	38.71 \pm 13.74	14.09

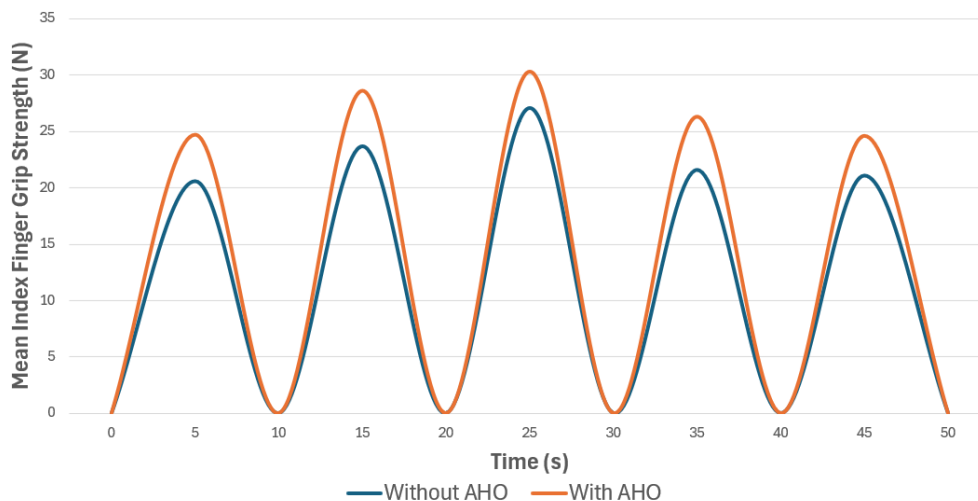


Figure 4.27: Average grip strength of the Index Finger for All Participants With and Without Wearing the AHO.

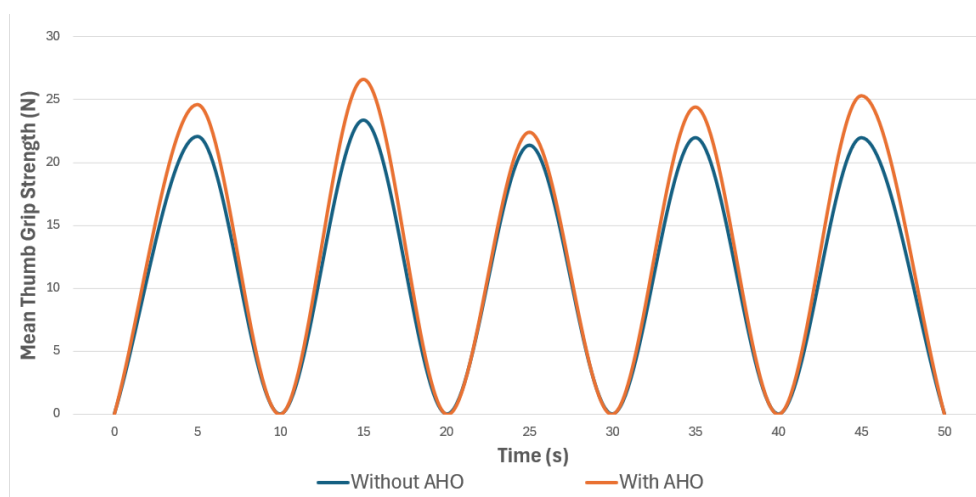


Figure 4.28: Average grip strength of the Thumb for All Participants With and Without Wearing the AHO.

4.7.4 Object Grasping Test

Object Grasping Test was performed to test the AHO ability in grasping objects with various sizes and shapes. Figure 4.29 shows the AHO (final prototype) grasping a ball of 3 cm (a), 6 cm (b), 7 cm (c) and 8 cm (d) when the AHO actuates grasping movement. This indicates the AHO's ability to grasp objects of various sizes.

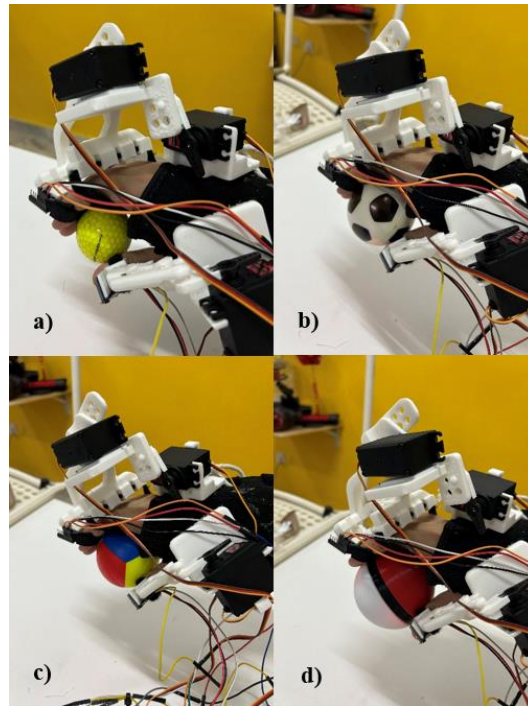


Figure 4.29: The AHO Grasping Balls of Various Sizes, a) $D = 3$ cm; b) $D = 6$ cm; c) $D = 7$ cm; d) $D = 8$ cm.

Figure 4.30 shows a cube (a), cylinder (b) and sphere (c) -shaped object being grasped when the AHO actuated grasping movement. This demonstrates the AHO's ability to grasp objects of various shapes. The AHO's grasping ability is useful for users with finger mobility issues and require practice on grasping objects, which is required in ADL, in order to regain back their fingers' grasping movement.

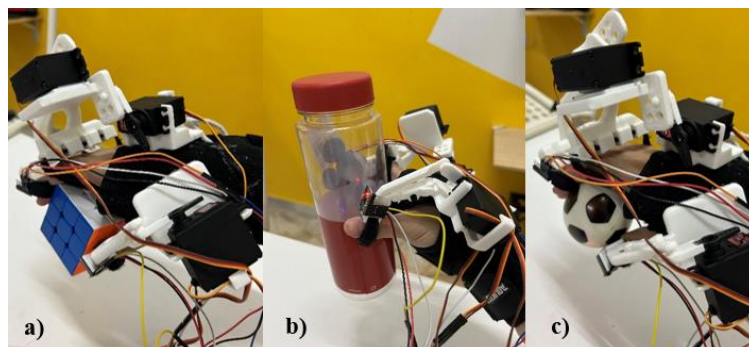


Figure 4.30: The AHO Grasping Objects of Different Shapes, a) Cube ; b) Cylinder ; c) Sphere.

4.7.5 Finger Range of Motion and Grip Strength Tests Based on Gender

Results of subject testing revealed that the standard error for finger extension was higher than flexion among all participants as shown in Table 4.8. This indicates that the exoskeleton can perform fingers flexion with more consistent index finger DIP joint ROMs as compared to extension. This could be due to the rotational angle of the servo motors responsible for actuating 4 fingers extension being insufficient. This difference can be reduced by increasing the rotational angle of the servo motor's arm so that it can pull the fingers upwards to a greater extent.

Table 4.8: Differences in Index Finger DIP joint ROM Between Male and Female Participants.

Movement	Mean \pm SD ($^{\circ}$)		Standard Error	Mean Square Error
	Male	Female		
<i>4 Fingers Flexion</i>	80.91 \pm 3.67	79.35 \pm 4.09	0.06	1.33
<i>4 Fingers Extension</i>	27.48 \pm 4.34	20.07 \pm 8.50	0.13	15.05

The results in Table 4.9 shows that there are differences in the amount of grip strength exhibited by both the male and female participants when wearing the AHO and without wearing it. A marked increase of 15 to 22% and 9 to 12% was observed in male and female cohort which proved that the exoskeleton could improve the grip strength for both male and female index finger and thumb.

Table 4.9: Differences in Grip Strength Without AHO and With AHO for Male and Female Participants.

Gender	Finger	Mean \pm SD ($^{\circ}$)		% Increase
		Without AHO	With AHO	
<i>Male</i>	<i>Index</i>	32.17 \pm 10.68	39.48 \pm 13.86	22.72
	<i>Thumb</i>	38.32 \pm 10.64	44.17 \pm 15.71	15.27
<i>Female</i>	<i>Index</i>	25.35 \pm 5.49	27.74 \pm 6.71	9.43
	<i>Thumb</i>	29.55 \pm 5.93	33.25 \pm 8.45	12.52

4.8 Summary

The final prototype 4 fingers part, thumb part, and junction box were designed using SOLIDWORKS. The final prototype consists of three servo motors for precise actuation of specific finger movements such as 4 fingers flexion/extension, thumb flexion/extension and grasping. It has two IMUs for collecting the index finger DIP and thumb IP joint ROMs, a portable power supply to power the electrical components, a junction box to house the microcontroller and PCB, Velcro straps providing adjustability to users of various finger diameters, and a wrist guard to house all the components together and ease of wear. It is lightweight (500 g) and cost-effective (RM 283.29). Initial designs on the mechanical frames encountered challenges, including mechanical joint rigidity and insufficient flexibility, which were addressed through multiple iterations. After redesigning on the thumb part, it showed significant improvement, with the thumb IP joint ROM increasing from 20.45° to 50.11° for thumb flexion and decreasing from 10.69° to 4.11° for thumb extension, making them close to their typical IP joint ROMs of 85° and 5°.

The prototype also demonstrated effective control over the index finger DIP joint ROM, achieving a mean flexion of 80.29°, with only a 10.1% deviation from its typical ROM, highlighting its accuracy. During finger ROM tests on the final prototype, it was found that the prototype produced quite consistent ROMs with a low standard deviation of less than 8 between all participants. Grip strength tests on the final prototype showed a marked increase when participants used the AHO. For the index finger, there was a 16% improvement in grip strength, and for the thumb, a 14% increase. This highlights the AHO's ability to improve in grip strength, an important feature for users with impaired motor skills. Additionally, the prototype was tested for its ability to grasp objects of varying sizes and shapes, successfully grasping balls between 3 cm and 8 cm in diameter, as well as cube, cylinder, and sphere-shaped objects. This flexibility demonstrates the AHO's potential for real-world applications where users need to handle a range of objects. The prototype's integration with its user-friendly Blynk IoT user interface which provides real-time finger ROMs data to be visualised and easy control over the device on actuating specific finger movements.

CHAPTER 5

CONCLUSIONS AND RECOMMENDATIONS

5.1 Conclusions

The project successfully demonstrated the proof-of-concept of the design and development of an assistive hand orthosis (AHO). This AHO was equipped with three servo motors that enables precise actuation on the users' fingers perform precise and specific finger movements such as 4 fingers flexion/extension, thumb flexion/extension and grasping. It was also equipped with IMUs for measuring finger ROMs. The angle readings on the IMUs proven to be accurate as the percentage differences between the IMU and digital goniometer readings are very low ($< 5\%$). The AHO is lightweight (500 g) and cost-effective (RM 283.29).

The prototype is integrated with a user friendly IoT user interface, which enables the users' rehabilitation data to be accessed and visualised remotely, and to be controlled easily using the Blynk IoT mobile app. This eases both the user and therapist in providing targeted and customisable assistance during fine motor trainings. The prototype's mechanical frames were made up of PLA and its electrical components were powered by a portable power source making it lightweight and portable. This enables the prototype to be easily carried around and used anywhere, allowing easy access to it. It's adjustability is proven as it was tested on subjects with a range of hand sizes.

After performing subject testing on this AHO, it shows that it can perform 4 fingers flexion/extension and thumb flexion/extension consistently with a low standard deviation of less than 10, and it can aid on users' grip strength with a percentage increase of 16.86% and 14.09% of the index finger and thumb respectively. The AHO also demonstrated the ability to grasp objects on different shapes and sizes. This is useful for users who have finger mobility issues and require practice on grasping objects, which is required in ADL, in order to regain back their fingers' grasping movement. This work is expected to serve as a foundation for the development of similar systems that will enhance

the accessibility, availability, affordability, and acceptability of exoskeleton rehabilitation systems in Malaysia.

5.2 Limitations

A limitation of this study is that the thumb part of the prototype cannot achieve a mean thumb IP joint ROM close to its typical ROM for thumb flexion, with a percentage error of 41.18%. Besides that, another limitation of this study is that fingers cannot be actuated and controlled individually when wearing the AHO, so it cannot perform finger movements such as finger pinching. Moreover, a limitation of this study is that the rigid attachments at the proximal end of the 4 fingers part are too rigid and contains no mechanical joints on it, so it can't produce ROM at the index finger MCP joint during 4 fingers flexion. Furthermore, the ROM for the other fingers such as middle, ring and small fingers can be collected on the prototype due to no IMUs being attached to these fingers. Additionally, the speed of the servo motors' actuation on the prototype's finger movements cannot be controlled, so some patients may feel uncomfortable when using the AHO. Lastly, the hinge at the junction box on the AHO broke due to it being too thin.

5.3 Recommendations for Future Work

A future work for this study is to use linear actuator instead of a servo motor to actuate the thumb part in order to produce a much greater thumb IP joint ROM during thumb flexion and so that it can get much closer to its typical ROM of 85°. Besides that, more servo motors can be added onto the AHO to allow individual actuation of the fingers so that the AHO can perform finger pinching. Moreover, mechanical joints can be added at the rigid attachments at the proximal end of the 4 fingers part, to increase flexibility at the proximal end and allow bending of the fingers at their MCP joint.

Furthermore, more IMUs can be added to the middle, ring and small fingers so that their ROMs can be tracked individually so that the therapist can carry out more specific targeted or customisable assistance on the patient's rehabilitation progress. Additionally, the AHO will need to have widgets on its IoT user interface which allows the servo motors' actuation speed to be

controlled on each of the servo motors, so that the user can feel more comfortable when using the AHO. Lastly, the hinge at the junction box on the AHO needs to be redesigned and to make it thicker so that it would not break in the future.

REFERENCES

Akyurek, G., Kars, S., Celik, Z., Koc, C. and Cesim, O. B., 2017. *Occupational Therapy - Occupation Focused Holistic Practice in Rehabilitation*. Turkey: InTechOpen.

Apoorve, 2015. *What is a Servo Motor? - Understanding the basics of Servo Motor Working*. Retrieved from <https://circuitdigest.com/article/servo-motor-working-and-basics>.

Baiju NT, 2022. *Pneumatic Artificial Muscle Robots: Benefits And Challenges*. Retrieved from <https://roboticsbiz.com/pneumatic-artificial-muscle-robots-benefits-and-challenges/>.

Barrett, A., 2020. *Advantages and Disadvantages of PLA*. Retrieved from <https://bioplasticsnews.com/2020/06/09/polylactic-acid-pla-dis-advantages/>.

Barrozo, 2023. *ESP32 Pinout: Everything You Need to Know*. Retrieved from <https://www.flux.ai/p/blog/esp32-pinout-everything-you-need-to-know>.

Basaraba, S. 2024. *Measuring Grip Strength for Health*. Retrieved from <https://www.verywellhealth.com/what-is-grip-strength-2224061>.

Basteris, A., Nijenhuis, S. M., Stienen, A. H. A., Buurke, J. H., Prange, G. B. and Amirabdollahian, F., 2014. Training modalities in robot-mediated upper limb rehabilitation in stroke: a framework for classification based on a systematic review. *Journal of NeuroEngineering and Rehabilitation*, 11(1), pp. 111. <https://doi.org/10.1186/1743-0003-11-111>.

Botnroll, n.d. *WEMOS® D1 R32 W/ ESP32 UNO R3 PINOUT*. Retrieved from <https://www.botnroll.com/en/esp32/3639-wemos-d1-r32-w-esp32-uno-r3-pinout.html>.

Butt, n.d. *How to use a flex sensor with Arduino*. Retrieved from <https://www.engineersgarage.com/how-to-use-a-flex-sensor-with-arduino/>.

Ceccarelli, M., and Cruz, C. M., 2021. A prototype characterization of ExoFinger, a finger exoskeleton. *International Journal of Advanced Robotic Systems*, 18(3). <https://doi.org/10.1177/17298814211024880>.

Chillibasket, 2015. *Calibrating & Optimising the MPU6050*. Retrieved from <https://wired.chillibasket.com/2015/01/calibrating-mpu6050/>.

Cleveland Clinic, 2023. *Hemiparesis*. Retrieved from <https://my.clevelandclinic.org/health/symptoms/24952-hemiparesis>.

Cunnington, R., 2016. *How our brain controls movement and makes new connections when parts are damaged*. Retrieved from <https://theconversation.com/how-our-brain-controls-movement-and-makes-new-connections-when-parts-are-damaged-63520>.

Cowan, R. E., Fregly, B. J., Boninger, M. L., Chan, L., Rodgers, M. M. and Reinkensmeyer, D. J., 2012 Recent trends in assistive technology for mobility. *Journal of NeuroEngineering and Rehabilitation*, 9. <https://doi.org/10.1186/1743-0003-9-20>.

Cytron Technologies, n.d.a. *GY-521 MPU6050 6DOF Accelerometer + Gyro*. Retrieved from <https://my.cytron.io/p-gy-521-mpu6050-6dof-accelerometer-plus-gyro>.

Cytron Technologies, n.d.b. *MG946R Metal Gear Servo*. Retrieved from <https://my.cytron.io/c-servo-motor/p-mg946r-metal-gear-servo>.

Cytron Technologies, n.d.c. *WiFi UNO Based ESP32*. Retrieved from <https://my.cytron.io/p-wifi-uno-based-esp32>.

Denslow, E., 2023. *Occupational Therapy Tools for Stroke Patients that Boost Independence*. Retrieved from <https://www.flintrehab.com/occupational-therapy-tools-for-stroke-patients/>.

Dychen, 2023. *A Comparison of Arduino IoT Cloud to Amazon AWS, Google Cloud, and Microsoft Azure*. Retrieved from <https://community.element14.com/technologies/internet-of-things/b/blog/posts/a-comparison-of-arduino-iot-cloud-to-amazon-aws-google-cloud-and-microsoft-azure>.

EJ Therapy, 2019. *What is the Difference Between Fine Motor and Gross Motor Skills?* Retrieved from <https://www.ejtherapy.com/blog/fine-motor-and-gross-motor-skills>.

Electricity-Magnetism, n.d.a. *Force Sensitive Resistor (FSR)*. Retrieved from <https://www.electricity-magnetism.org/force-sensitive-resistor-fsr/>.

Electricity-Magnetism, n.d.b. *Linear Motors*. Retrieved from <https://www.electricity-magnetism.org/linear-motors/>.

Electronic Wings, n.d. *MPU6050 Accelerometer and Gyroscope Sensor Guide with Arduino Programming*. Retrieved from <https://www.electronicwings.com/sensors-modules/mpu6050-gyroscope-accelerometer-temperature-sensor-module>.

Enabnit, A. and Warren, A., 2023. *Fine Motor Disability: Understanding, Evaluation, and Support*. Retrieved from <https://www.dovemed.com/health->

topics/focused-health-topics/fine-motor-disability-understanding-evaluation-and-support.

Esposito, D., Centracchoi, J., Andreozzi, E., Savino, S., Gargiulo, G. D., Naik, G. R. and Bifulco, P., 2022. Design of a 3D-Printed Hand Exoskeleton Based on Force-Myography Control for Assistance and Rehabilitation. *Feature Papers to Celebrate the First Impact Factor of Machines*, 10(1), pp.57. <https://doi.org/10.3390/machines10010057>.

Fahaam, H. A., Davis, S. and Meziani, S. N., 2016. *Wrist rehabilitation exoskeleton robot based on pneumatic soft actuators*. In: IEEE (Institute of Electrical and Electronics Engineers): International Conference for Students on Applied Engineering (ICSAE). Newcastle Upon Tyne, UK, 2016. Manchester: University of Salford.

Farinha, D., Dias, J., Neves, P., Pereira, K., Ferreira, C. and Pires, G., 2019. *Assistive Robotic Hand Orthosis (ARHO) controlled with EMG: evaluation of a preliminary prototype*. In: IEEE (Institute of Electrical and Electronics Engineers): 6th Portuguese Meeting on Bioengineering (ENBENG). Lisbon, Portugal, 2019. Tomar: Polytechnic Institute of Tomar.

Fergus, K. n.d. *Down Syndrome: Symptoms and Intellectual and Physical Traits*. Retrieved from <https://www.verywellhealth.com/symptoms-of-down-syndrome-1120463>.

Forgeahead, 2022. *What Are The 4 Stages Of IoT Architecture?* Retrieved from https://forgeahead.io/blog/4-stages-of-iot-architecture/#4_Layers_of_IoT_Architecture_Explained.

Gutierrez, C. A. and Biswas, R., 2023. *What are the pros and cons of using motion tracking vs rotoscoping for different types of shots and scenes?* Retrieved from <https://www.linkedin.com/advice/1/what-pros-cons-using-motion-tracking-vs-rotoscoping>.

Hankun, 2023. *Advantages and Disadvantages of Pneumatic Actuators*. Retrieved from <https://www.hankunfluid.com/article/88/45.html>.

Harrison, D., 2023. *Electromyography (EMG): Definition, Uses, and What to Expect*. Retrieved from <https://www.spineinfo.com/diagnostics/electromyography-emg/electromyography-emg-definition-uses-and-what-to-expect/>.

Heason, 2020. *Advantages of Servo Motors*. Retrieved from <https://www.heason.com/news-media/technical-blog-archive/advantages-of-servo-motors>.

Husam, A. and Husi, G., 2021. Design and Development of Continuous Passive Motion (CPM) for Fingers and Wrist Grounded-Exoskeleton Rehabilitation System. *Applied Sciences*, 11(2), pp. 815. <https://doi.org/10.3390/app11020815>.

Indian Institute of Embedded Systems, n.d. *Unleashing the Power of Blynk Cloud for IoT Innovations*. Retrieved from <https://iies.in/blog/unleashing-the-power-of-blynk-cloud-for-iot-innovations/>.

Inertial Labs, 2023. *Advantages and Disadvantages of Inertial Measurement Units*. Retrieved from <https://inertiallabs.com/advantages-and-disadvantages-of-inertial-measurement-units/>.

IQS Directory, n.d. *Hydraulic Cylinders*. Retrieved from <https://www.iqsdirectory.com/articles/hydraulic-cylinder.html>.

Ismail, R., Ariyanto, M., Pambudi, K. A., Syafei, J. W. and Ananto, G. P., 2017. *Extra robotic thumb and exoskeleton robotic fingers for patient with hand function disability*. In: IEEE (Institute of Electrical and Electronics Engineers): 4th International Conference on Electrical Engineering, Computer Science and Informatics (EECSI). Yogyakarta, Indonesia, 2017. Semarang: Diponegoro University.

Ison, M., and Artemiadis, P., 2014. The role of muscle synergies in myoelectric control: Trends and challenges for simultaneous multifunction control. *Journal of NeuroEngineering and Rehabilitation*, 11(1), pp. 1-20. <https://doi.org/10.1186/1743-0003-11-43>.

Last Minute Engineers, n.d. *ESP32 Pinout Reference*. Retrieved from <https://lastminuteengineers.com/esp32-pinout-reference/>.

Lelong, M., Zysset, A., Nievergelt, M., Luder, R., Gotz, U., Schulze, C. and Wieber, F., 2021. How effective is fine motor training in children with ADHD? A scoping review. *BMC Pediatr*, 21, pp.490. <https://doi.org/10.1186/s12887-021-02916-5>.

Levin, M. F., Kleim, J. A., and Wolf, S. L., 2009. What Do Motor 'Recovery' and 'Compensation' Mean in Patients Following Stroke? *Neurorehabilitation and Neural Repair*, 23(4), pp. 313-319. <https://doi.org/10.1177/1545968308328727>.

Li, H., Cheng, L., Sun, N. and Cao, R., 2021. Design and Control of an Underactuated Finger Exoskeleton for Assisting Activities of Daily Living. *IEEE/ASME Transactions on Mechatronics*, 27(5), pp.2699-2709. <https://doi.org/10.1109/TMECH.2021.3120030>.

Li, Z., Yuan, M., Mao, K. and Zheng, L., 2023. *Finger Rehabilitation Training Robot Mechanism Design*. In: IEEE (Institute of Electrical and Electronics Engineers): 5th International Symposium on Robotics & Intelligent

Manufacturing Technology (ISRIMT). Changzhou, China, 2023. Changzhou: Hohai University.

Maciejasz, P., Eschweiler, J., Gerlach-Hahn, K., Jansen-Troy, A and Leonhardt, S., 2014. A survey on robotic devices for upper limb rehabilitation. *Journal of NeuroEngineering and Rehabilitation*, 11(1) pp. 3. <https://doi.org/10.1186/1743-0003-11-3>.

Mayo Clinic, n.d. *Movement Disorder*. Retrieved from <https://www.mayoclinic.org/diseases-conditions/movement-disorders/symptoms-causes/syc-20363893>.

Mercyshalinie, E. R. S., Ghadge, A., Ifejika, N. and Tadesse, Y., 2023. NOHAS: A Novel Orthotic Hand Actuated by Servo Motors and Mobile App for Stroke Rehabilitation. *AI for Robotic Exoskeletons and Prostheses*, 12(6), pp.169. <https://doi.org/10.3390/robotics12060169>.

Meta Motion, n.d. *Optical Motion Capture Systems*. Retrieved from <https://metamotion.com/motion-capture/optical-motion-capture-1.htm>.

Motion Analysis, 2023. *What is Optical Motion Capture?* Retrieved from <https://www.motionanalysis.com/biomechanics/what-is-optical-motion-capture/>.

Motzki, P. and Rizzello, G., 2023. Smart Shape Memory Alloy Actuator Systems and Applications. In: Chowdhury, M. A. and Rahman, M. M., ed. 2024. *Shape Memory Alloys - New Advances*. IntechOpen. <https://doi.org/10.5772/intechopen.1002632>.

Mybotic, n.d. *TCA9548A I2C MULTIPLEXER MODULE*. Retrieved from <https://www.mybotic.com.my/sensor/tca9548a-i2c-multiplexer-module>.

Nycz, C. J., Butzer, T., Lamercy, O., Arata, J., Fischer, G. S. and Gassert, R., 2016. Design and Characterization of a Lightweight and Fully Portable Remote Actuation System for Use With a Hand Exoskeleton. *IEEE Robotics and Automation Letters*, 1(2), pp.976-983. <https://doi.org/10.1109/LRA.2016.2528296>.

Othman, A., Hamzah, N., Hussain, N., Baharudin, R., Rosli, A. D. and Ani, A. I. C., 2016. *Design and development of an adjustable angle sensor based on rotary potentiometer for measuring finger flexion*. In: IEEE (Institute of Electrical and Electronics Engineers): International Conference on Control System, Computing and Engineering (ICCSCE). Penang, Malaysia, 2021. Permatang Pauh: UiTM Pulau Pinang.

PainScale, n.d. *The Pros and Cons of Occupational Therapy*. Retrieved from <https://www.painscale.com/article/pros-and-cons-of-occupational-therapy>.

Park, J., Heo, P., Kim, J. and Na, Y., 2020. A Finger Grip Force Sensor with an Open-Pad Structure for Glove-Type Assistive Devices. *Physical Sensors*, 20(1), pp.4. <https://doi.org/10.3390/s20010004>.

Physiopedia, n.d. *Grip Strength*. Retrieved from https://www.physiopedia.com/Grip_Strength.

Physiotutors, n.d. *Wrist/Hand Active Range of Motion (AROM) Assessment*. Retrieved from <https://www.physiotutors.com/wiki/wrist-hand-active-range-of-motion/>.

Positek, n.d. *Rotary Position Sensors: Basic Guide and Specifications*. Retrieved from <https://www.positek.com/news-media/blog-archive/rotary-position-sensors-basic-guide-and-specifications>.

Rad, A., 2023. *Types of movements in the human body*. Retrieved from <https://www.kenhub.com/en/library/anatomy/types-of-movements-in-the-human-body>.

RAYPCB, n.d. *Stripboard Vs Perfboard Vs Breadboard: What's Difference*. Retrieved from <https://www.raypcb.com/stripboard-vs-perfboard-vs-breadboard/>.

Rincon, C., Delgado, P., Hakansson, N. A. and Yihun, Y., 2023. Modeling of Human-Exoskeleton Alignment and Its Effect on the Elbow Flexor and Extensor Muscles during Rehabilitation. *Modelling*, 4(3), pp. 351-365. <https://doi.org/10.3390/modelling4030020>.

Rosenthal, R., Rosnow, R. L. and Rubin, D. B., 2000. *Contrasts and effect sizes in behavioral research: A correlational approach*. Cambridge, England: Cambridge University Press.

RS Malaysia, n.d. *Festo Pneumatic Cylinder - 19232, 16mm Bore, 100mm Stroke, DSNU Series, Double Acting*. Retrieved from <https://my.rs-online.com/web/p/pneumatic-piston-rod-cylinders/1214710>.

Serrano, D., Copaci, D. S., Moreno, L. and Blanco, D., 2018. *SMA based wrist exoskeleton for rehabilitation therapy*. In: IEEE (Institute of Electrical and Electronics Engineers): International Conference on Intelligent Robots and Systems (IROS). Madrid, Spain, 2018. Madrid: Carlos III University of Madrid.

Shahid, T., Gouwanda, D., Nurzaman, S. G., Gopalai, A. A. and Kheng, T. K., 2021. *Development of an Electrooculogram-activated Wearable Soft Hand Exoskeleton*. In: IEEE (Institute of Electrical and Electronics Engineers): Conference on Biomedical Engineering and Sciences (IECBES). Langkawi Island, Malaysia, 2021. Bandar Sunway: Monash University Malaysia.

Shea, C. 2021. *Explaining the Difference Between Occupational and Physiotherapy*. Retrieved from <https://napacentre.com.au/explaining-the-difference-between-occupational-and-physical-therapy/>.

Shilleh, M. M., 2023. *How to Calibrate Gyroscope with MPU6050*. Retrieved from <https://www.hackster.io/Shilleh/how-to-calibrate-gyroscope-with-mpu6050-6ca10f>.

Singh, N., Saini, M., Kumar, N., Srivastava, M. V. P. and Mehndiratta, A., 2021. Evidence of neuroplasticity with robotic hand exoskeleton for post-stroke rehabilitation: a randomized controlled trial. *Journal of NeuroEngineering and Rehabilitation*, 76(2021), pp. 18. <https://doi.org/10.1186/s12984-021-00867-7>.

Skaramagkas, V., Andrikopoulos, G. and Manesis, S., 2020. *An Experimental Investigation of Essential Hand Tremor Suppression via a Soft Exoskeletal Glove*. In: IEEE (Institute of Electrical and Electronics Engineers): European Control Conference (ECC). St. Petersburg, Russia, 2020. Rio: University of Patras.

Soft Robotics Kit, n.d. *Pneumatic Artificial Muscles*. Retrieved from <https://softroboticstoolkit.com/book/pneumatic-artificial-muscles>.

Soft Robotics Kit, n.d. *PneuNets Bending Actuators*. Retrieved from <https://softroboticstoolkit.com/book/pneunets-bending-actuator>.

Tarr, C. 2022. *Hand Injuries*. Retrieved from https://www.emedicinehealth.com/hand_injuries/article_em.htm.

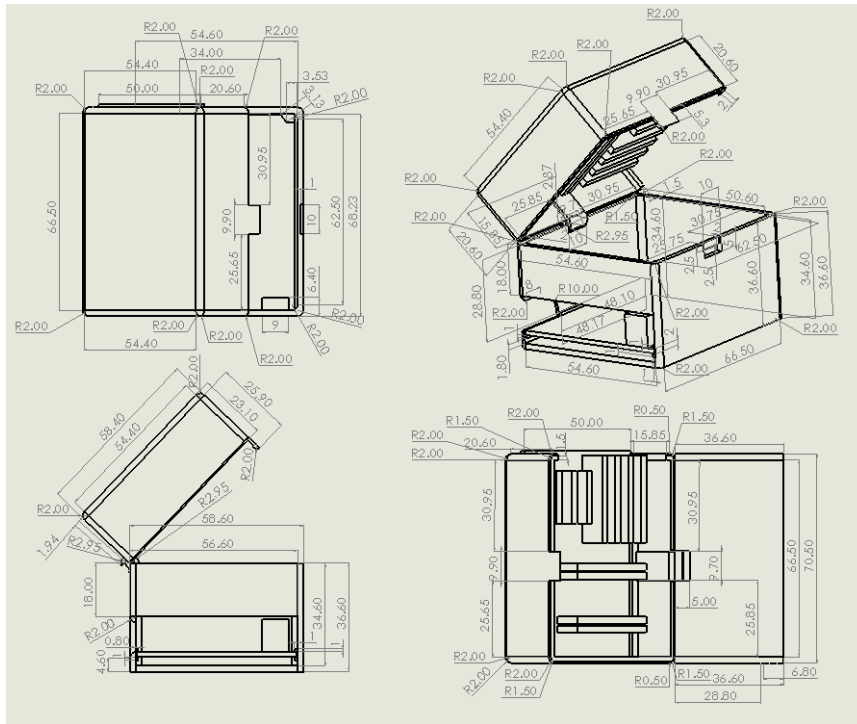
Tkachuk, H. and Horn, S., 2020. Evaluation of the accuracy and precision of digital force gauges used in hand strength assessments. *Journal of Applied Biomechanics*, 36(5), pp. 359-365. <https://doi.org/10.1123/jab.2020-0045>.

Tolomatic, 2016. *Hydraulic linear actuator advantages and disadvantages*. Retrieved from <https://www.tolomatic.com/blog/hydraulic-linear-actuator-advantages-and-disadvantages/>.

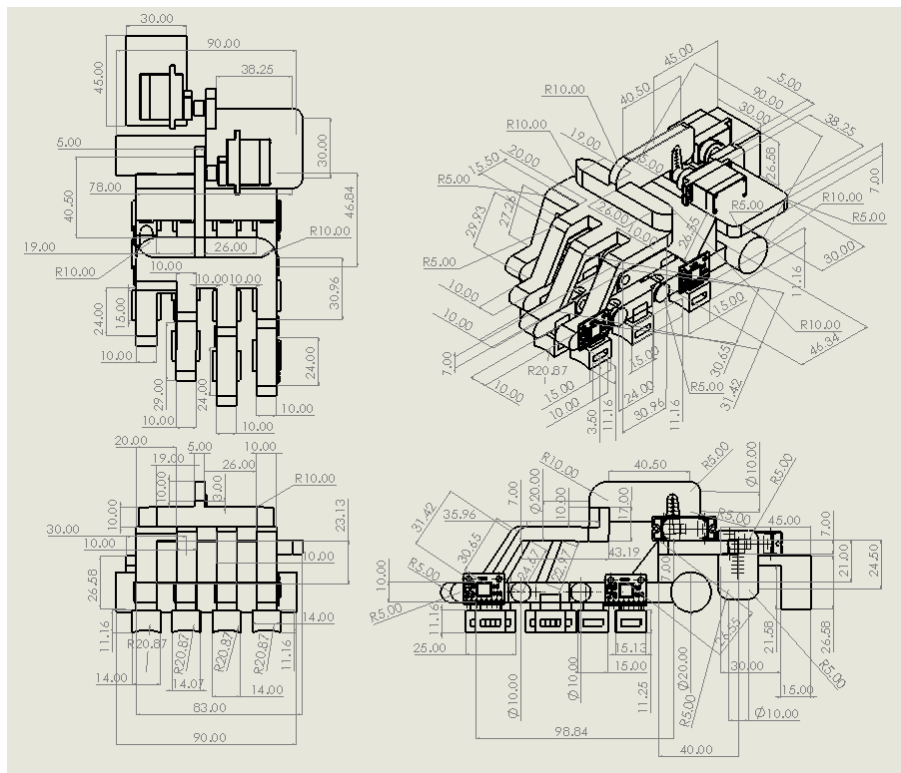
Vectornav Technologies, n.d. *WHAT IS AN INERTIAL MEASUREMENT UNIT?* Retrieved from <https://www.vectornav.com/resources/inertial-navigation-articles/what-is-an-inertial-measurement-unit-imu>.

What Things Weigh, n.d. *Weight of a Hand*. Retrieved from <https://whatthingsweigh.com/how-much-does-a-hand-weigh/>.

Yap, H., K., Lim, J. H., Nasrallah, F., Goh, J. C. H. and Yeow, R. C. H., 2015. *A soft exoskeleton for hand assistive and rehabilitation application using pneumatic actuators with variable stiffness*. In: IEEE (Institute of Electrical and Electronics Engineers): International Conference on Robotics and Automation (ICRA). Seattle, USA, 2015. Singapore: National University of Singapore.



Appendix G: Technical Drawings of the Final Prototype Junction Box with Dimensions in Multiple Views.



Appendix H: Technical Drawings of the Second Iterative 4 Fingers Part with Dimensions in Multiple Views.

Development of a 3D-Printed IoT-Enabled Finger Exoskeleton for Fine Motor Training

Chi Heim Wong
Dept of Mechatronics and Biomedical
Engineering
Universiti Tunku Abdul Rahman
Kajang, Malaysia
wongchiheim@utar.my

Ming Jack Choo
Dept of Mechatronics and Biomedical
Engineering
Universiti Tunku Abdul Rahman
Kajang, Malaysia
cmjack1907@utar.my

Yu Zheng Chong**
Dept of Mechatronics and Biomedical
Engineering
Universiti Tunku Abdul Rahman
Kajang, Malaysia
chongyz@utar.edu.my

Joo Ling Loo*
Dept of Mechatronics and Biomedical
Engineering
Universiti Tunku Abdul Rahman
Kajang, Malaysia
loojl@utar.edu.my

Abstract— There are currently lack of assistive devices connected to internet-of-things (IoT), which enables precise real-time and, remote control and monitoring of the patients during finger fine motor rehabilitation. This study aimed to enhance existing hand therapy tool by developing a portable, affordable (~MYR 300) and remotely controllable finger exoskeleton to enhance fine motor training of fingers. The exoskeleton was designed to assist in actuating flexion-extension movements of all 4 fingers and thumb in the metacarpophalangeal (MCP) joint, and grasping movement. The mechanical frame was designed using computer-aided software (CAD) and additive manufactured with polylactic acid (PLA) filaments. The functional components include inertial measurement units (IMUs) that measure the range of motion of the index finger and thumb; servo motors that enable precise linear actuation in performing specific finger and thumb movements; a microcontroller as the control system; and a simple IoT user interface that aids the therapists in monitoring rehabilitation progress of individual, as well as controlling the exoskeleton remotely. This exoskeleton can perform 4 fingers flexion/extension and thumb flexion/extension on subjects with various hand sizes (15.5 cm to 18 cm) consistently with a low standard deviation ($SD < 8$), and it can aid on users' grip strength with a percentage increase of 16.86% and 14.09% for index finger and thumb, respectively. Experimental outcomes showed that the exoskeleton was able to acquire, display and store relevant data accurately when assisting participants to perform repetitive flexion/extension movement and practice grasping on objects of various shapes and sizes. This proof of concept demonstrated the exoskeleton can assist and has the potential to improve the effectiveness of fine motor trainings in finger rehabilitation, besides providing more convenience to the users and therapists.

Keywords— Internet of things, fine motor training, finger exoskeleton, servo motor, range of motion, grip strength

I. INTRODUCTION

People with fine motor impairments face difficulties in performing precise and coordinated movements such as finger flexion/extension, finger abduction/adduction, gripping, pinching and more [1][2]. Fine motor impairments are caused by various conditions such as stroke, cerebral palsy, traumatic

*Corresponding author: J.L. Loo

#Y. Z. Chong and J. L. Loo are with the Centre for Healthcare Science and Technology, University Tunku Abdul Rahman, Selangor, Malaysia

**Y. Z. Chong is Senior, IEEE member

brain injury, bone fractures and more [3]. As a result, having fine motor impairments can impact the activities of daily living (ADL) such as writing, using utensils, button clothes and more [4]. Therefore, fine motor training to regain and improve fine motor control, coordination, strength and dexterity of fingers is required [2].


Traditional hand therapy tools, such as therapy putty, finger exercisers, and fine motor skill training devices, are still widely used in finger fine motor rehabilitation in Malaysia. Fine motor skills rehabilitation, such as finger movement and coordination, usually requires a relatively long time compared to gross motor skills. Usually, individuals with fine motor impairments would undergo occupational therapy sessions, which focuses recovery on fine motor movements instead of gross motor movements [5], by practicing basic hand and finger exercises like ball grip, pinching objects, gripping and grasping objects to improve their pinch force and grip strength [2]. Assistive devices such as exoskeletons, adaptive utensils and video gaming tools are sometimes adopted to help individuals perform fine motor trainings more effectively and easily during occupational therapy [6].

Despite the increased interest, these assistive devices were reported to be lacking the precision and adaptability needed for addressing the unique needs, and quantitatively track and evaluate the performance of individual patient for finger fine motor rehabilitation [7]. Therefore, an active finger exoskeleton containing sensors and motors is a solution to enable measurements of the biomechanical parameters accurately and precisely, so that therapists can use these data to assess and provide accurate, targeted and customizable therapy for individual patient during fine motor trainings. Moreover, there is currently a lack of rehabilitation devices that can be controlled over a user interface [8].

Pneumatic actuators are commonly used in hand and wrist exoskeletons, as seen in the work of Yap et al. [9] and Fahaam et al. [10]. However, these actuators struggle with precision control, which is essential for finger exoskeletons that assist fine motor movements [11]. To overcome this, recent designs have shifted to electrical actuation using servo motors, as demonstrated by Esposito et al. [12], and Ceccarelli and Cruz [13]. Servo motors offer greater precision for controlling fine motor movements as demonstrated by an electrically actuated

Appendix K: Conference Manuscript Based on This Project Accepted to be Presented at the IECBES 2024 Conference.

CCC RightsLink Sign in/Register



Assistive Robotic Hand Orthosis (ARHO) controlled with EMG: evaluation of a preliminary prototype
 Conference Proceedings: 2019 IEEE 6th Portuguese Meeting on Bioengineering (ENBENG)
 Author: Diogo Farinha
 Publisher: IEEE
 Date: February 2019
Copyright © 2019, IEEE

Thesis / Dissertation Reuse

The IEEE does not require individuals working on a thesis to obtain a formal reuse license, however, you may print out this statement to be used as a permission grant:

Requirements to be followed when using any portion (e.g., figure, graph, table, or textual material) of an IEEE copyrighted paper in a thesis:

- 1) In the case of textual material (e.g., using short quotes or referring to the work within these papers) users must give full credit to the original source (author, paper, publication) followed by the IEEE copyright line © 2011 IEEE.
- 2) In the case of illustrations or tabular material, we require that the copyright line © [Year of original publication] IEEE appear prominently with each reprinted figure and/or table.
- 3) If a substantial portion of the original paper is to be used, and if you are not the senior author, also obtain the senior author's approval.

Appendix L: An Assistive Robotic Hand Orthosis (Farinha, et al., 2019).

Reprinted with permission from Copyright 2019 IEEE.

CCC RightsLink CW



A soft exoskeleton for hand assistive and rehabilitation application using pneumatic actuators with variable stiffness
 Conference Proceedings: 2015 IEEE International Conference on Robotics and Automation (ICRA)
 Author: Hong Kai Yap
 Publisher: IEEE
 Date: May 2015
Copyright © 2015, IEEE

Thesis / Dissertation Reuse


The IEEE does not require individuals working on a thesis to obtain a formal reuse license, however, you may print out this statement to be used as a permission grant:

Requirements to be followed when using any portion (e.g., figure, graph, table, or textual material) of an IEEE copyrighted paper in a thesis:

- 1) In the case of textual material (e.g., using short quotes or referring to the work within these papers) users must give full credit to the original source (author, paper, publication) followed by the IEEE copyright line © 2011 IEEE.
- 2) In the case of illustrations or tabular material, we require that the copyright line © [Year of original publication] IEEE appear prominently with each reprinted figure and/or table.
- 3) If a substantial portion of the original paper is to be used, and if you are not the senior author, also obtain the senior author's approval.

Appendix M: The ExoGlove (Yap, et al., 2015). Reprinted with permission from Copyright 2022 IEEE.

CCC RightsLink CW



SMA based wrist exoskeleton for rehabilitation therapy
 Conference Proceedings: 2018 IEEE/RSJ International Conference on Intelligent Robots and Systems (IROS)
 Author: David Serrano
 Publisher: IEEE
 Date: October 2018
Copyright © 2018, IEEE

Thesis / Dissertation Reuse

The IEEE does not require individuals working on a thesis to obtain a formal reuse license, however, you may print out this statement to be used as a permission grant:

Requirements to be followed when using any portion (e.g., figure, graph, table, or textual material) of an IEEE copyrighted paper in a thesis:

- 1) In the case of textual material (e.g., using short quotes or referring to the work within these papers) users must give full credit to the original source (author, paper, publication) followed by the IEEE copyright line © 2011 IEEE.
- 2) In the case of illustrations or tabular material, we require that the copyright line © [Year of original publication] IEEE appear prominently with each reprinted figure and/or table.
- 3) If a substantial portion of the original paper is to be used, and if you are not the senior author, also obtain the senior author's approval.

Appendix N: A SMA Based Wrist Exoskeleton (Serrano, et al., 2018).

Reprinted with permission from Copyright 2018 IEEE.